*materials*

MDPI

*Supplementary Materials*

# Synthesis, Absolute Configuration, Antibacterial and Antifungal Activities of Novel Benzofuryl *β*-Amino Alcohols

## 1. NMR Spectra

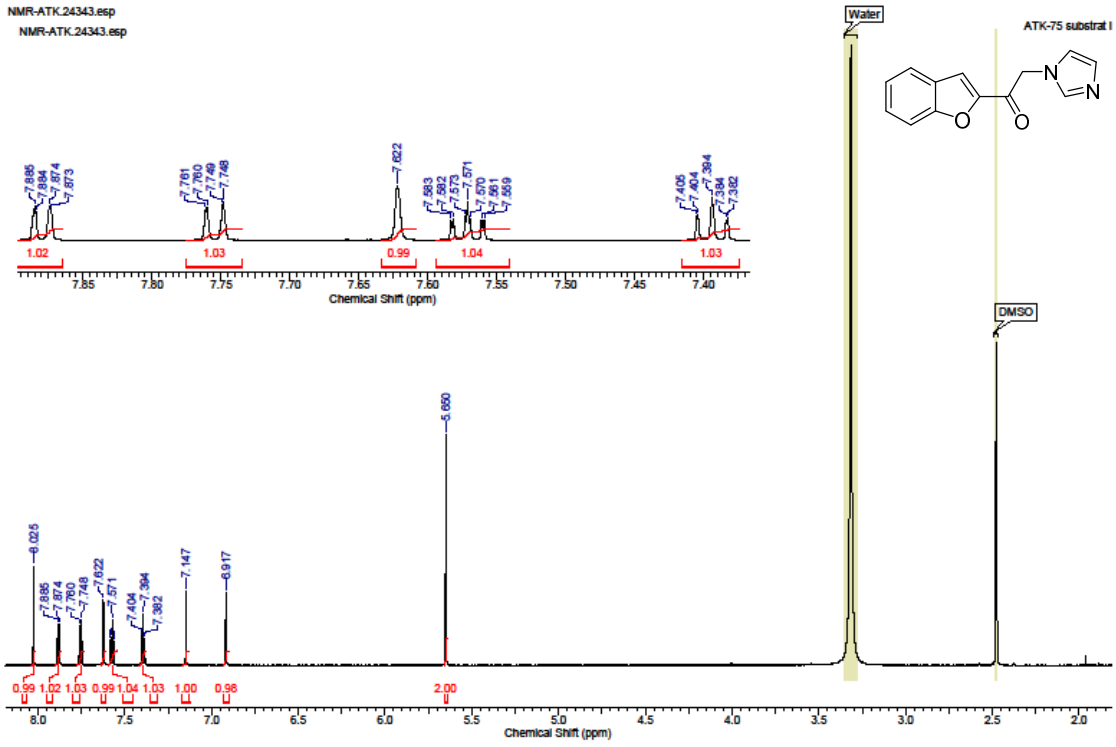


(**a**)

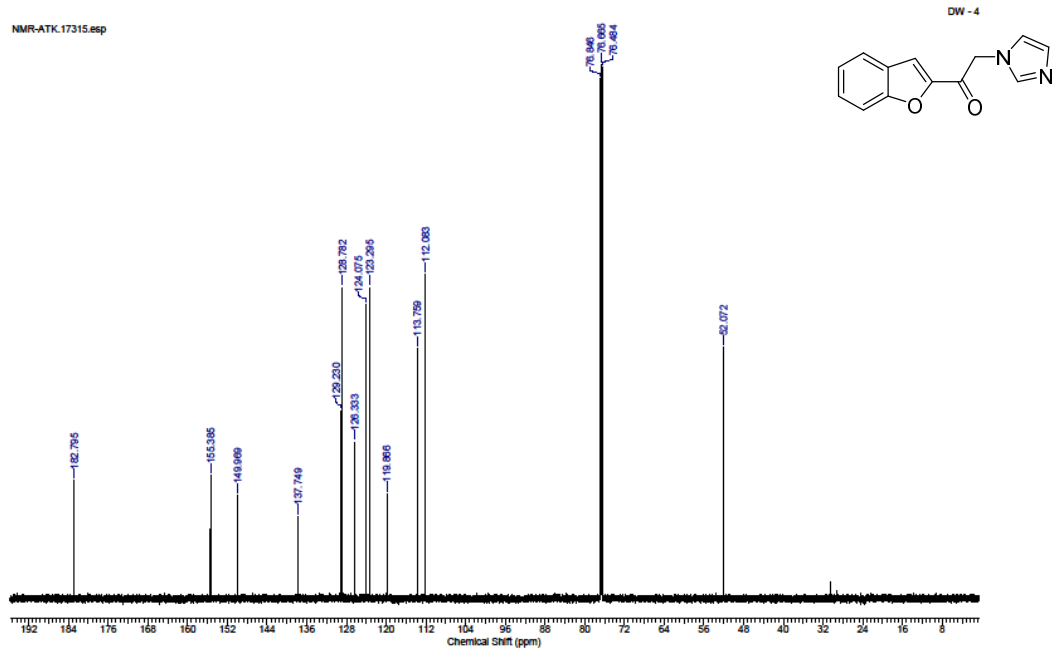


(**b**)

**Figure 1.** (**a**) $^{1}$H NMR and (**b**) $^{13}$C NMR spectra of 1-(benzofuran-2-yl)-2-(1*H*-imidazol-1-yl)ethanone (**5**).

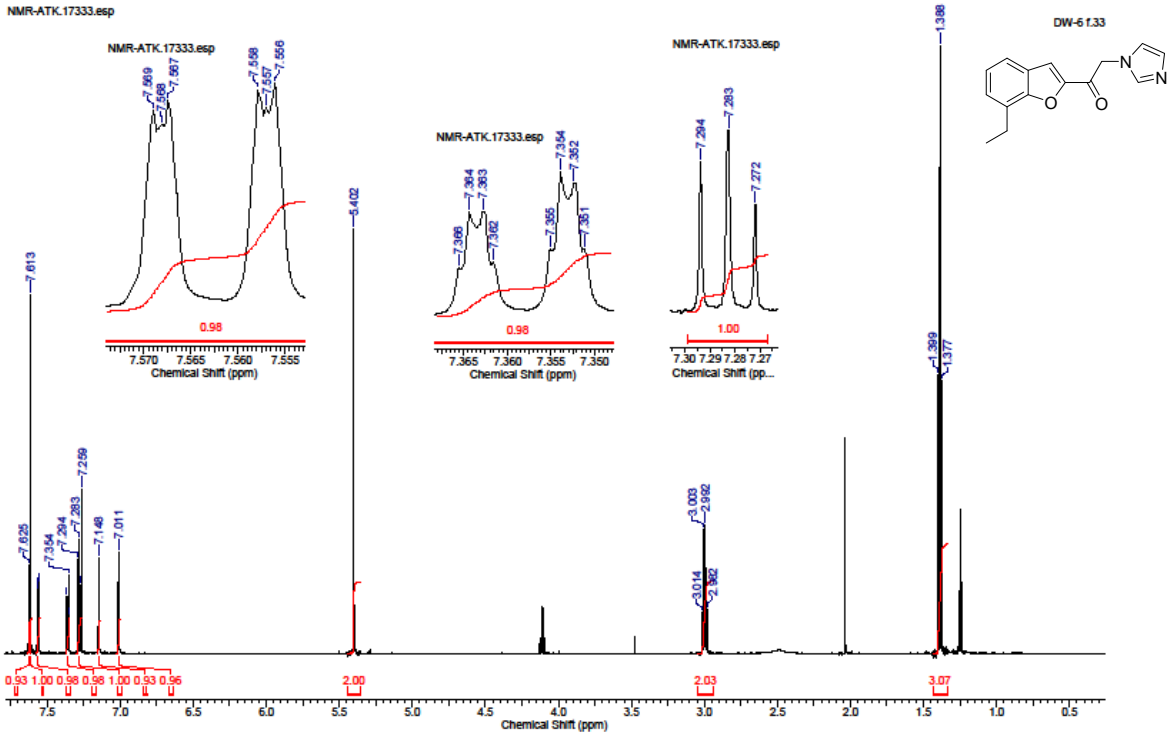


(**a**)

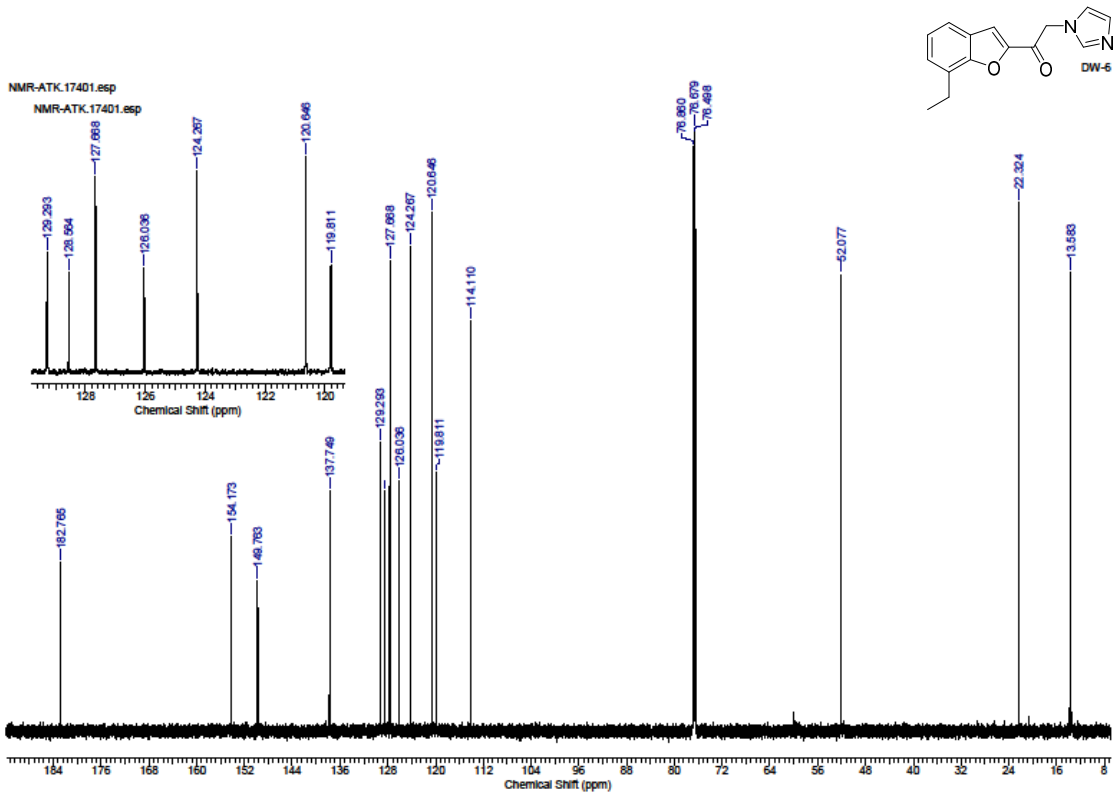


(**b**)

**Figure S2.** (**a**) $^{1}$H NMR and (**b**) $^{13}$C NMR spectra of 1-(7-ethylbenzofuran-2-yl)-2-(1*H*-imidazol-1-yl)ethanone (**6**).

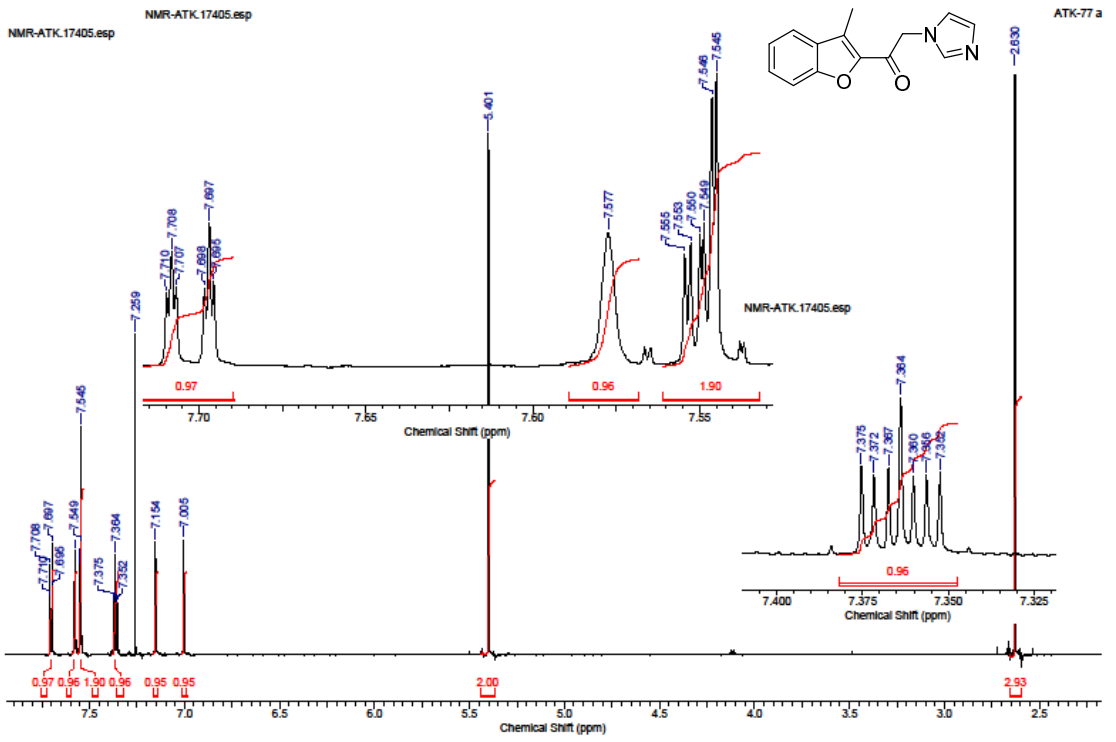

(**a**)

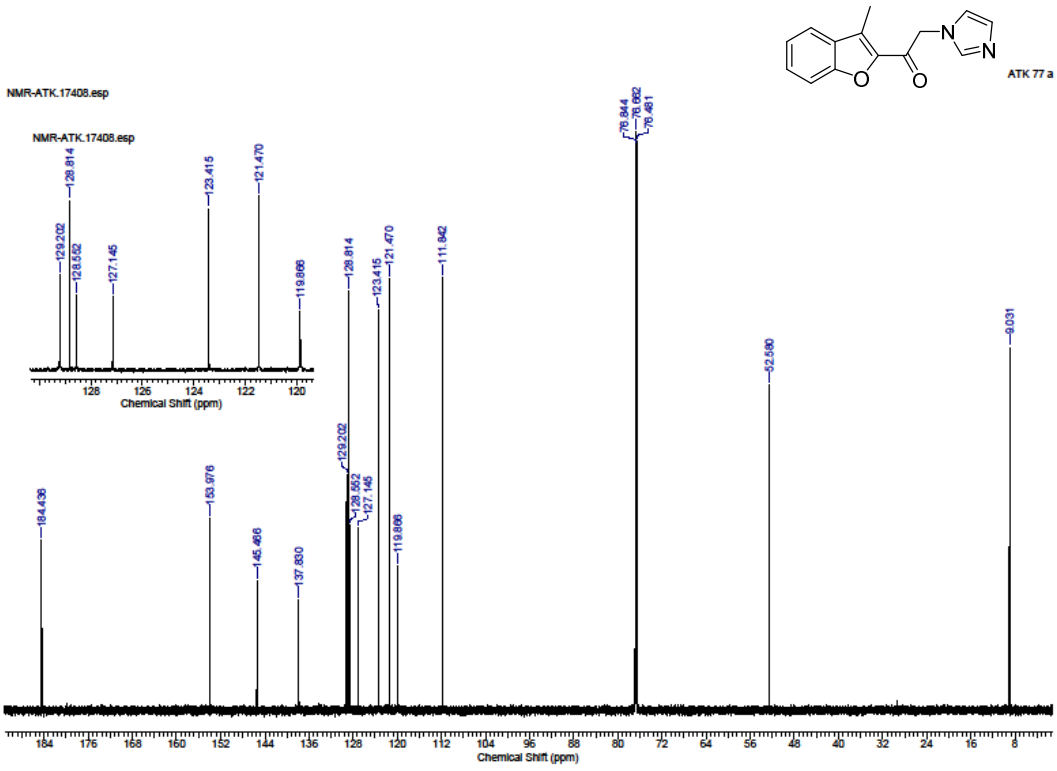


(**b**)

**Figure 3.** (**a**) $^{1}$H NMR and (**b**) $^{13}$C NMR spectra of 2-(1*H*-imidazol-1-yl)-1-(3-methylbenzofuran-2-yl)ethanone (**7**).

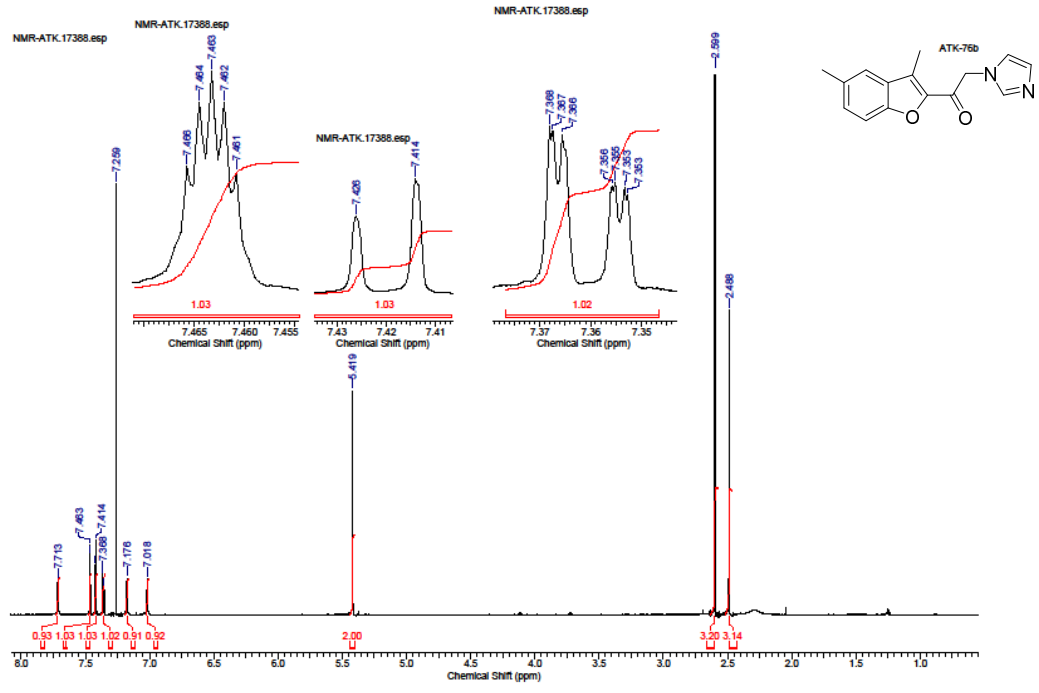


(**a**)

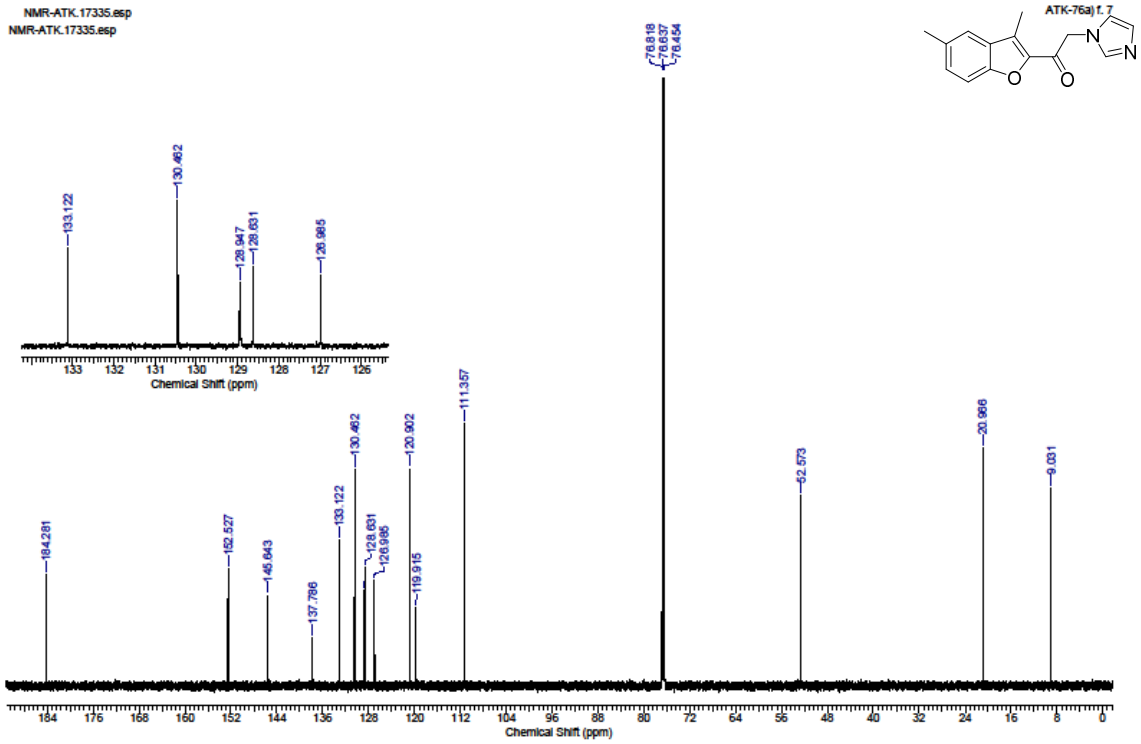


(**b**)

**Figure 4.** (a) $^{1}$H NMR and (**b**) $^{13}$C NMR spectra of 1-(3,5-dimethylbenzofuran-2-yl)-2-(1*H*-imidazol-1-yl)ethanone (**8**).

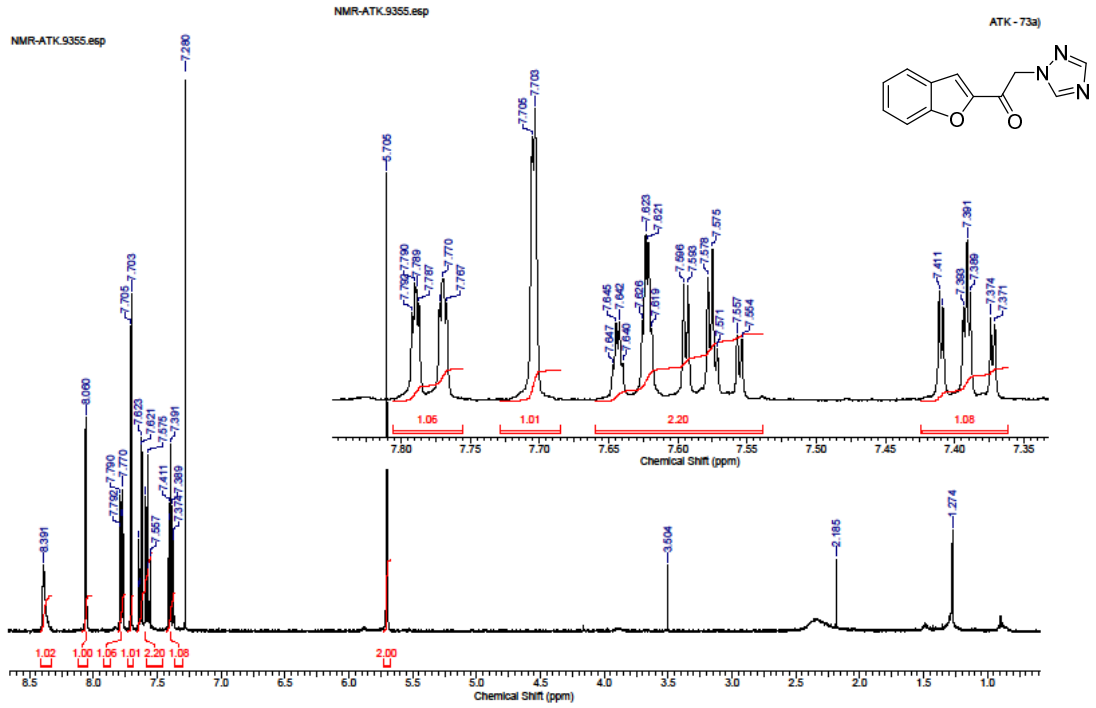


(**a**)

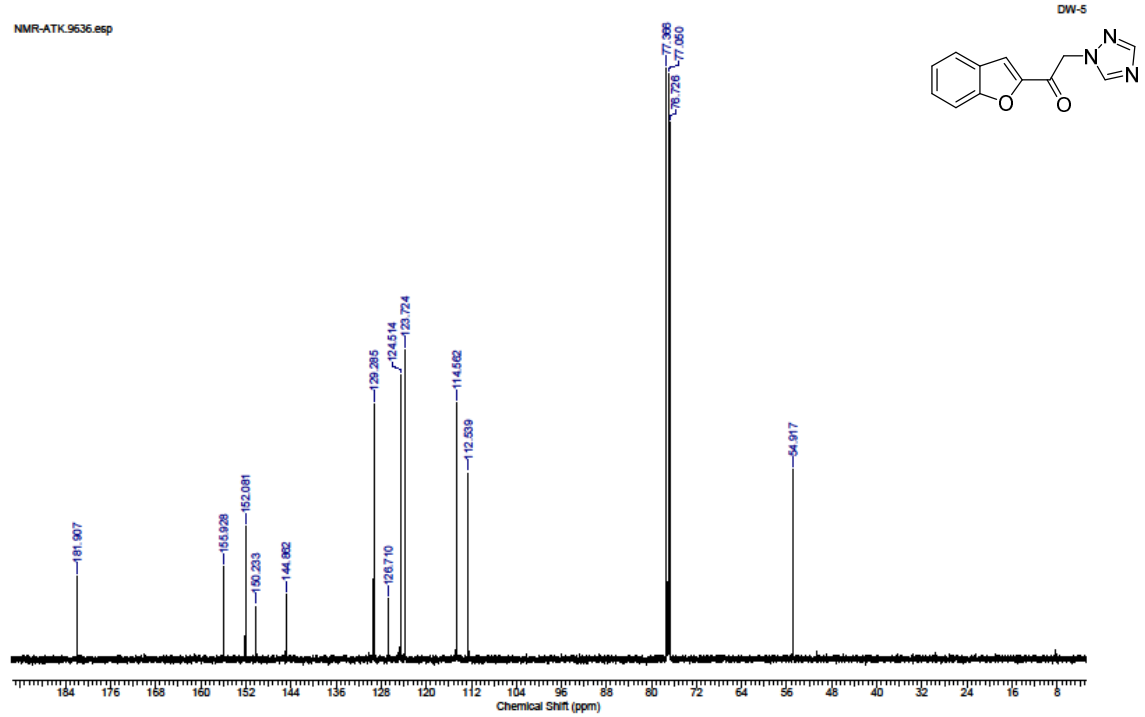


(**b**)

**Figure 5.** (**a**) $^{1}$H NMR and (**b**) $^{13}$C NMR spectra of 1-(benzofuran-2-yl)-2-(1*H*-1,2,4-triazol-1-yl)ethanone (**9**).

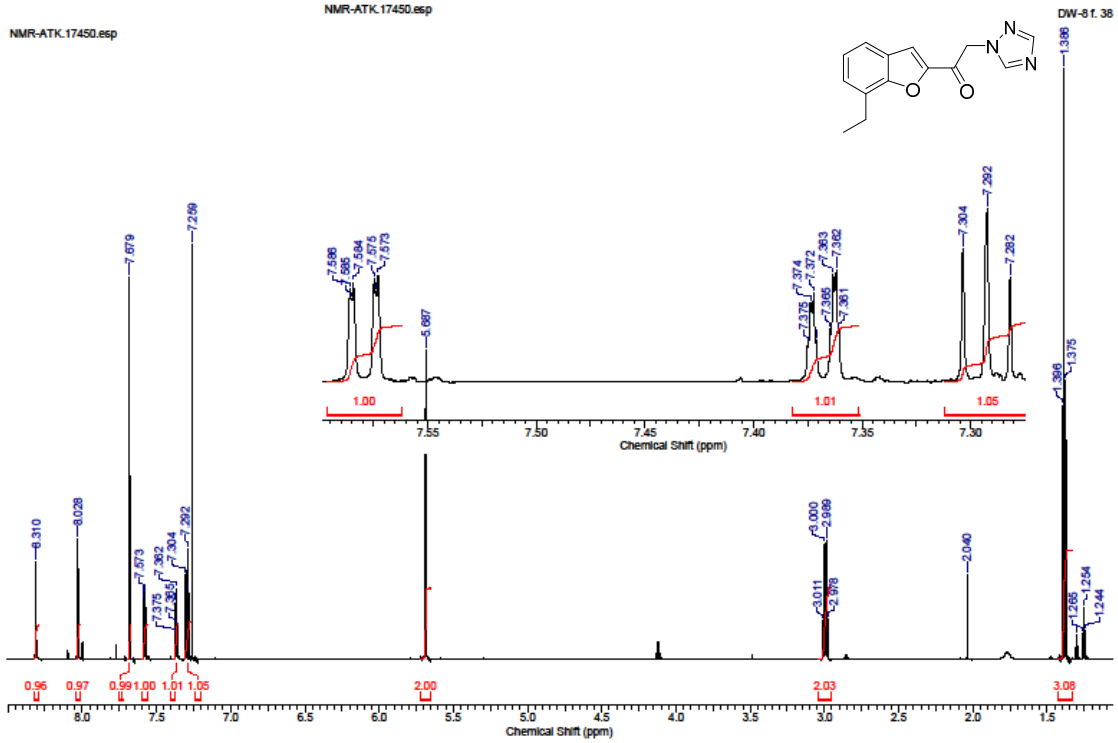


(**a**)

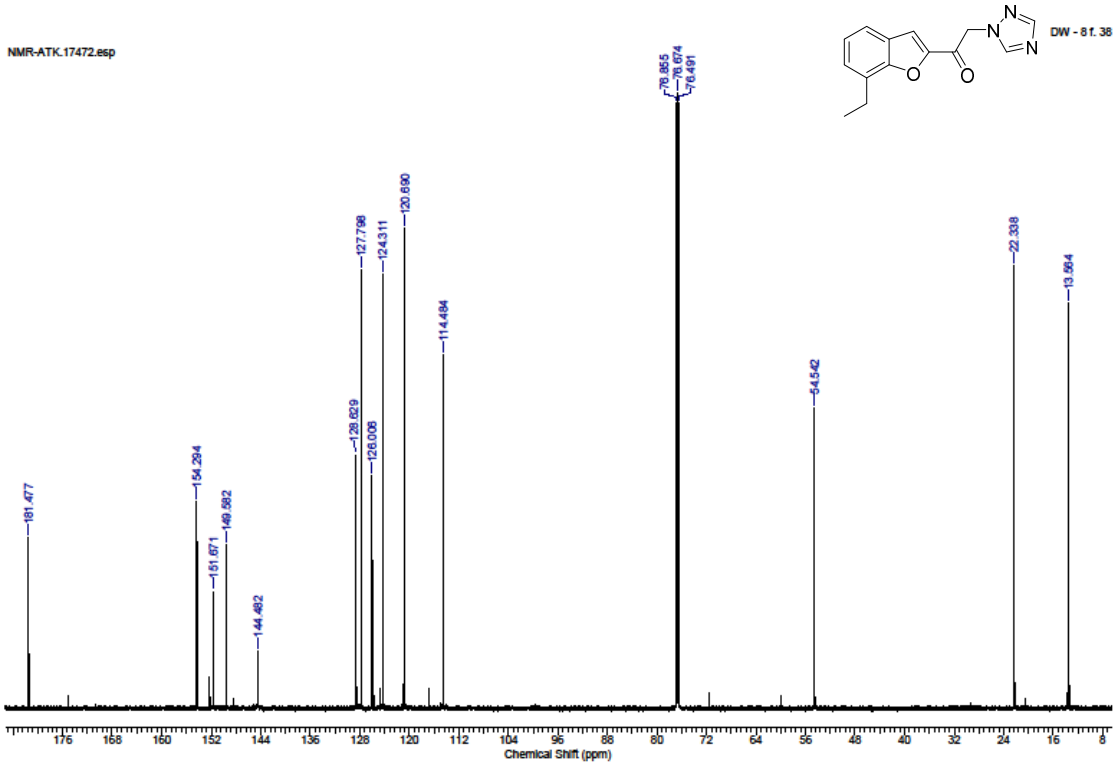


(**b**)

**Figure 6.** (**a**) $^{1}$H NMR and (**b**) $^{13}$C NMR spectra of 1-(7-ethylbenzofuran-2-yl)-2-(1*H*-1,2,4-triazol-1-yl)ethanone (**10**).

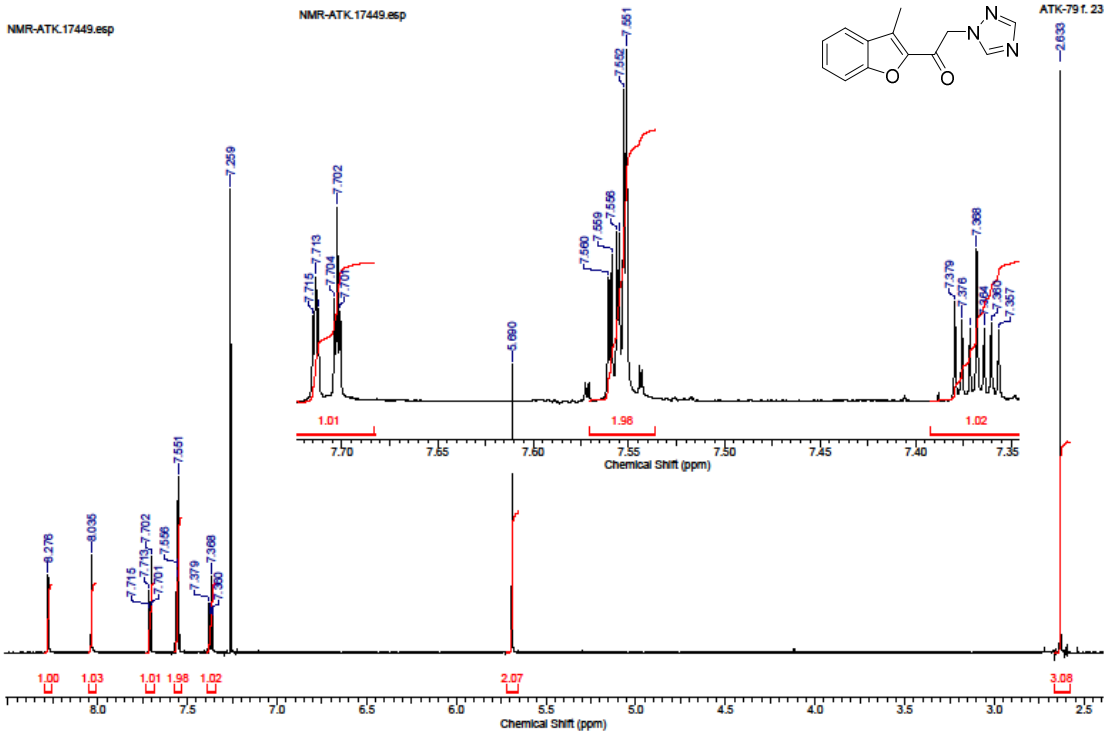


(**a**)

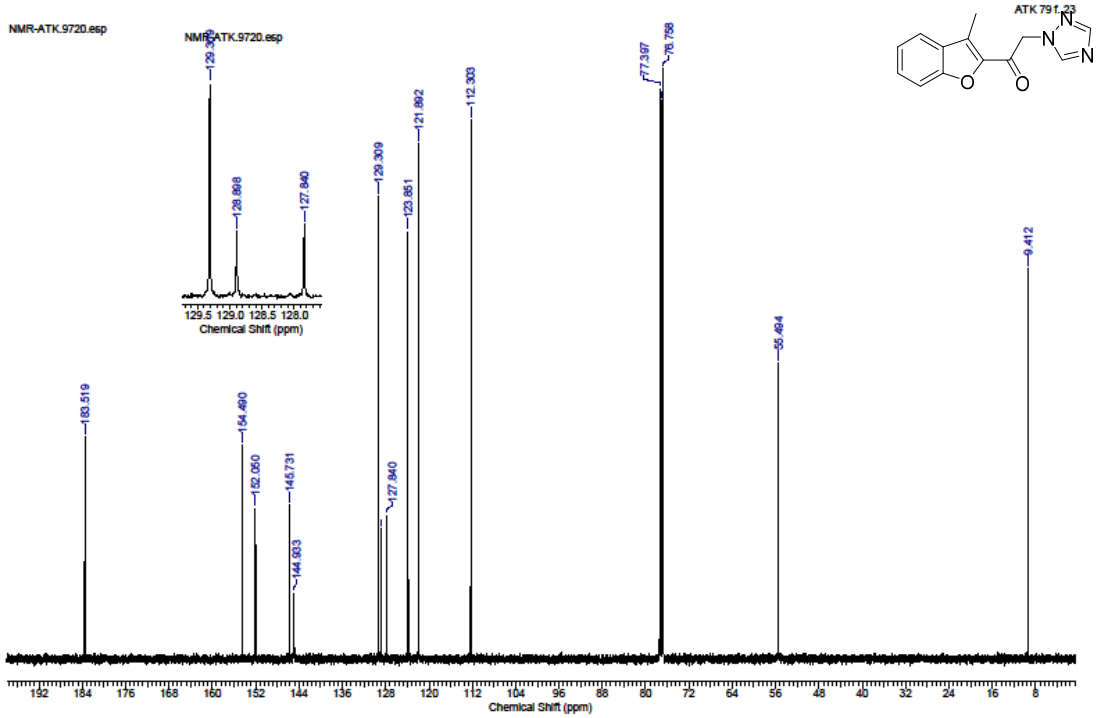


(**b**)

**Figure 7.** (**a**) $^{1}$H NMR and (**b**) $^{13}$C NMR spectra of 1-(3-methylbenzofuran-2-yl)-2-(1*H*-1,2,4-triazol-1-yl)ethanone (**11**).

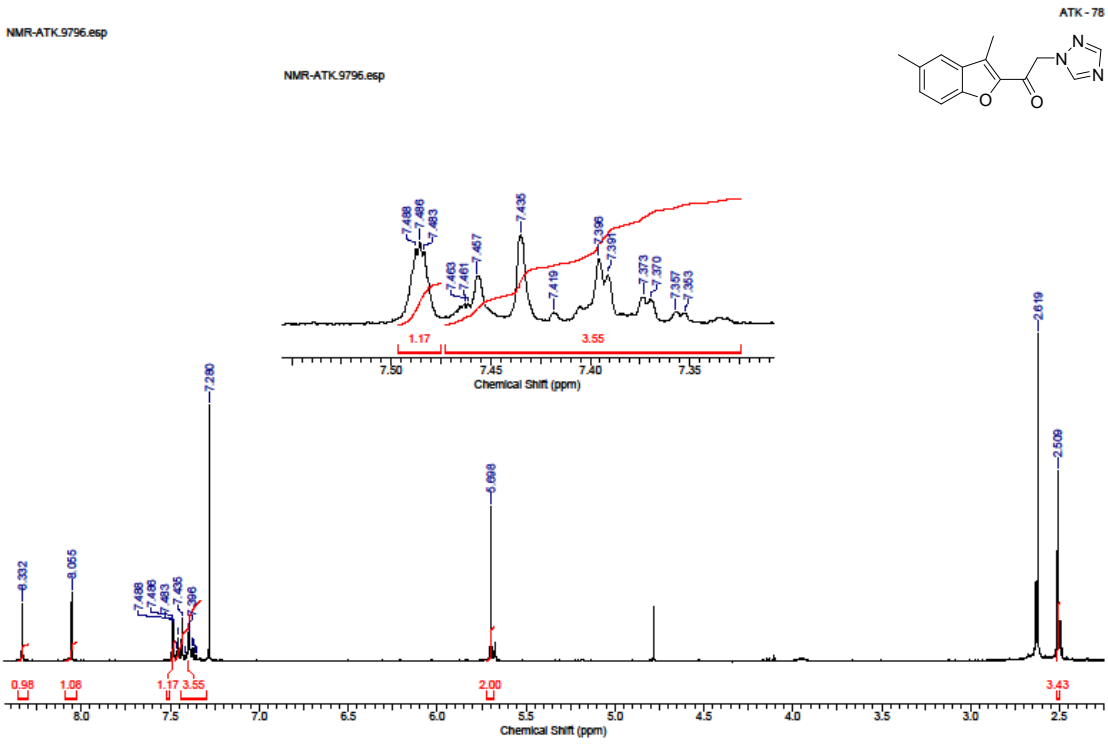


(**a**)

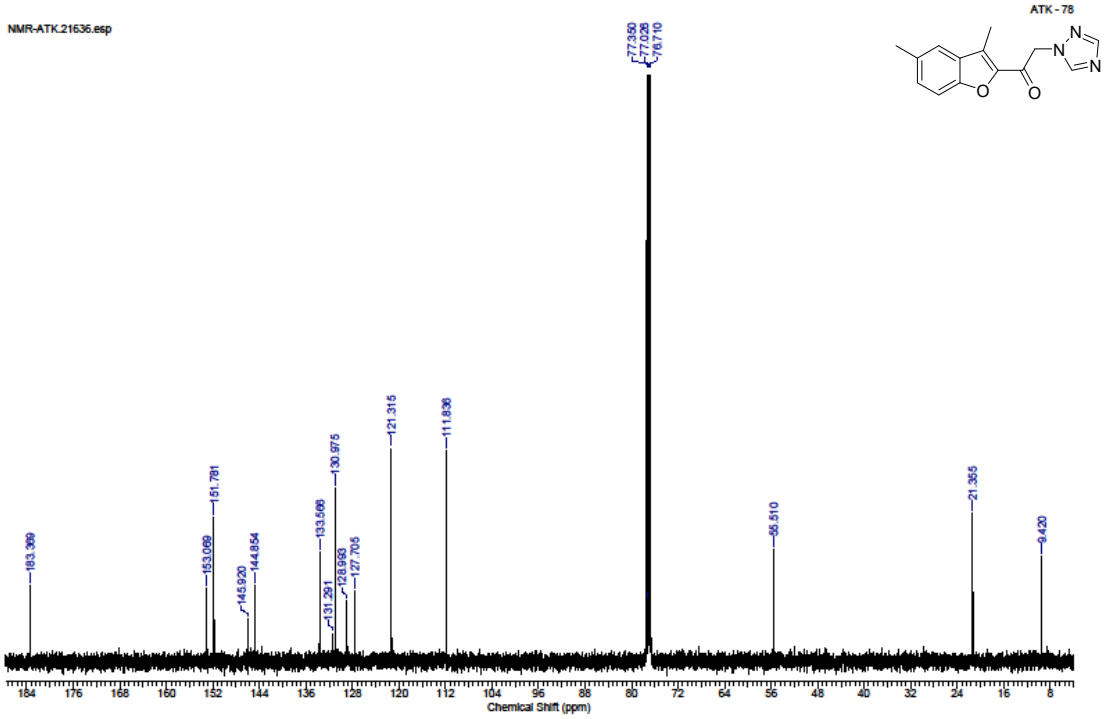


(**b**)

**Figure S8.** (**a**) $^{1}$H NMR and (**b**) $^{13}$C NMR spectra of 1-(3,5-dimethylbenzofuran-2-yl)-2-(1*H*-1,2,4-triazol-1-yl)ethanone (**12**).

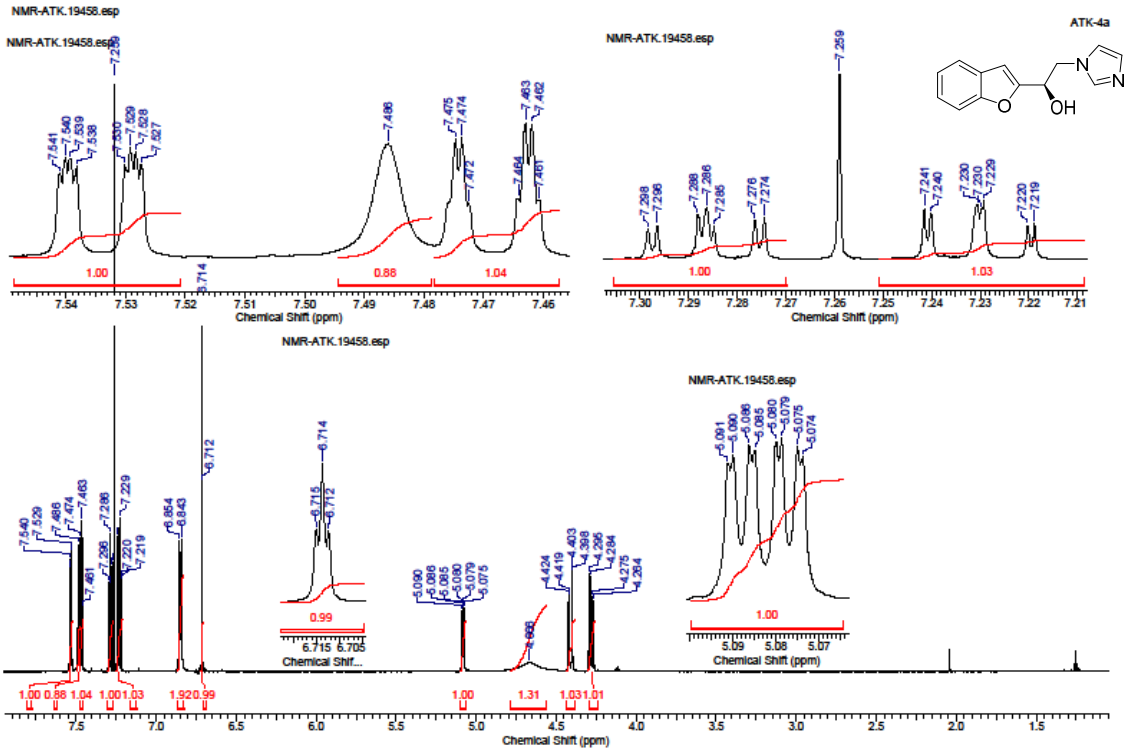


(**a**)

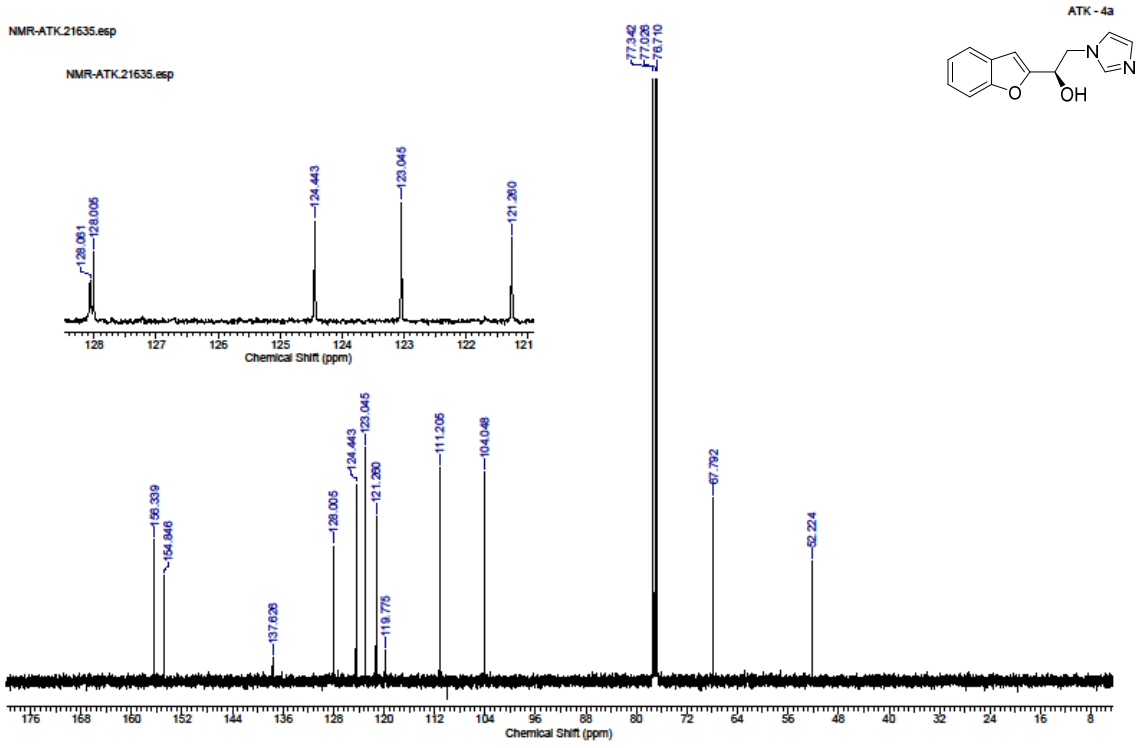


(**b**)

**Figure S9.** (**a**) $^{1}$H NMR and (**b**) $^{13}$C NMR spectra of (*R*)-1-(benzofuran-2-yl)-2-(1*H*-imidazol-1-yl)ethan-1-ol (**13**).

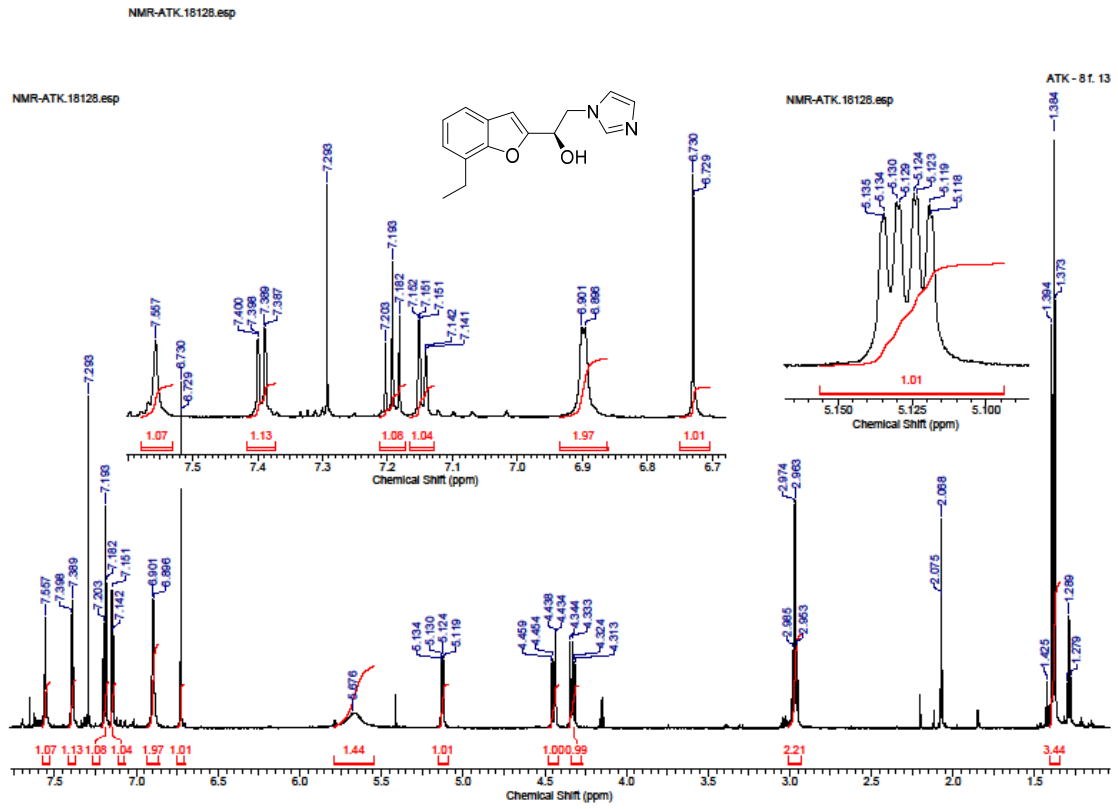


(**a**)

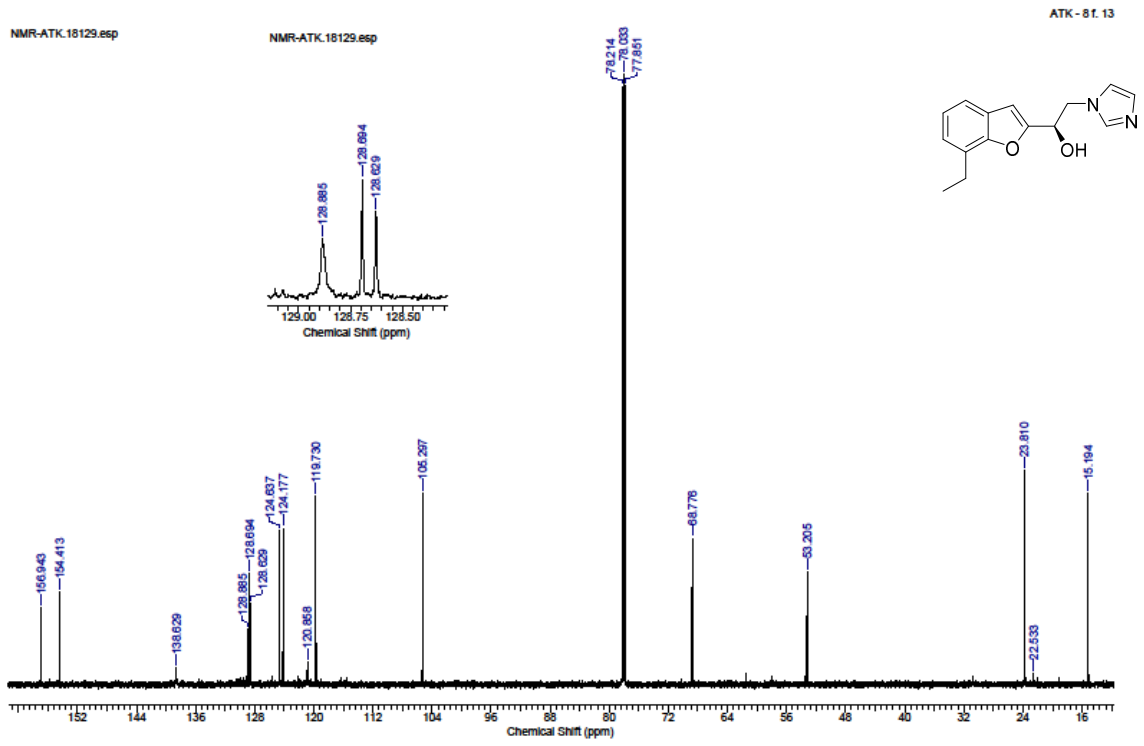


(**b**)

**Figure S10.** (**a**) $^{1}$H NMR and (**b**) $^{13}$C NMR spectra of (*R*)-1-(7-ethylbenzofuran-2-yl)-2-(1*H*-imidazol-1-yl)ethan-1-ol (**14**).

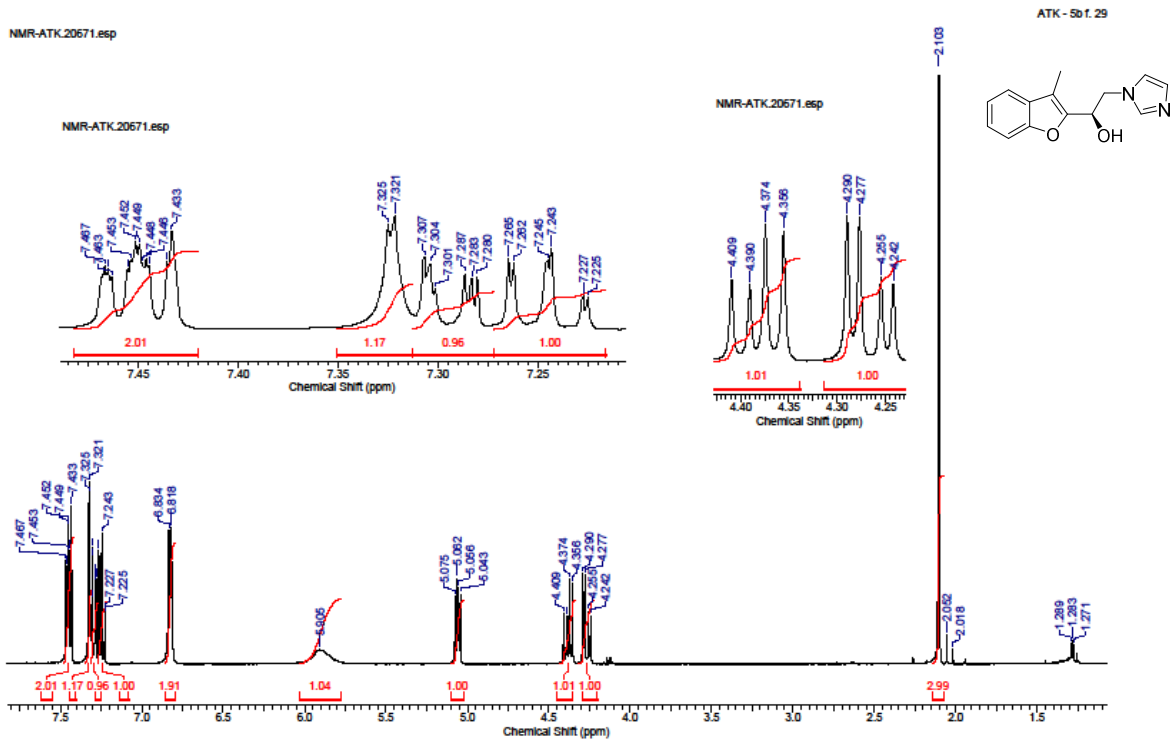


(**a**)

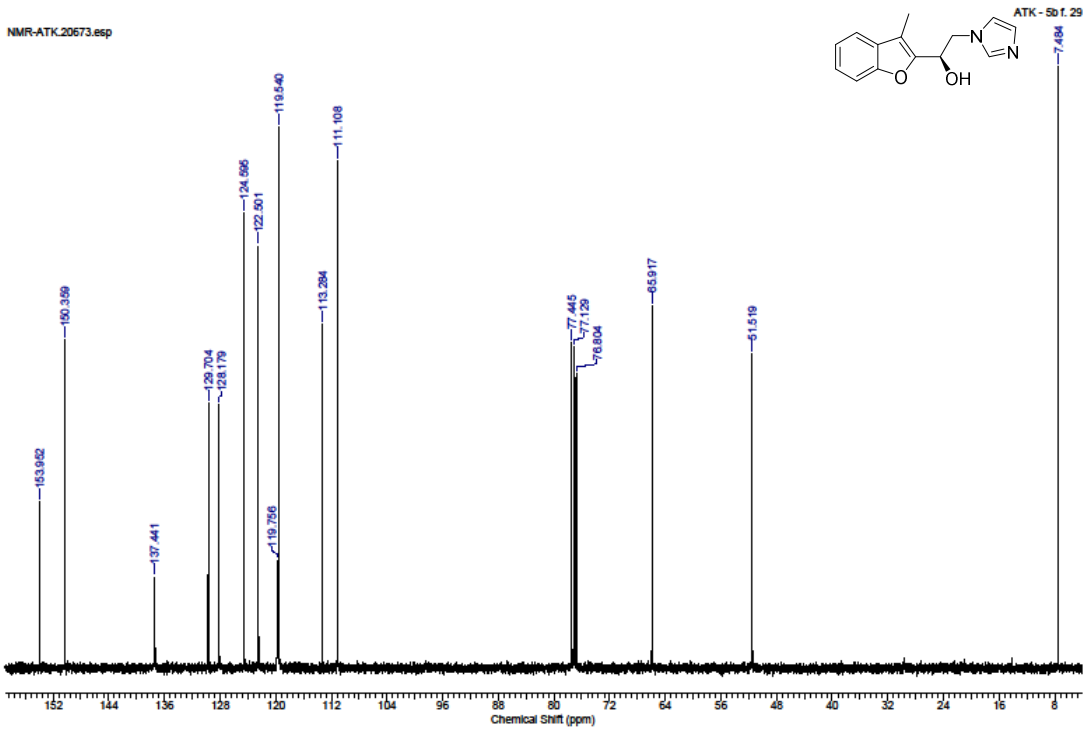


(**b**)

**Figure S11.** (**a**) $^{1}$H NMR and (**b**) $^{13}$C NMR spectra of (*R*)-2-(1*H*-imidazol-1-yl)-1-(3-methylbenzofuran-2-yl)ethan-1-ol (**15**).

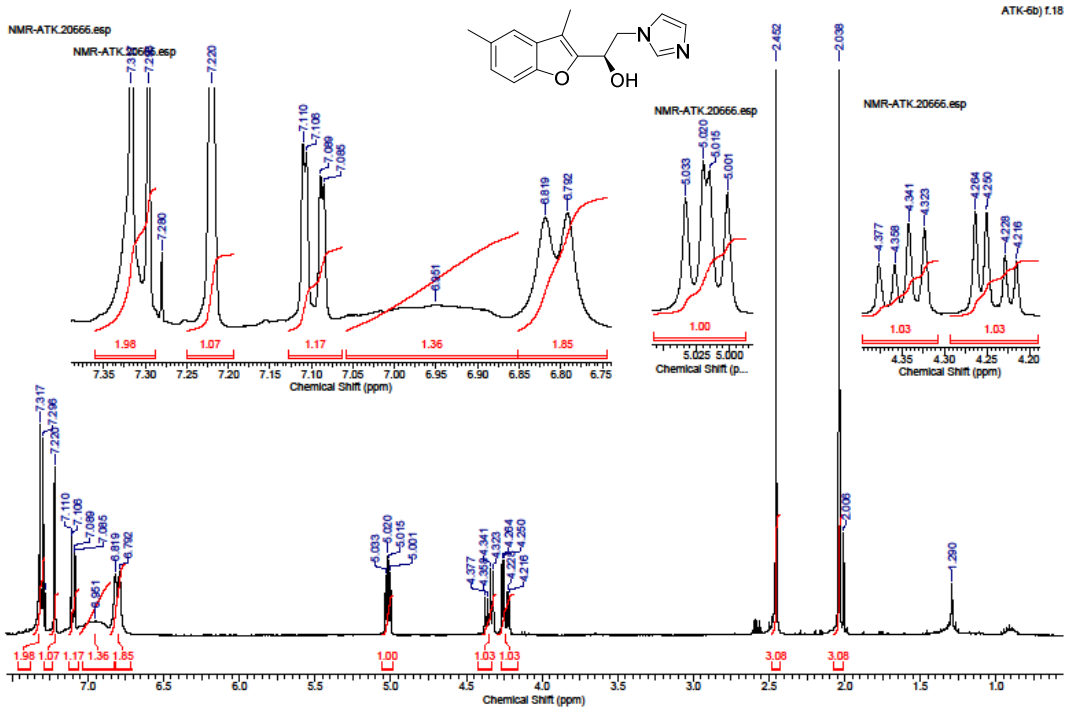


(**a**)

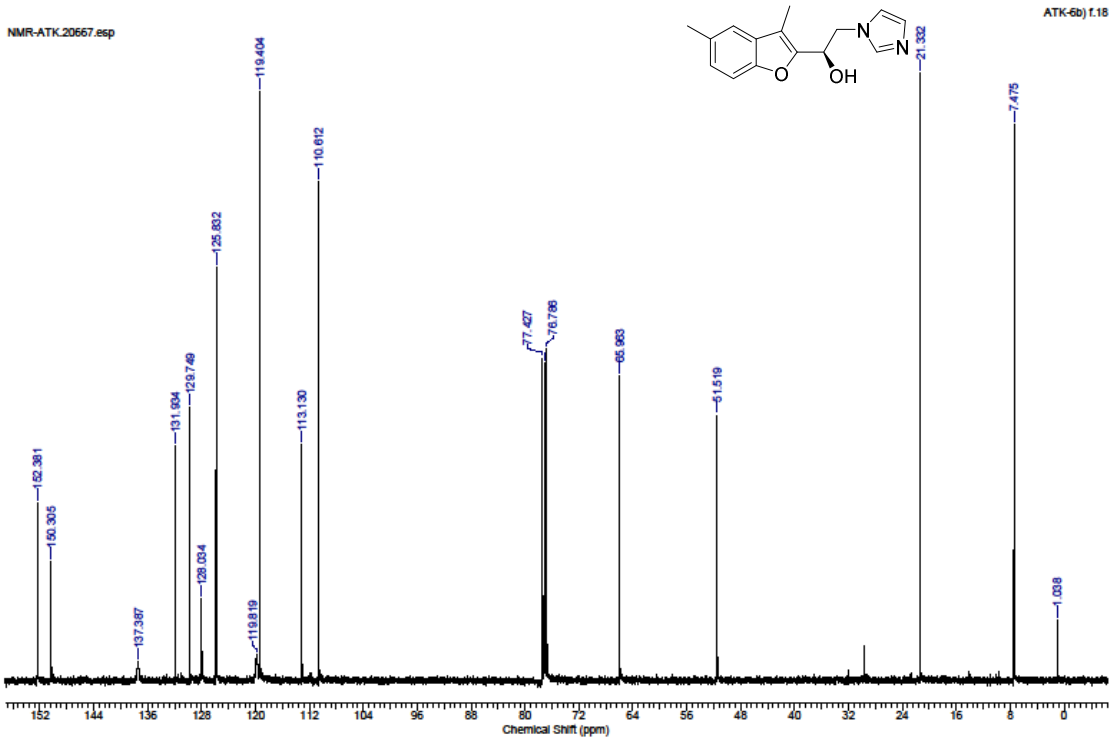


(**b**)

**Figure 12.** (**a**) $^{1}$H NMR and (**b**) $^{13}$C NMR spectra of (*R*)-1-(3,5-dimethylbenzofuran-2-yl)-2-(1*H*-imidazol-1-yl)ethan-1-ol (**16**).

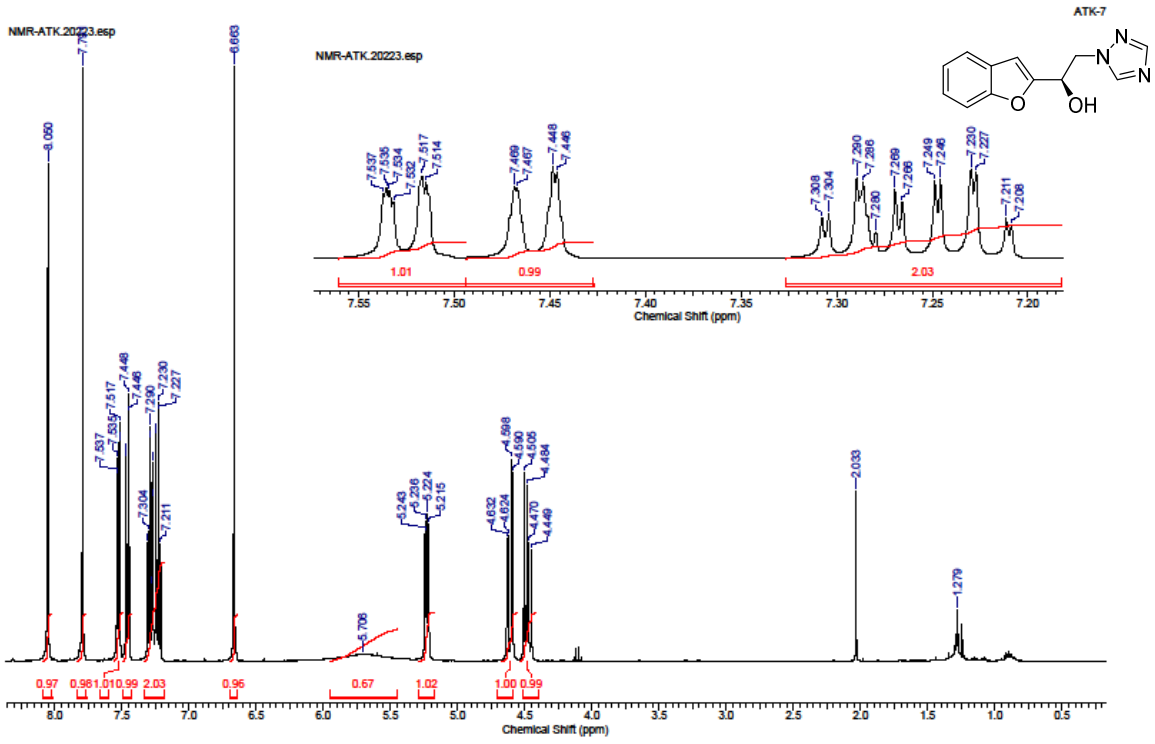


(**a**)

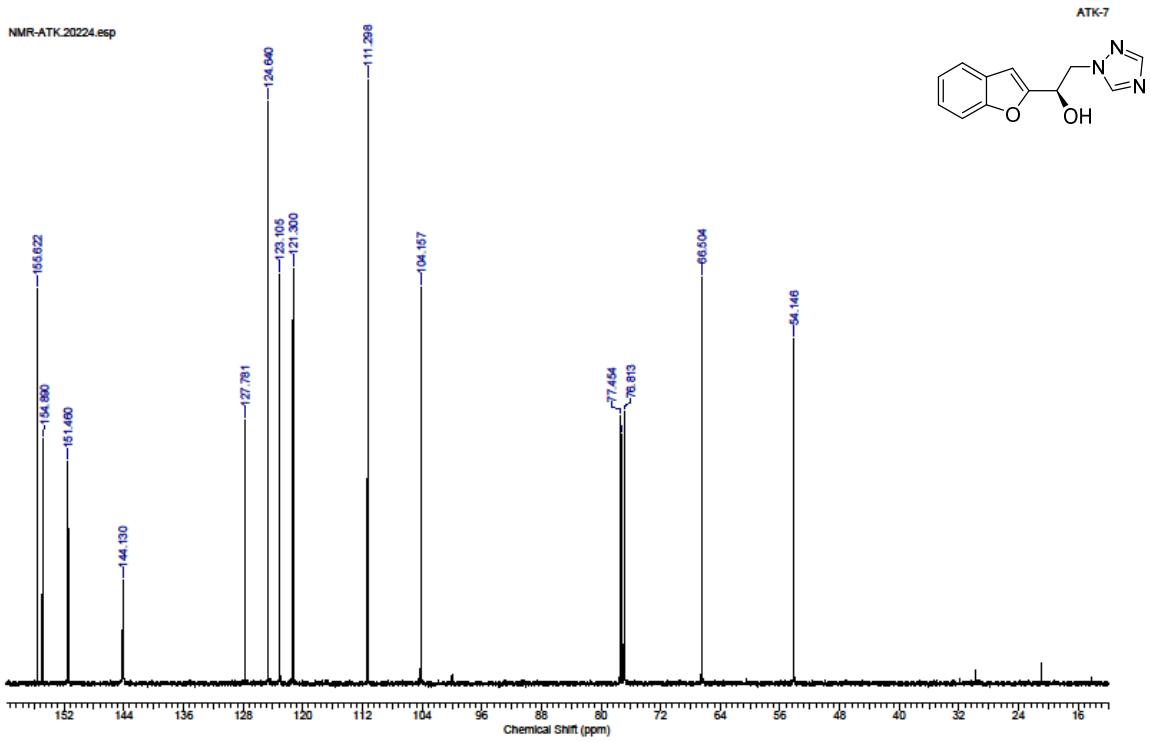


(**b**)

**Figure 13.** (**a**) $^{1}$H NMR and (**b**) $^{13}$C NMR spectra of (*R*)-1-(benzofuran-2-yl)-2-(1*H*-1,2,4-triazol-1-yl)ethan-1-ol (**17**).

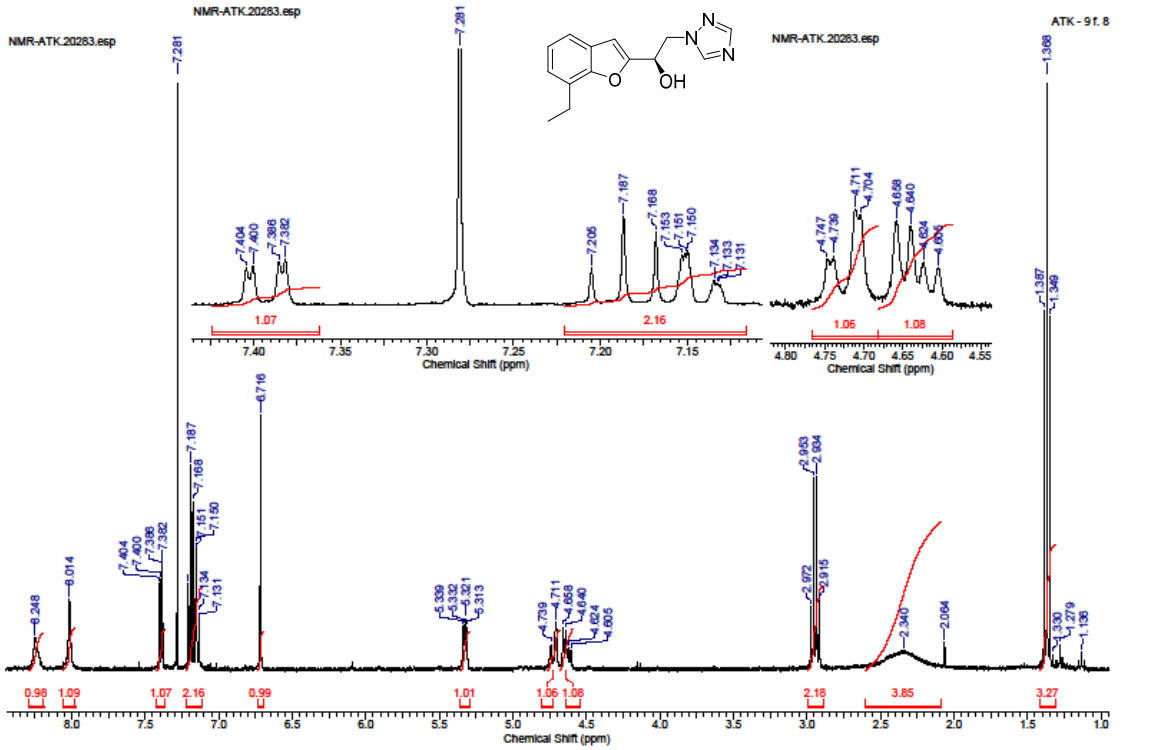

(**a**)

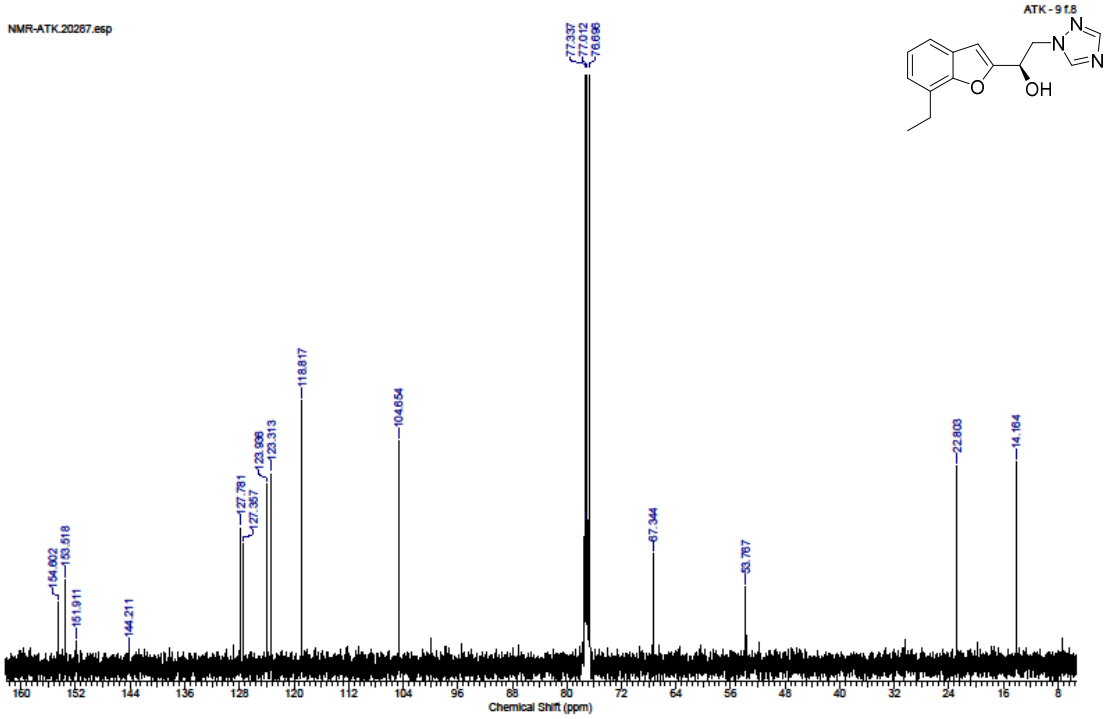


(**b**)

**Figure 14.** (**a**) $^{1}$H NMR and (**b**) $^{13}$C NMR spectra of (*R*)-1-(7-ethylbenzofuran-2-yl)-2-(1*H*-1,2,4-triazol-1-yl)ethan-1-ol (**18**).

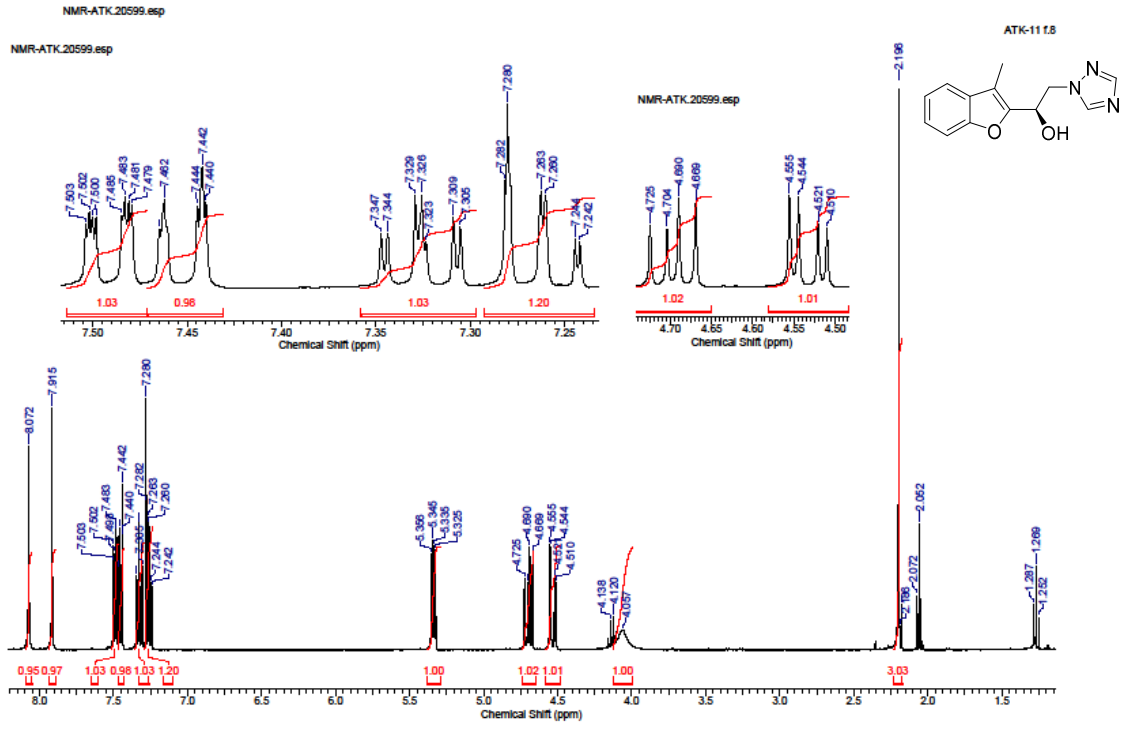

(**a**)

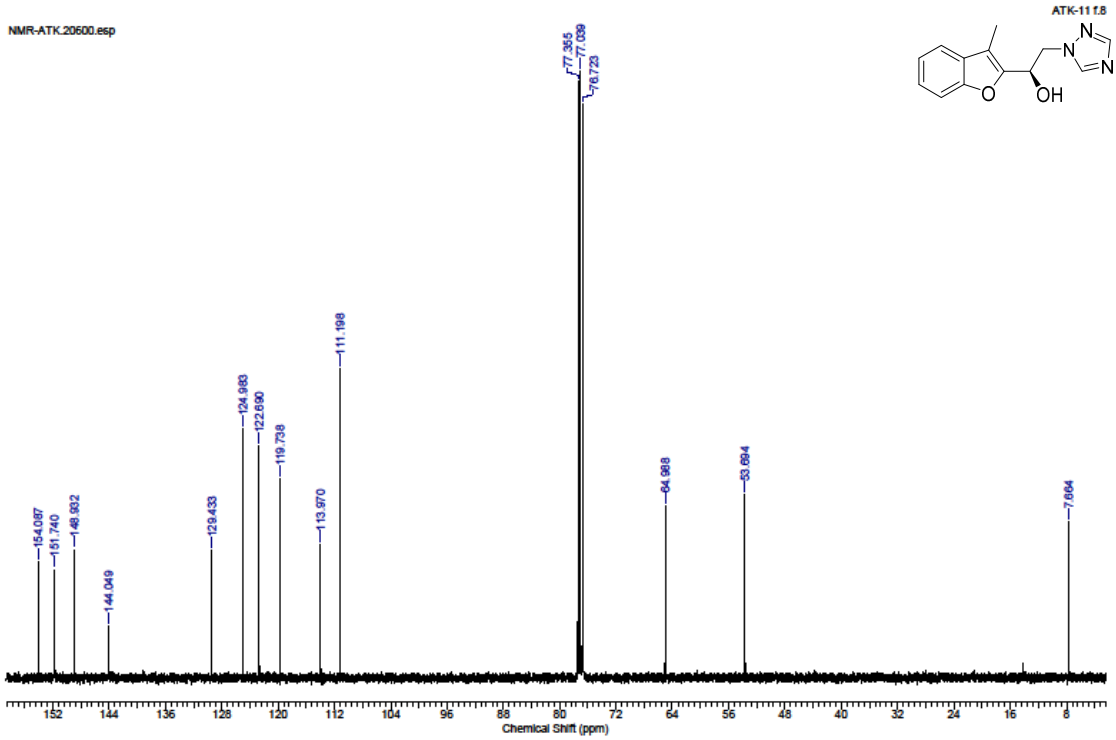


(**b**)

**Figure 15.** (**a**) $^{1}$H NMR and (**b**) $^{13}$C NMR spectra of (*R*)-1-(3-methylbenzofuran-2-yl)-2-(1*H*-1,2,4-triazol-1-yl)ethan-1-ol (**19**).

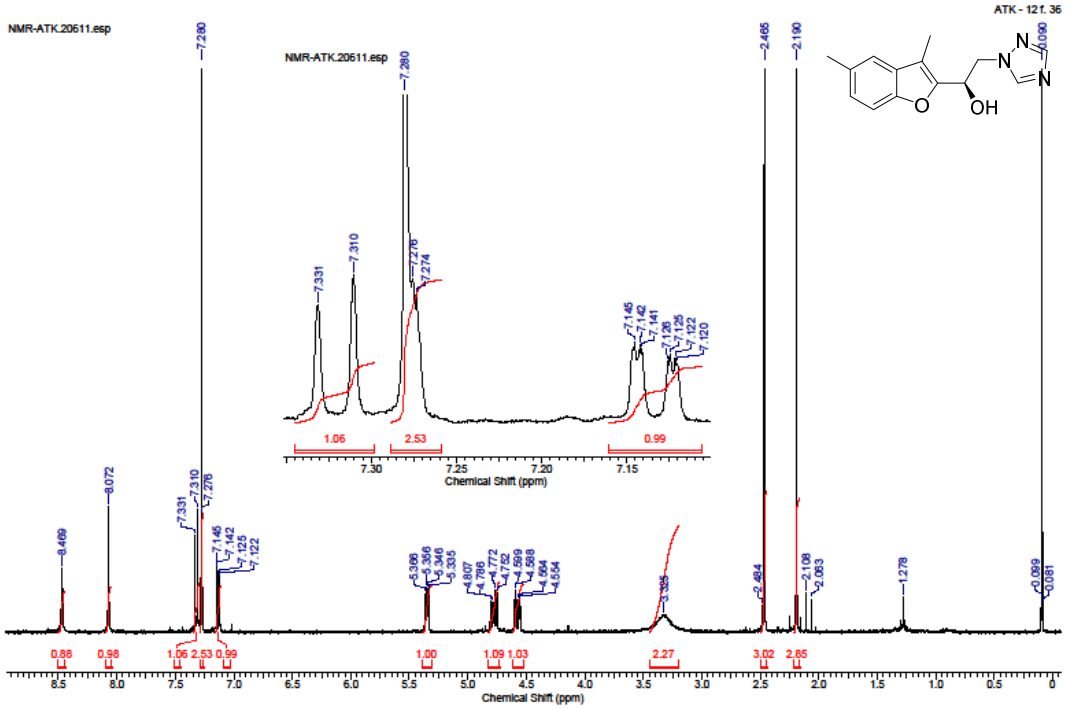

(**a**)

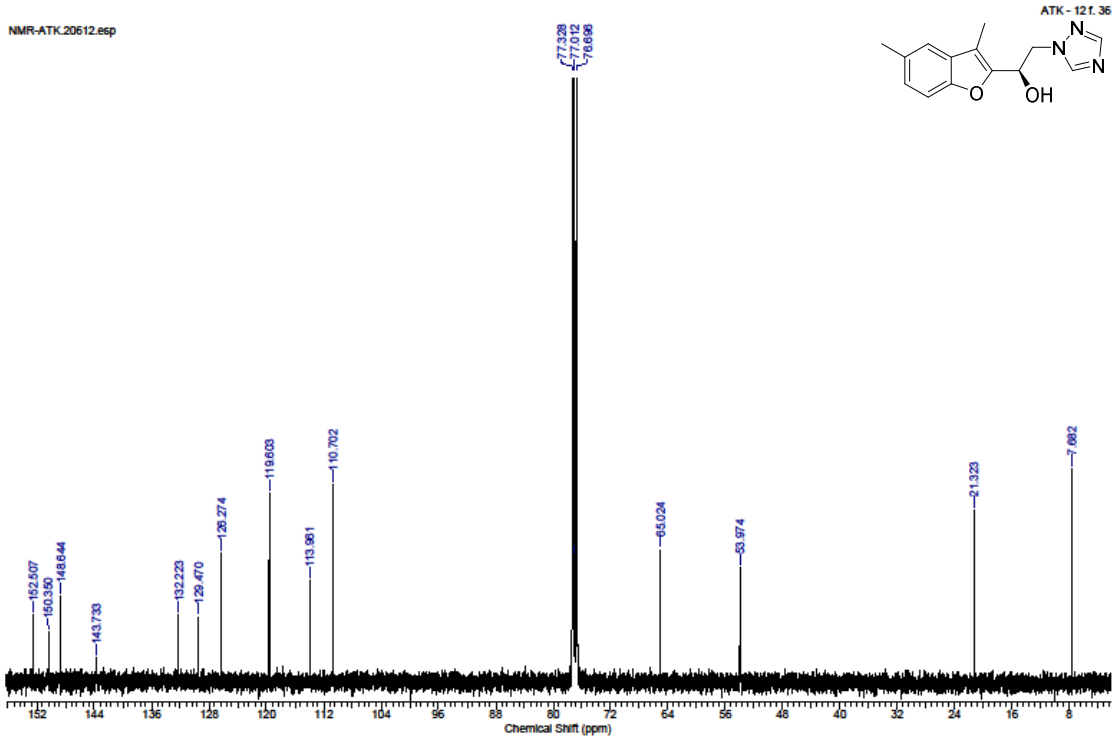


(**b**)

**Figure 16.** (**a**) $^{1}$H NMR and (**b**) $^{13}$C NMR spectra of (*R*)-1-(3,5-dimethylbenzofuran-2-yl)-2-(1H-1,2,4-triazol-1-yl)ethan-1-ol (**20**).

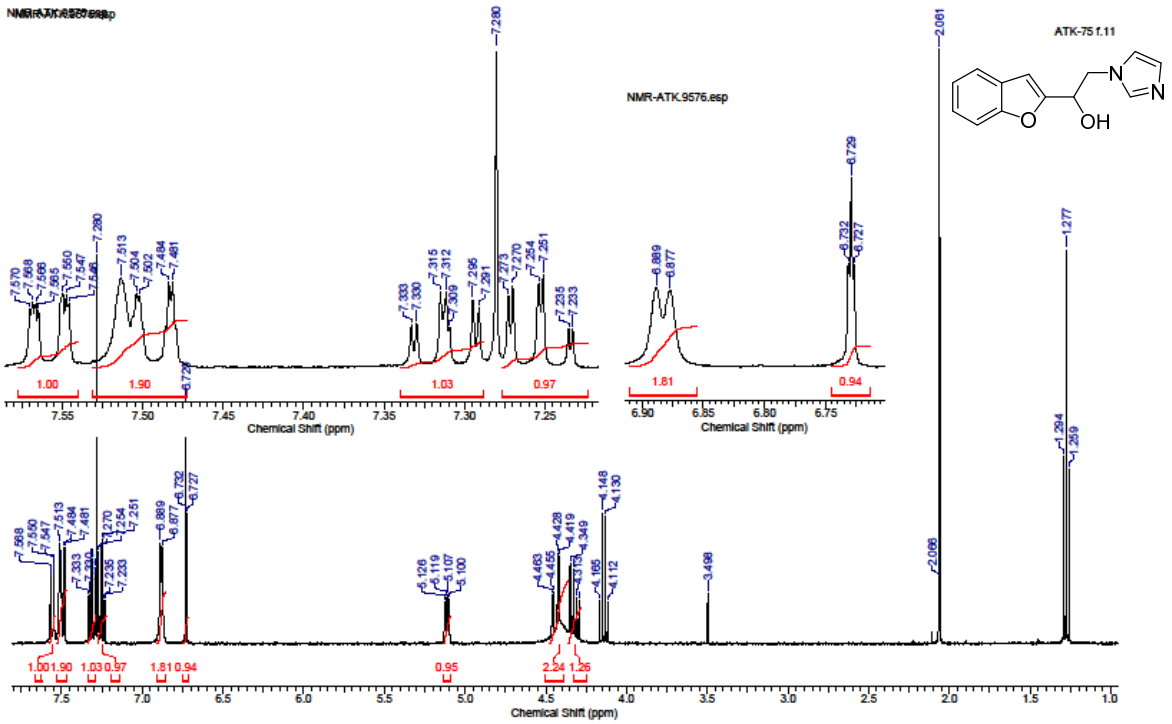
NMR-ATK.9576.esp
ATK-75 f.11
Chemical Shift (ppm)

(**a**)

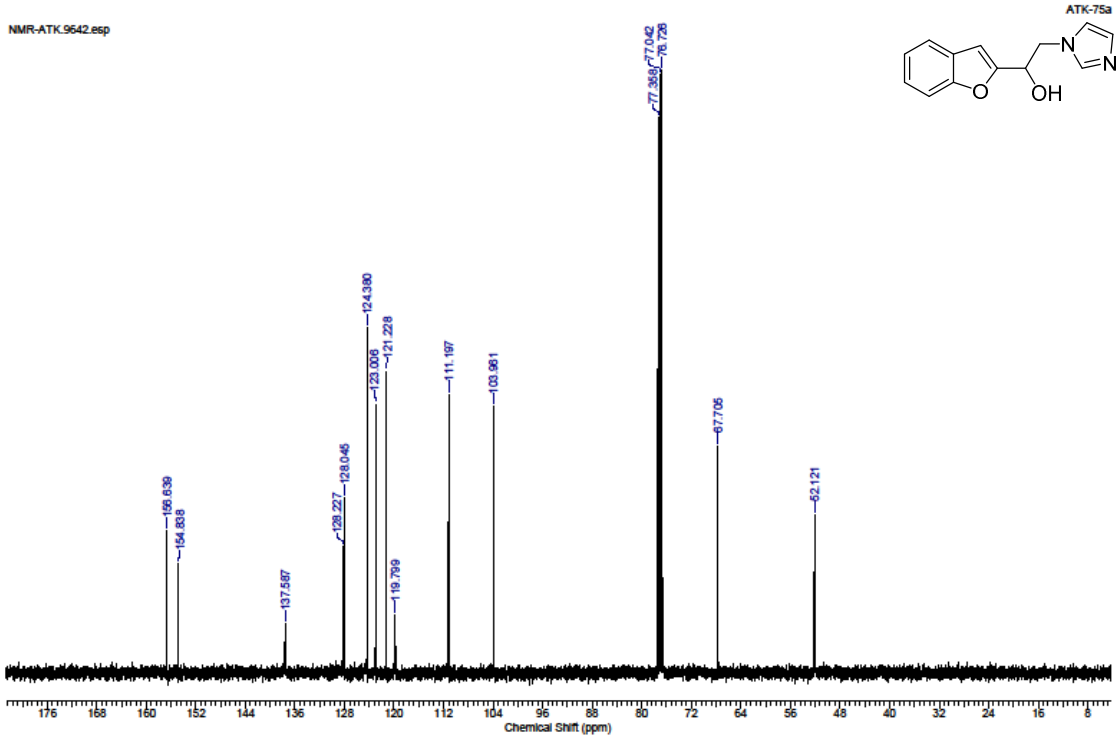
NMR-ATK.9642.esp
ATK-75a
Chemical Shift (ppm)

(**b**)

**Figure 17.** (**a**) $^{1}$H NMR and (**b**) $^{13}$C NMR spectra of 1-(benzofuran-2-yl)-2-(1*H*-imidazol-1-yl)ethan-1-ol (**21**).

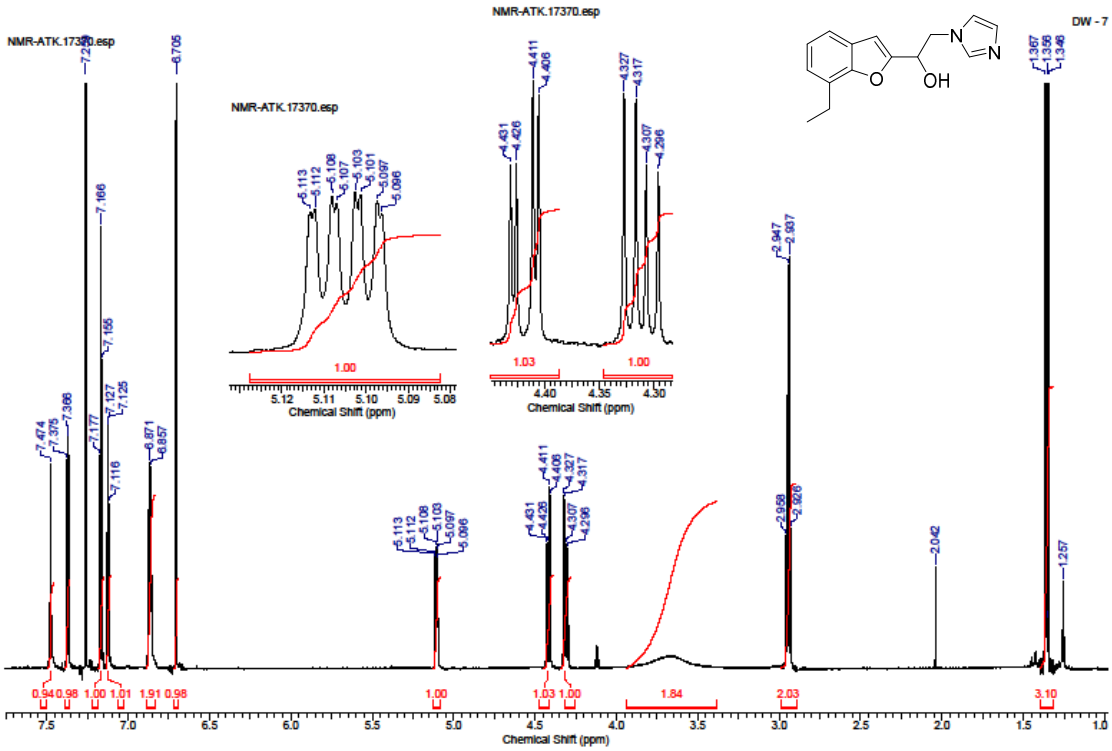


(**a**)

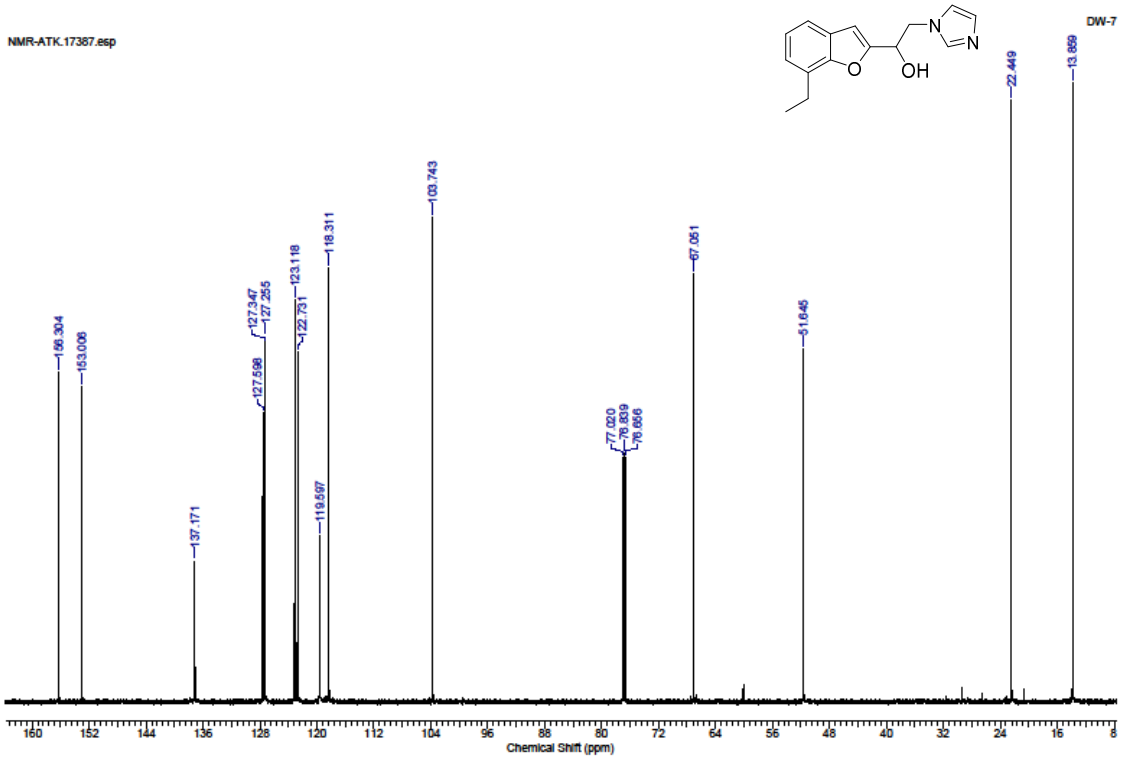

(**b**)

**Figure 18.** (**a**) $^{1}$H NMR and (**b**) $^{13}$C NMR spectra of 1-(7-ethylbenzofuran-2-yl)-2-(1*H*-imidazol-1-yl)ethan-1-ol (**22**).

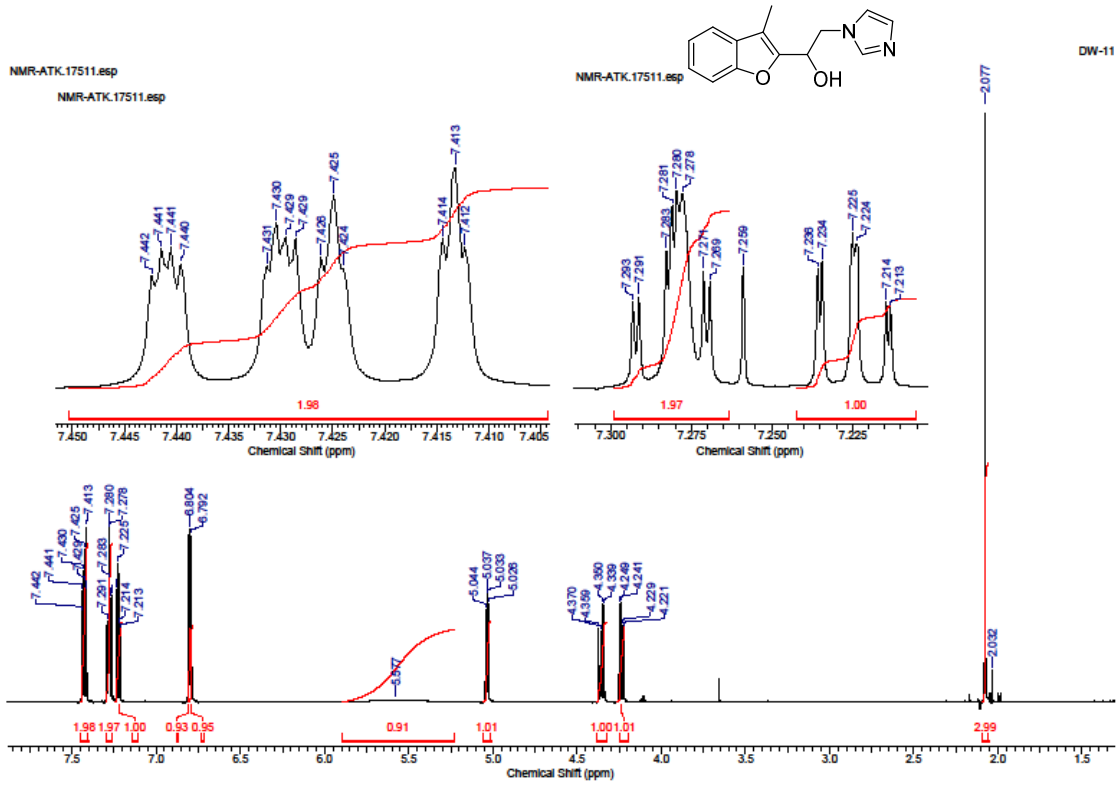


.

(**a**)

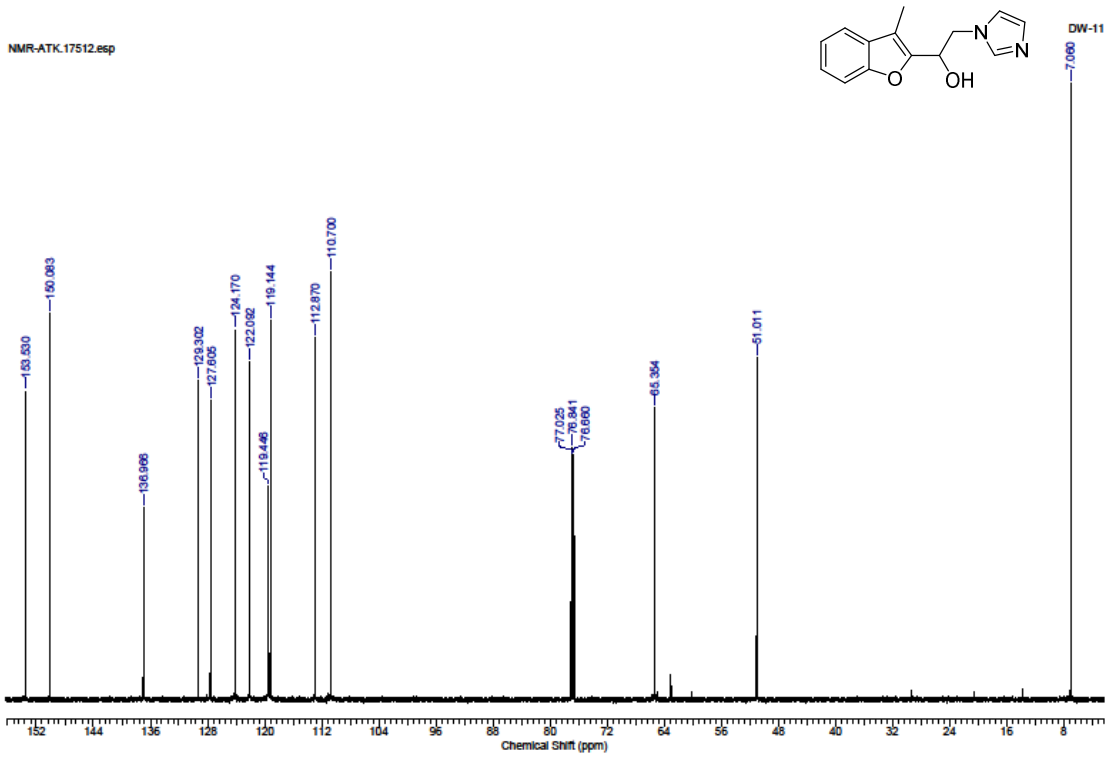


(**b**)

**Figure S19.** (**a**) $^{1}$H NMR and (**b**) $^{13}$C NMR spectra of 2-(1*H*-imidazol-1-yl)-1-(3-methylbenzofuran-2-yl)ethan-1-ol (**23**).

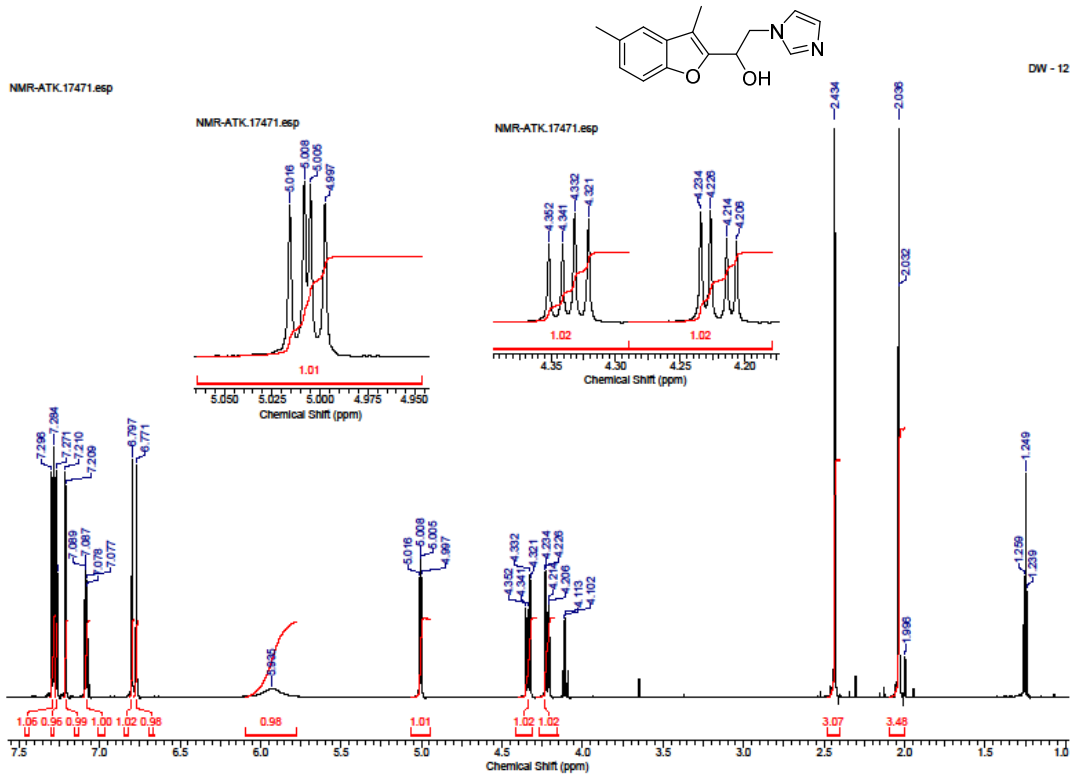

(**a**)

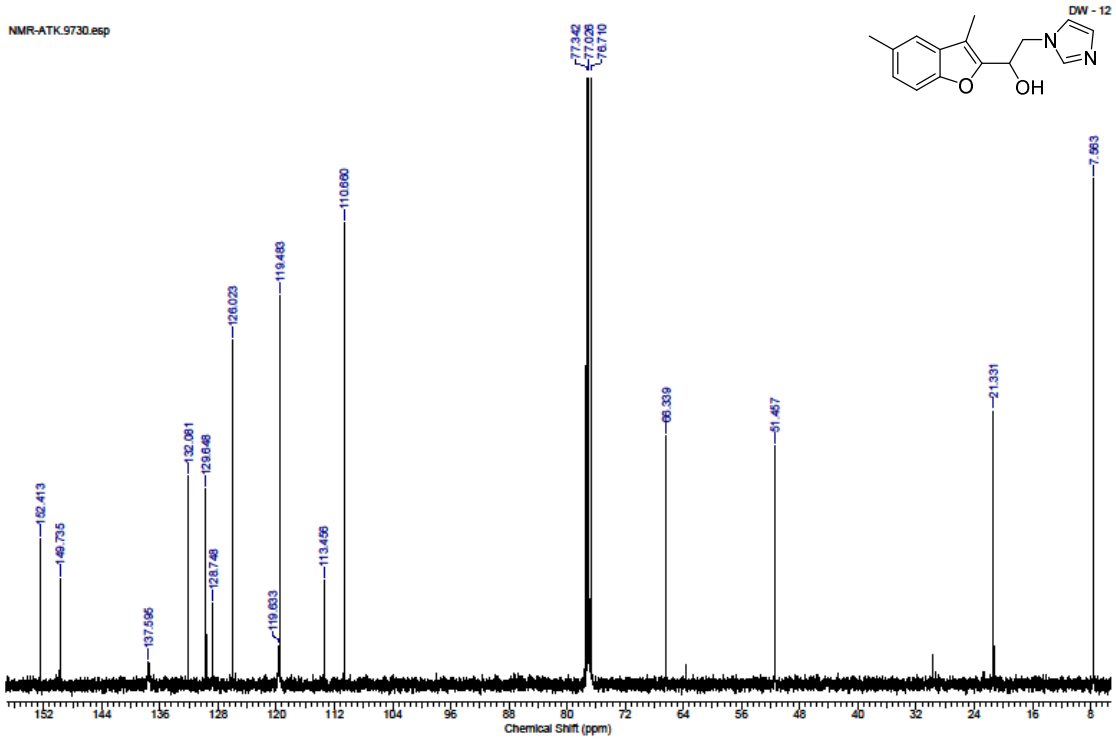


(**b**)

**Figure 20.** (a) $^{1}$H NMR and (b) $^{13}$C NMR spectra of 1-(3,5-dimethylbenzofuran-2-yl)-2-(1*H*-imidazol-1-yl)ethan-1-ol (24).

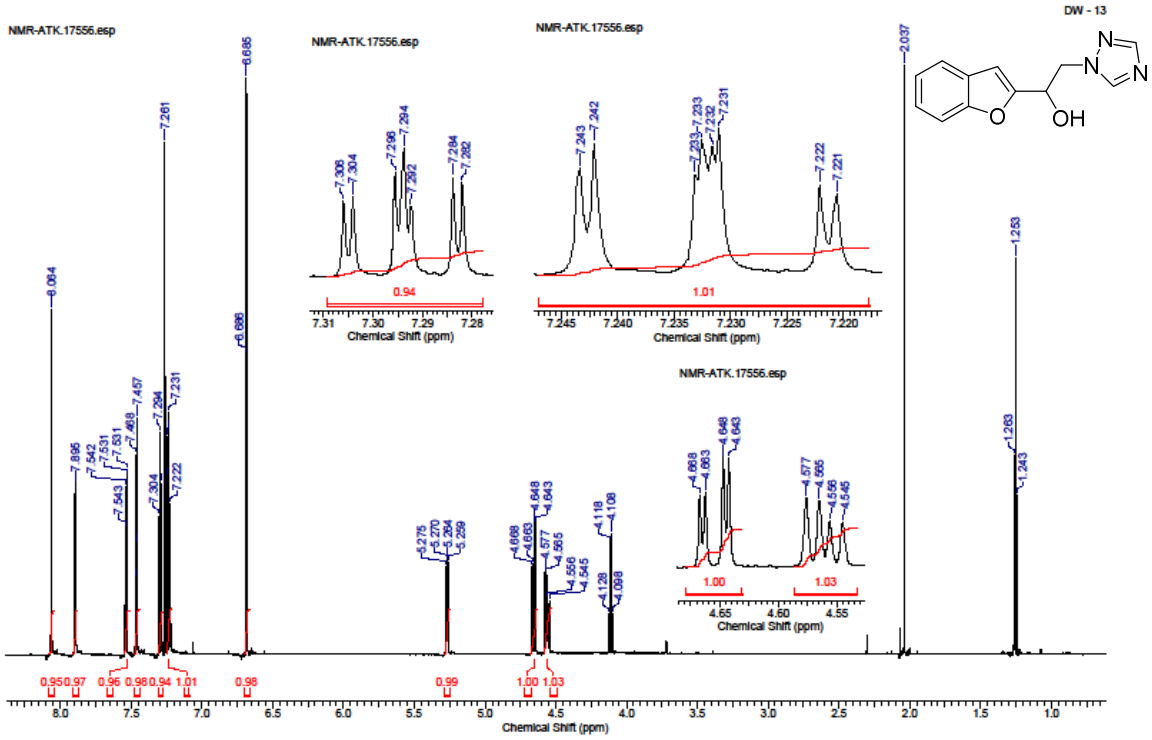
NMR-ATK.17556.esp
DW - 13
Chemical Shift (ppm)

(**a**)

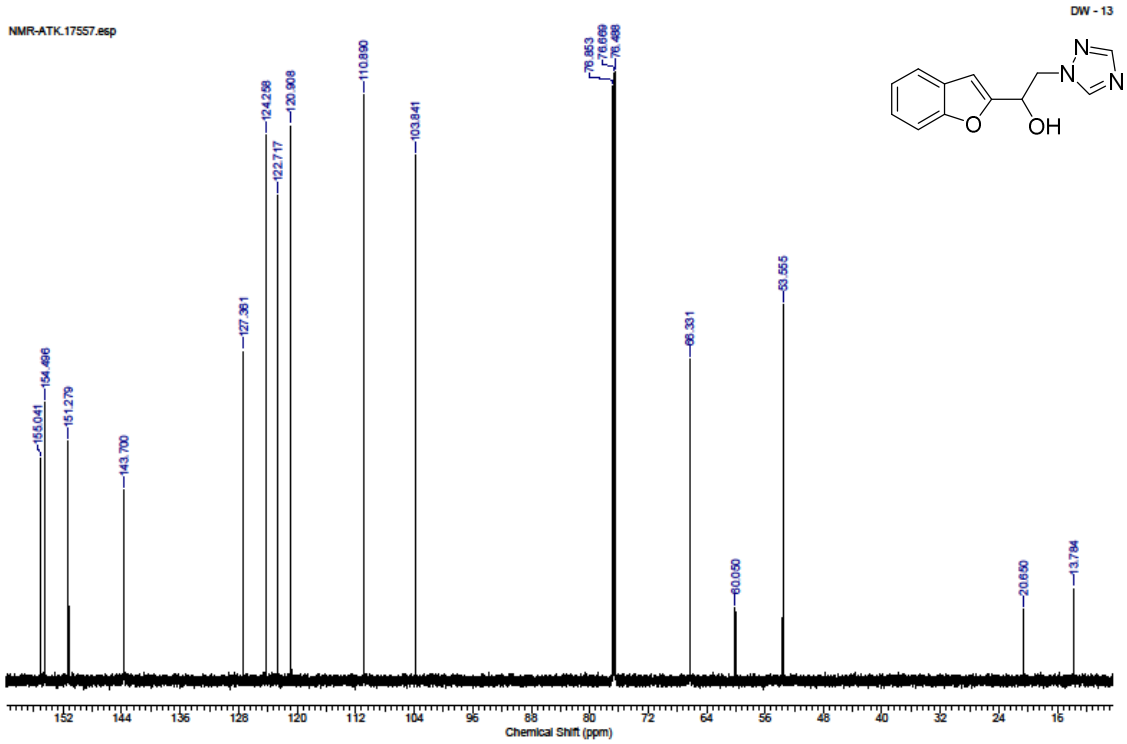
NMR-ATK.17557.esp
DW - 13
Chemical Shift (ppm)

(**b**)

**Figure 21.** (**a**) $^{1}$H NMR and (**b**) $^{13}$C NMR spectra of 1-(benzofuran-2-yl)-2-(1*H*-1,2,4-triazol-1-yl)ethan-1-ol (**25**).

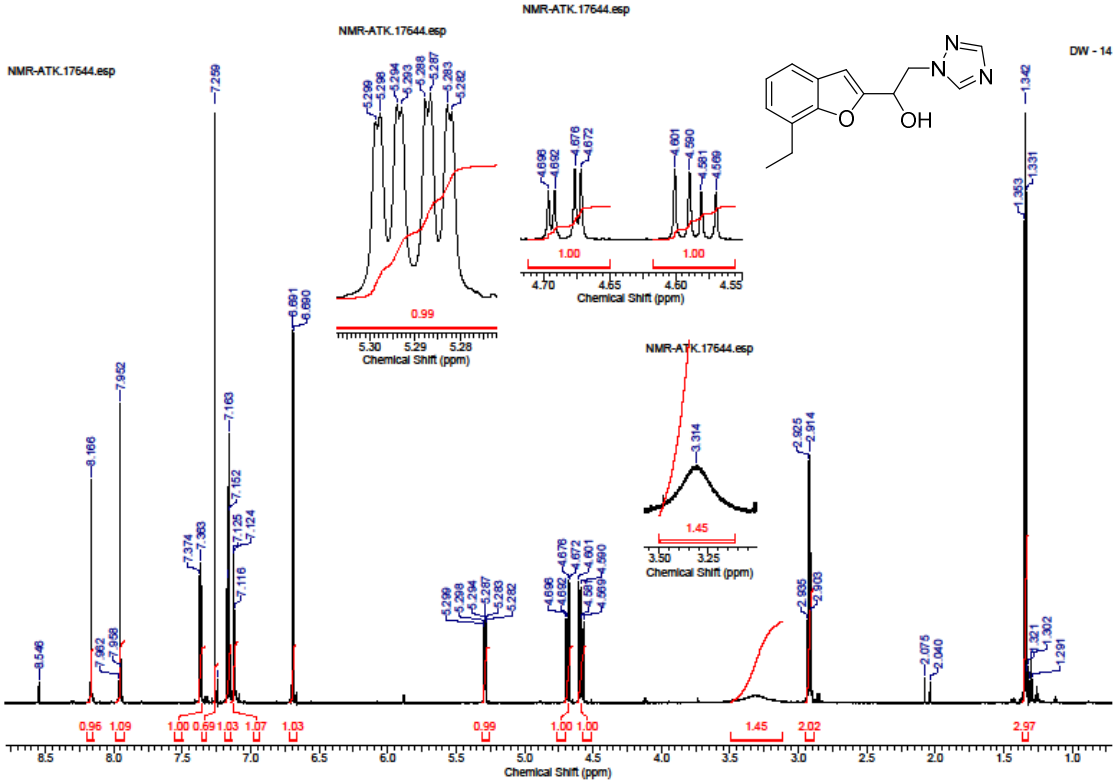


(**a**)

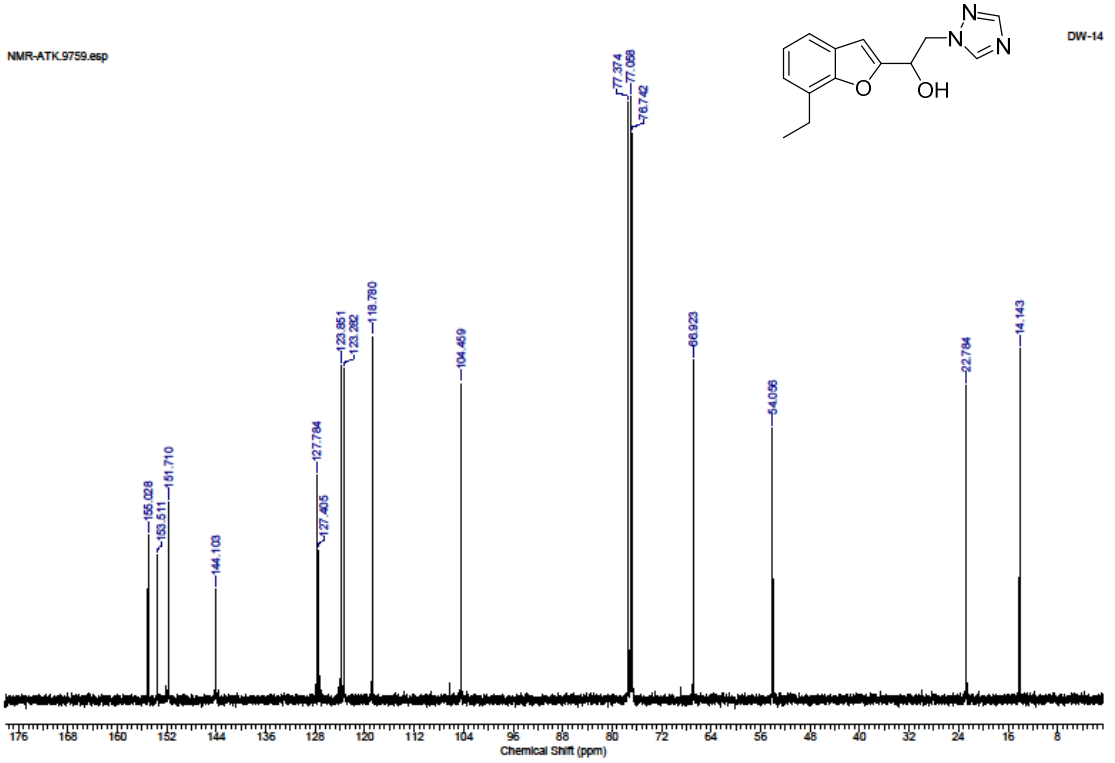

(**b**)

**Figure 22.** (**a**) $^{1}$H NMR and (**b**) $^{13}$C NMR spectra of 1-(7-ethylbenzofuran-2-yl)-2-(1*H*-1,2,4-triazol-1-yl)ethan-1-ol (**26**).

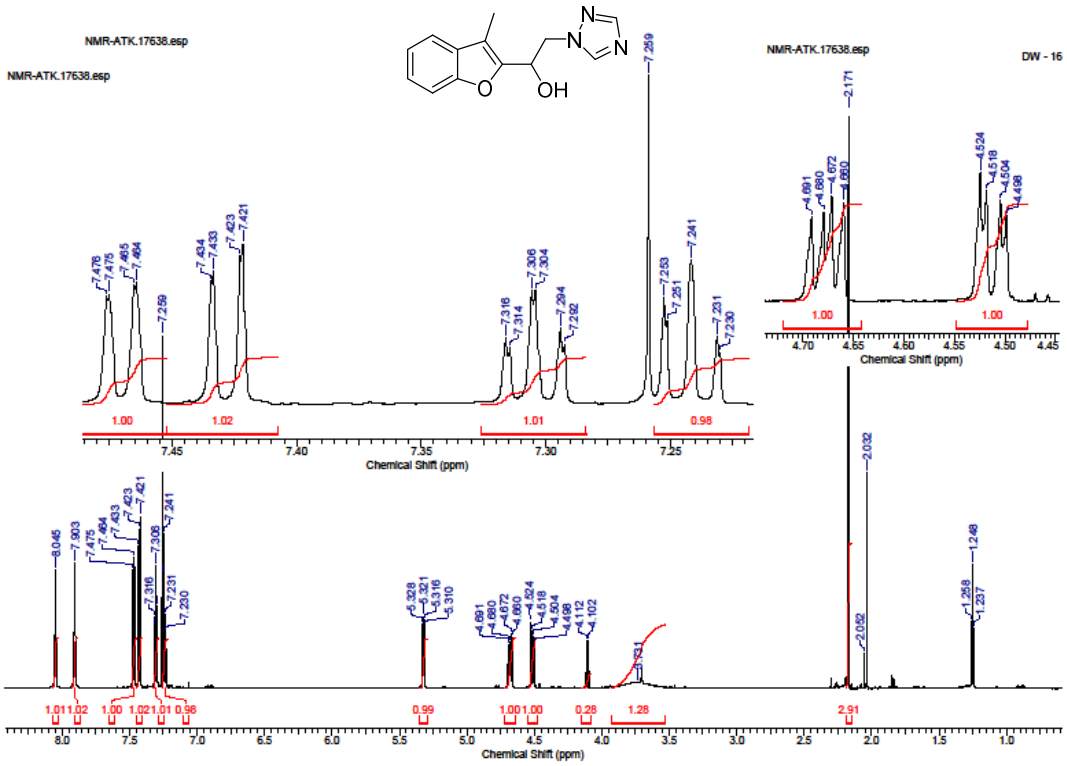


(**a**)

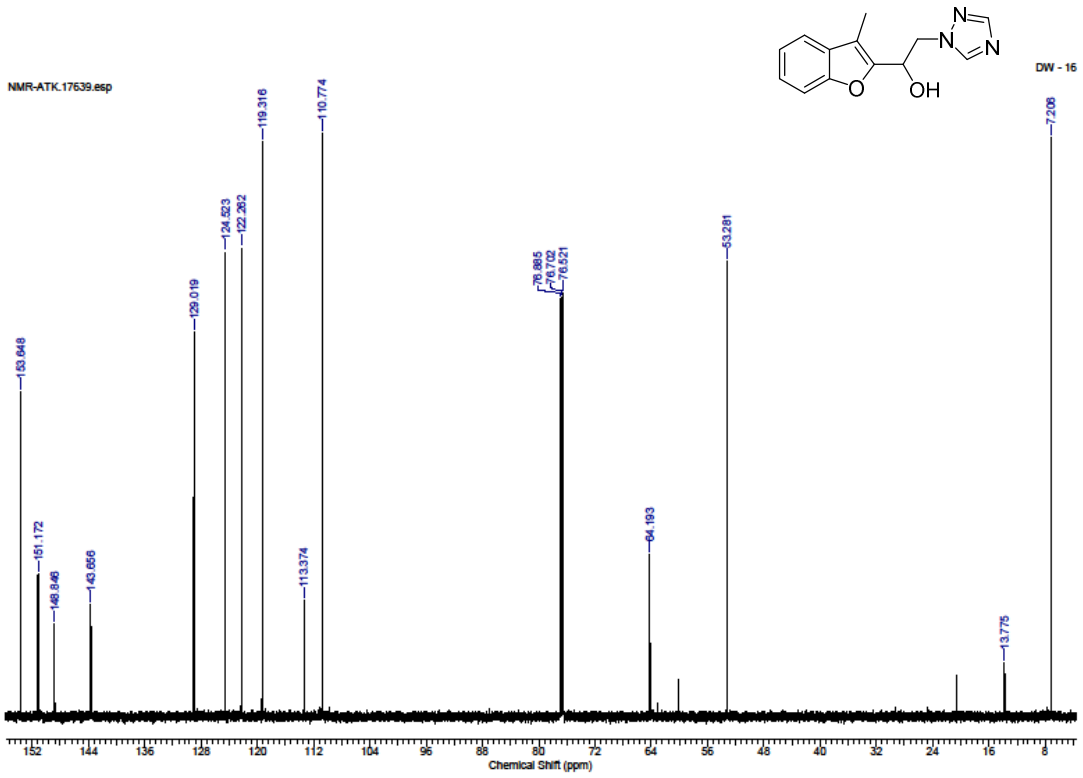


(**b**)

**Figure S23.** (**a**) $^{1}$H NMR and (**b**) $^{13}$C NMR spectra of 1-(3-methylbenzofuran-2-yl)-2-(1*H*-1,2,4-triazol-1-yl)ethan-1-ol (**27**).

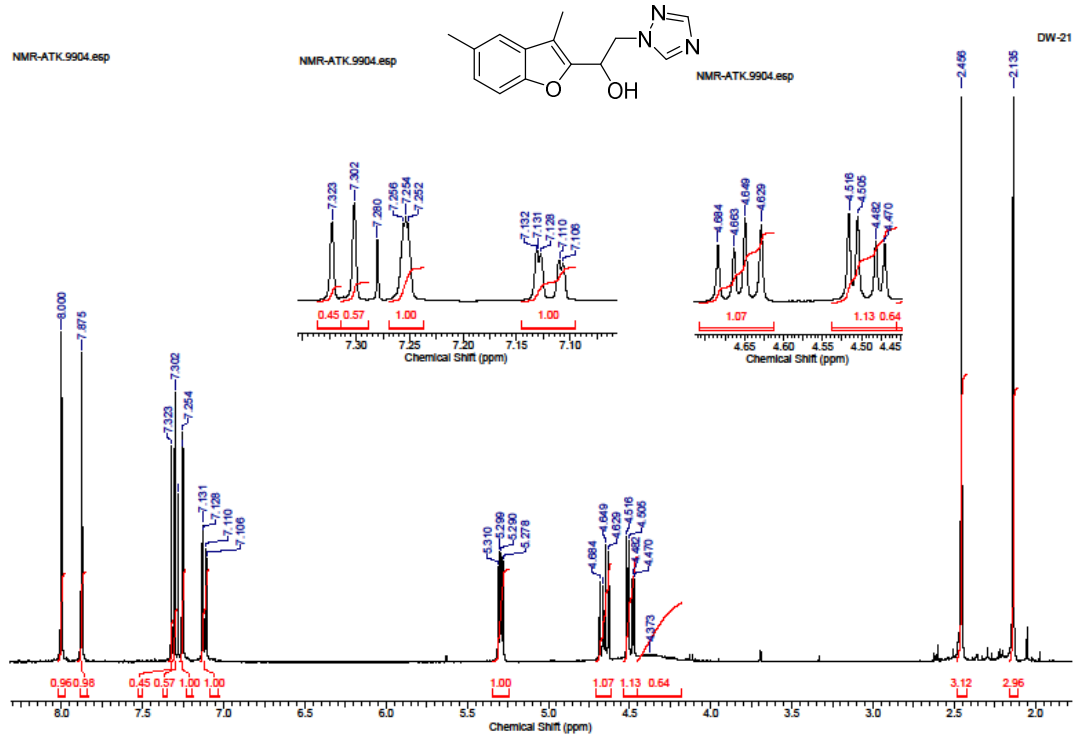


(**a**)

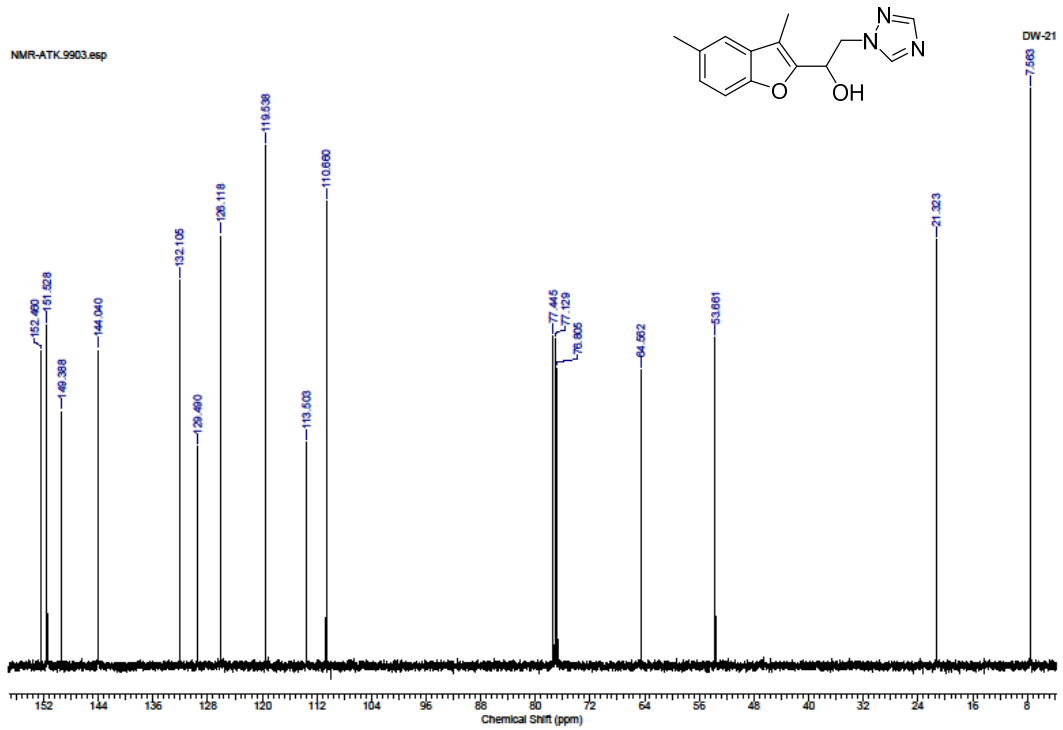


(**b**)

**Figure 24.** (**a**) $^{1}$H NMR and (**b**) $^{13}$C NMR spectra of 1-(3,5-dimethylbenzofuran-2-yl)-2-(1*H*-1,2,4-triazol-1-yl)ethan-1-ol (**28**).

## 2. Calculations Details

The theoretical approach that has been used in this work is common to all studied structures and includes (i) conformational search at molecular mechanics level (MM3); (ii) pre-optimization at the B3LYP/6-31G(d) level to reduce the number of thermally accessible conformers; (iii) parallel re-optimization of conformers found at low-DFT level at B3LYP/6-311++G(d,p) level and with the use of the IEFPCM solvent model, respectively, for acetonitrile and chloroform, followed by frequency calculations to confirm stability of received structures; (iv) calculations on relative energies ($\Delta E_{DFT}$ and $\Delta\Delta G_{DFT}$) using Boltzmann distribution at T = 298.15 K; (v) rotatory strengths calculations at the TD-DFT/6-311++G(d,p) level for all stable conformers of relative energies ranging from 0.0 to 2.0 kcal mol$^{-1}$; (vi) optical rotation calculations at the IEFPCM($CHCl_3$)/B3LYP/*aug*-cc-pVTZ level for all stable conformers of relative energies ranging from 0.0 to 2.0 kcal mol$^{-1}$.

Preliminary conformer distribution search was performed by the Scigress package [1] using the MM3 molecular mechanics force field. All possible conformers were analyzed using the systematic search methodology. Minimum energy conformers of relative steric energies ($\Delta E_{SE}$) up to 10 kcal mol$^{-1}$ found by molecular mechanics were further fully optimized at the B3LYP/6-31G(d) level as implemented in the Gaussian09 package [2], which significantly reduced the number of conformers. Higher accuracy calculations were performed at the IEFPCM/B3LYP/6-311++G(d,p) level [3].

The conformers obtained at the DFT/6-311++G(d,p) level were the real minima (no imaginary frequencies have been found). Total and free energy values have been calculated and used to obtain the Boltzmann population of conformers at 298.15 K. Only the results for conformers that differ from the most stable one by less than 2 kcal mol$^{-1}$ have been taken into account for further calculations, following a generally accepted protocol [4].

The TD-DFT/6-311++G(2d,2p) calculations of ECD were performed for all structures re-optimized at higher levels of theory. We used three different density functionals for calculations of rotatory strengths, namely CAM-B3LYP [5], M06-2X [6] and ωB97-XD [7] functional. Rotatory

strengths were calculated using both length and velocity representations. In the present study, the differences between the length and velocity representations of the calculated values of rotatory strengths were quite small, and for this reason only the velocity representations were further used. The CD spectra were simulated by overlapping Gaussian functions for each transition according to the procedure previously described and using half band width 0.4 eV [8]. It should be noted, that there are not substantial differences between ECD spectra calculated with these three functionals for the same molecule, therefore we discussed here only results obtained with the use of ωB97-XD functional.

The cartesian coordinates and structures of individual conformers of **13–20** calculated at the various levels of theory are available on request (300 pages) from the authors.

**Table S1.** Total (E, in Hartree) and relative energies (*ΔE*, *ΔΔG*, in kcal mol$^{-1}$), percentage populations (Pop.) and number of imaginary frequencies calculated at the IEFPCM(MeCN)/B3LYP/6-311++G(d,p) level for low-energy conformers of **13**.

| Conformer [a] | E | *ΔE* | Pop. | *ΔΔG* | Pop. | #ImFreq |
|---|---|---|---|---|---|---|
| 1 | −762.756385 | 1.14 | 2.93 | 1.61 | 1.09 | 0 |
| 3 | −762.757133 | 0.67 | 6.48 | 0.63 | 5.81 | 0 |
| 4 | −762.756378 | 1.14 | 2.91 | 1.45 | 1.46 | 0 |
| 6 | −762.756791 | 0.89 | 4.51 | 0.53 | 6.81 | 0 |
| 14 | −762.757456 | 0.47 | 9.12 | 0.27 | 10.66 | 0 |
| 16 | −762.756425 | 1.11 | 3.06 | 1.09 | 2.64 | 0 |
| 18 | −762.757051 | 0.72 | 5.94 | 0.69 | 5.18 | 0 |
| 20 | −762.75602 | 1.37 | 1.99 | 1.47 | 1.4 | 0 |
| 29 | −762.757585 | 0.39 | 10.45 | 0.00 | 16.73 | 0 |
| 32 | −762.756444 | 1.10 | 3.12 | 1.14 | 2.45 | 0 |
| 33 | −762.755814 | 1.50 | 1.6 | 1.33 | 1.77 | 0 |
| 34 | −762.757362 | 0.53 | 8.26 | 0.62 | 5.89 | 0 |
| 35 | −762.755439 | 1.73 | 1.08 | 1.66 | 1.01 | 0 |
| 39 | −762.755962 | 1.41 | 1.87 | 1.17 | 2.33 | 0 |
| 43 | −762.755724 | 1.55 | 1.45 | 1.73 | 0.9 | 0 |
| 44 | −762.755417 | 1.75 | 1.05 | 1.74 | 0.88 | 0 |
| 46 | −762.756699 | 0.94 | 4.09 | 1.23 | 2.11 | 0 |
| 51 | −762.756741 | 0.92 | 4.27 | 0.59 | 6.14 | 0 |
| 52 | −762.756414 | 1.12 | 3.02 | 0.51 | 7.08 | 0 |
| 53 | −762.758202 | 0.00 | 20.09 | 0.05 | 15.45 | 0 |
| 60 | −762.756313 | 1.18 | 2.72 | 1.2 | 2.21 | 0 |

[a] conformers are numbered according to their appearance during conformational search.

**Table S2.** Total (E, in Hartree) and relative energies (*ΔE*, *ΔΔG*, in kcal mol$^{-1}$), percentage populations (Pop.) and number of imaginary frequencies calculated at the IEFPCM($CHCl_3$)/B3LYP/6−311++G(d,p) level for low-energy conformers of **13**.

| Conformer [a] | E | *ΔE* | Pop. | *ΔΔG* | Pop. | #ImFreq |
|---|---|---|---|---|---|---|
| 1 | −762.752203 | 0.56 | 4.53 | 1.18 | 1.94 | 0 |
| 3 | −762.752527 | 0.36 | 6.39 | 0.58 | 5.32 | 0 |
| 4 | −762.752303 | 0.50 | 5.04 | 1.15 | 2.03 | 0 |
| 6 | −762.752317 | 0.49 | 5.11 | 0.80 | 3.69 | 0 |
| 14 | −762.752261 | 0.52 | 4.82 | 0.68 | 4.51 | 0 |
| 16 | −762.751182 | 1.20 | 1.54 | 1.34 | 1.47 | 0 |
| 18 | −762.752022 | 0.67 | 3.74 | 0.80 | 3.66 | 0 |
| 20 | −762.750943 | 1.35 | 1.19 | 1.81 | 0.66 | 0 |
| 26 | −762.74997 | 1.96 | 0.42 | 2.50 | 0 | 0 |
| 29 | −762.753095 | 0.00 | 11.66 | 0.00 | 14.23 | 0 |

| | | | | | | |
|---|---|---|---|---|---|---|
| 32 | −762.750624 | 1.55 | 0.85 | 1.37 | 1.41 | 0 |
| 33 | −762.751114 | 1.24 | 1.43 | 1.27 | 1.68 | 0 |
| 35 | −762.750874 | 1.39 | 1.11 | 1.57 | 1.01 | 0 |
| 39 | −762.750318 | 1.74 | 0.61 | 1.89 | 0.58 | 0 |
| 40 | −762.753024 | 0.04 | 10.81 | 0.27 | 8.98 | 0 |
| 43 | −762.751167 | 1.21 | 1.51 | 1.57 | 1.01 | 0 |
| 44 | −762.750897 | 1.38 | 1.13 | 1.53 | 1.07 | 0 |
| 46 | −762.752089 | 0.63 | 4.02 | 1.18 | 1.95 | 0 |
| 51 | −762.752571 | 0.33 | 6.69 | 0.15 | 11.11 | 0 |
| 52 | −762.752289 | 0.51 | 4.96 | 0.28 | 8.82 | 0 |
| 53 | −762.753087 | 0.01 | 11.56 | 0.03 | 13.44 | 0 |
| 54 | −762.752863 | 0.15 | 9.12 | 0.25 | 9.37 | 0 |
| 60 | −762.751302 | 1.13 | 1.74 | 1.15 | 2.06 | 0 |

[a] conformers are numbered according to their appearance during conformational search.

**Table S3.** Total (E, in Hartree) and relative energies ($\Delta E$, $\Delta\Delta G$, in kcal mol$^{-1}$), percentage populations (Pop.) and number of imaginary frequencies calculated at the IEFPCM(MeCN)/B3LYP/6-311++G(d,p) level for low-energy conformers of **14**.

| **Conformer** [a] | **E** | $\Delta E$ | **Pop.** | $\Delta\Delta G$ | **Pop.** | **#ImFreq** |
|---|---|---|---|---|---|---|
| 1 | −841.4092792 | 0.71 | 2.86 | 1.40 | 1.15 | 0 |
| 2 | −841.4093205 | 0.68 | 2.99 | 0.74 | 3.49 | 0 |
| 3 | −841.408859 | 0.97 | 1.83 | 0.73 | 3.59 | 0 |
| 4 | −841.4090019 | 0.88 | 2.13 | 1.28 | 1.41 | 0 |
| 5 | −841.4097618 | 0.41 | 4.77 | 0.56 | 4.71 | 0 |
| 6 | −841.4097633 | 0.40 | 4.78 | 0.66 | 4.02 | 0 |
| 7 | −841.4086642 | 1.09 | 1.49 | 1.02 | 2.19 | 0 |
| 8 | −841.4087367 | 1.05 | 1.61 | 1.00 | 2.24 | 0 |
| 9 | −841.4077823 | 1.65 | 0.59 | 0.96 | 2.4 | 0 |
| 10 | −841.4096896 | 0.45 | 4.42 | 0.71 | 3.66 | 0 |
| 11 | −841.4096811 | 0.46 | 4.38 | 0.79 | 3.2 | 0 |
| 12 | −841.4074238 | 1.87 | 0.4 | 1.98 | 0.43 | 0 |
| 14 | −841.409473 | 0.59 | 3.52 | 0.70 | 3.75 | 0 |
| 15 | −841.4079711 | 1.53 | 0.72 | 1.70 | 0.69 | 0 |
| 16 | −841.4095086 | 0.56 | 3.65 | 0.88 | 2.76 | 0 |
| 17 | −841.4076186 | 1.75 | 0.49 | 1.97 | 0.44 | 0 |
| 18 | −841.4076186 | 1.75 | 0.49 | 2.26 | 0 | 0 |
| 19 | −841.4074977 | 1.83 | 0.43 | 2.70 | 0 | 0 |
| 20 | −841.4088512 | 0.98 | 1.82 | 0.87 | 2.81 | 0 |
| 21 | −841.4089465 | 0.92 | 2.01 | 1.19 | 1.63 | 0 |
| 22 | −841.4088784 | 0.96 | 1.87 | 0.77 | 3.32 | 0 |
| 23 | −841.4088876 | 0.95 | 1.89 | 0.97 | 2.36 | 0 |
| 24 | −841.4083488 | 1.29 | 1.07 | 2.15 | 0 | 0 |
| 25 | −841.4104077 | 0.00 | 9.47 | 0.17 | 9.15 | 0 |
| 26 | −841.4079246 | 1.56 | 0.68 | 2.16 | 0 | 0 |
| 27 | −841.4103746 | 0.02 | 9.14 | 0.00 | 12.22 | 0 |
| 28 | −841.4092667 | 0.72 | 2.83 | 1.12 | 1.83 | 0 |
| 29 | −841.4092517 | 0.73 | 2.78 | 1.20 | 1.6 | 0 |
| 30 | −841.4085481 | 1.17 | 1.32 | 0.72 | 3.62 | 0 |
| 31 | −841.4083761 | 1.27 | 1.1 | 2.13 | 0 | 0 |
| 32 | −841.4085795 | 1.15 | 1.36 | 1.15 | 1.76 | 0 |
| 33 | −841.4085 | 1.18 | 1.29 | 1.64 | 0.76 | 0 |
| 34 | −841.4085521 | 1.16 | 1.33 | 1.75 | 0.64 | 0 |

| | | | | | | |
|---|---|---|---|---|---|---|
| 35 | −841.4101 | 0.22 | 6.56 | 0.39 | 6.36 | 0 |
| 36 | −841.4101 | 0.21 | 6.65 | 0.53 | 4.99 | 0 |
| 37 | −841.4078 | 1.65 | 0.59 | 1.64 | 0.76 | 0 |
| 38 | −841.4079702 | 1.53 | 0.72 | 1.07 | 2 | 0 |
| 39 | −841.4083705 | 1.28 | 1.09 | 1.56 | 0.88 | 0 |
| 40 | −841.4084726 | 1.21 | 1.22 | 1.29 | 1.38 | 0 |
| 41 | −841.4080105 | 1.50 | 0.75 | 1.39 | 1.17 | 0 |
| 42 | −841.4081858 | 1.39 | 0.9 | 1.73 | 0.65 | 0 |

[a] conformers are numbered according to their appearance during conformational search.

**Table S4.** Total (E, in Hartree) and relative energies ($\Delta E$, $\Delta\Delta G$, in kcal mol$^{-1}$), percentage populations (Pop.) and number of imaginary frequencies calculated at the IEFPCM($CHCl_3$)/B3LYP/6-311++G(d,p) level for low-energy conformers of **14**.

| Conformer [a] | E | $\Delta E$ | Pop. | $\Delta\Delta G$ | Pop. | #ImFreq |
|---|---|---|---|---|---|---|
| 1 | −841.404568 | 0.53 | 2.73 | 0.75 | 2.18 | 0 |
| 2 | −841.4046253 | 0.50 | 2.9 | 0.25 | 5.1 | 0 |
| 3 | −841.4043308 | 0.68 | 2.12 | 0.94 | 1.59 | 0 |
| 4 | −841.404419 | 0.63 | 2.33 | 0.68 | 2.44 | 0 |
| 5 | −841.4052385 | 0.11 | 5.56 | 0.05 | 7.13 | 0 |
| 6 | −841.4052739 | 0.09 | 5.77 | 0.24 | 5.17 | 0 |
| 7 | −841.404065 | 0.85 | 1.6 | 1.25 | 0.94 | 0 |
| 8 | −841.4041139 | 0.82 | 1.69 | 0.78 | 2.09 | 0 |
| 9 | −841.4032474 | 1.36 | 0.67 | 1.41 | 0.72 | 0 |
| 10 | −841.4044759 | 0.59 | 2.48 | 0.68 | 2.45 | 0 |
| 11 | −841.4044657 | 0.6 | 2.45 | 0.69 | 2.4 | 0 |
| 12 | −841.4030072 | 1.51 | 0.52 | 1.22 | 0.98 | 0 |
| 13 | −841.4028025 | 1.64 | 0.42 | 1.77 | 0.39 | 0 |
| 14 | −841.405157 | 0.16 | 5.1 | 0.00 | 7.74 | 0 |
| 15 | −841.4033826 | 1.28 | 0.78 | 1.36 | 0.78 | 0 |
| 16 | −841.4052241 | 0.12 | 5.47 | 0.45 | 3.61 | 0 |
| 17 | −841.4031676 | 1.41 | 0.62 | 1.56 | 0.56 | 0 |
| 18 | −841.4032388 | 1.37 | 0.67 | 1.90 | 0.31 | 0 |
| 19 | −841.4031231 | 1.44 | 0.59 | 2.43 | 0 | 0 |
| 20 | −841.4042695 | 0.72 | 1.99 | 0.86 | 1.81 | 0 |
| 21 | −841.4042805 | 0.71 | 2.01 | 0.46 | 3.56 | 0 |
| 22 | −841.4046642 | 0.47 | 3.02 | 0.35 | 4.3 | 0 |
| 23 | −841.4047078 | 0.44 | 3.17 | 0.59 | 2.84 | 0 |
| 24 | −841.4040851 | 0.83 | 1.64 | 1.25 | 0.94 | 0 |
| 25 | −841.405415 | 0.00 | 6.7 | 0.30 | 4.69 | 0 |
| 26 | −841.4035105 | 1.20 | 0.89 | 1.90 | 0.31 | 0 |
| 27 | −841.4054154 | 0.00 | 6.7 | 0.07 | 6.85 | 0 |
| 28 | −841.4042273 | 0.75 | 1.9 | 0.47 | 3.53 | 0 |
| 29 | −841.4042325 | 0.74 | 1.91 | 1.10 | 1.21 | 0 |
| 30 | −841.4044084 | 0.63 | 2.31 | 0.43 | 3.74 | 0 |
| 31 | −841.4042349 | 0.74 | 1.92 | 1.53 | 0.58 | 0 |
| 32 | −841.4044565 | 0.60 | 2.43 | 0.82 | 1.95 | 0 |
| 33 | −841.4043187 | 0.69 | 2.1 | 1.28 | 0.89 | 0 |
| 34 | −841.4044428 | 0.61 | 2.39 | 1.11 | 1.19 | 0 |
| 35 | −841.4053426 | 0.05 | 6.21 | 0.16 | 5.94 | 0 |
| 36 | −841.405375 | 0.03 | 6.42 | 0.09 | 6.69 | 0 |
| 37 | −841.4022158 | 2.01 | 0 | 1.69 | 0.45 | 0 |
| 38 | −841.402473 | 1.85 | 0.3 | 2.15 | 0 | 0 |

| | | | | | | |
|---|---|---|---|---|---|---|
| 39 | −841.4026 | 1.75 | 0.35 | 1.56 | 0.55 | 0 |
| 40 | −841.4028 | 1.61 | 0.44 | 1.81 | 0.36 | 0 |
| 41 | −841.4025 | 1.81 | 0.32 | 1.62 | 0.5 | 0 |
| 42 | −841.4027 | 1.68 | 0.4 | 1.59 | 0.53 | 0 |

[a] conformers are numbered according to their appearance during conformational search.

**Table S5.** Total (E, in Hartree) and relative energies ($\Delta E$, $\Delta\Delta G$, in kcal mol$^{-1}$), percentage populations (Pop.) and number of imaginary frequencies calculated at the IEFPCM(MeCN)/B3LYP/6-311++G(d,p) level for low-energy conformers of **15**.

| Conformer [a] | E | $\Delta E$ | Pop. | $\Delta\Delta G$ | Pop. | #ImFreq |
|---|---|---|---|---|---|---|
| 2 | −802.086052 | 0.26 | 18.16 | 0.00 | 25.67 | 0 |
| 11 | −802.085808 | 0.41 | 14.02 | 0.56 | 10.01 | 0 |
| 18 | −802.086014 | 0.28 | 17.44 | 0.40 | 13.1 | 0 |
| 21 | −802.08646 | 0.00 | 27.99 | 0.00 | 25.81 | 0 |
| 25 | −802.084802 | 1.04 | 4.83 | 0.82 | 6.5 | 0 |
| 26 | −802.08374 | 1.71 | 1.57 | 1.93 | 1 | 0 |
| 27 | −802.084488 | 1.24 | 3.46 | 0.56 | 9.97 | 0 |
| 28 | −802.083416 | 1.91 | 1.11 | 2.11 | 0 | 0 |
| 34 | −802.083513 | 1.85 | 1.23 | 2.22 | 0 | 0 |
| 39 | −802.08361 | 1.79 | 1.36 | 2.02 | 0 | 0 |
| 44 | −802.083657 | 1.76 | 1.44 | 1.49 | 2.09 | 0 |
| 45 | −802.083325 | 1.97 | 1.01 | 1.72 | 1.4 | 0 |
| 46 | −802.084535 | 1.21 | 3.64 | 1.48 | 2.11 | 0 |
| 49 | −802.084269 | 1.38 | 2.74 | 1.42 | 2.35 | 0 |

[a] conformers are numbered according to their appearance during conformational search.

**Table S6.** Total (E, in Hartree) and relative energies ($\Delta E$, $\Delta\Delta G$, in kcal mol$^{-1}$), percentage populations (Pop.) and number of imaginary frequencies calculated at the IEFPCM($CHCl_3$)/B3LYP/6-311++G(d,p) level for low-energy conformers of **15**.

| Conformer [a] | E | $\Delta E$ | Pop. | $\Delta\Delta G$ | Pop. | #ImFreq |
|---|---|---|---|---|---|---|
| 2 | −802.081609 | 0.00 | 22.5 | 0.07 | 21.58 | 0 |
| 4 | −802.078456 | 1.98 | 0.8 | 2.87 | 0 | 0 |
| 11 | −802.081502 | 0.07 | 20.09 | 0.49 | 10.72 | 0 |
| 18 | −802.081024 | 0.37 | 12.1 | 0.14 | 19.35 | 0 |
| 21 | −802.081282 | 0.21 | 15.9 | 0.00 | 24.35 | 0 |
| 25 | −802.080332 | 0.80 | 5.82 | 0.58 | 9.15 | 0 |
| 26 | −802.079039 | 1.61 | 1.48 | 2.16 | 0 | 0 |
| 27 | −802.080233 | 0.86 | 5.23 | 0.78 | 6.5 | 0 |
| 28 | −802.078857 | 1.73 | 1.22 | 2.33 | 0 | 0 |
| 34 | −802.079279 | 1.46 | 1.9 | 2.17 | 0 | 0 |
| 39 | −802.079406 | 1.38 | 2.18 | 2.12 | 0 | 0 |
| 44 | −802.079418 | 1.37 | 2.21 | 1.36 | 2.46 | 0 |
| 45 | −802.079112 | 1.57 | 1.6 | 1.53 | 1.85 | 0 |
| 46 | −802.079953 | 1.04 | 3.89 | 1.49 | 1.97 | 0 |
| 49 | −802.079736 | 1.18 | 3.09 | 1.46 | 2.08 | 0 |

[a] conformers are numbered according to their appearance during conformational search.

**Table S7.** Total (E, in Hartree) and relative energies ($\Delta E$, $\Delta\Delta G$, in kcal mol$^{-1}$), percentage populations (Pop.) and number of imaginary frequencies calculated at the IEFPCM(MeCN)/B3LYP/6-311++G(d,p) level for low-energy conformers of **16**.

| Conformer [a] | E | *ΔE* | Pop. | *ΔΔG* | Pop. | #ImFreq |
|---|---|---|---|---|---|---|
| 2 | −841.412875 | 0.33 | 11.61 | 0.47 | 11.19 | 0 |
| 9 | −841.412566 | 0.52 | 8.36 | 0.00 | 24.76 | 0 |
| 15 | −841.413289 | 0.07 | 17.99 | 0.41 | 12.38 | 0 |
| 16 | −841.412838 | 0.35 | 11.16 | 0.60 | 9.05 | 0 |
| 22 | −841.411558 | 1.16 | 2.87 | 1.36 | 2.51 | 0 |
| 23 | −841.410499 | 1.82 | 0.94 | 1.82 | 1.14 | 0 |
| 25 | −841.411259 | 1.34 | 2.09 | 1.27 | 2.89 | 0 |
| 35 | −841.410267 | 1.97 | 0.73 | 2.17 | 0 | 0 |
| 38 | −841.41037 | 1.90 | 0.82 | 2.46 | 0 | 0 |
| 39 | −841.411393 | 1.26 | 2.41 | 1.64 | 1.56 | 0 |
| 40 | −841.410446 | 1.85 | 0.88 | 1.86 | 1.06 | 0 |
| 43 | −841.411125 | 1.43 | 1.82 | 1.70 | 1.41 | 0 |
| 46 | −841.413293 | 0.07 | 18.06 | 0.50 | 10.64 | 0 |
| 48 | −841.413401 | 0.00 | 20.26 | 0.09 | 21.41 | 0 |

[a] conformers are numbered according to their appearance during conformational search.

**Table S8.** Total (E, in Hartree) and relative energies (*ΔE*, *ΔΔG*, in kcal mol$^{-1}$), percentage populations (Pop.) and number of imaginary frequencies calculated at the IEFPCM($CHCl_3$)/B3LYP/6-311++G(d,p) level for low-energy conformers of **16**.

| Conformer[a] | E | *ΔE* | Pop. | *ΔΔG* | Pop. | #ImFreq |
|---|---|---|---|---|---|---|
| 2 | −841.40849 | 0.08 | 15.59 | 0.36 | 11.26 | 0 |
| 9 | −841.408313 | 0.19 | 12.92 | 0.23 | 13.96 | 0 |
| 15 | −841.408156 | 0.29 | 10.94 | 0.29 | 12.69 | 0 |
| 16 | −841.407944 | 0.42 | 8.74 | 0.43 | 10.07 | 0 |
| 22 | −841.407118 | 0.94 | 3.64 | 0.84 | 4.99 | 0 |
| 23 | −841.405844 | 1.74 | 0.94 | 1.96 | 0.75 | 0 |
| 24 | −841.405643 | 1.87 | 0.76 | 1.95 | 0.77 | 0 |
| 25 | −841.407019 | 1.00 | 3.28 | 0.60 | 7.54 | 0 |
| 35 | −841.406071 | 1.60 | 1.2 | 1.96 | 0.75 | 0 |
| 38 | −841.406193 | 1.52 | 1.37 | 2.18 | 0 | 0 |
| 39 | −841.406801 | 1.14 | 2.6 | 1.42 | 1.9 | 0 |
| 40 | −841.406217 | 1.50 | 1.4 | 1.49 | 1.68 | 0 |
| 43 | −841.406597 | 1.27 | 2.1 | 1.56 | 1.5 | 0 |
| 46 | −841.408557 | 0.04 | 16.74 | 0.35 | 11.44 | 0 |
| 48 | −841.408615 | 0.00 | 17.79 | 0.00 | 20.71 | 0 |

[a] conformers are numbered according to their appearance during conformational search.

**Table S9.** Total (E, in Hartree) and relative energies (*ΔE*, *ΔΔG*, in kcal mol$^{-1}$), percentage populations (Pop.) and number of imaginary frequencies calculated at the IEFPCM(MeCN)/B3LYP/6-311++G(d,p) level for low-energy conformers of **17**.

| Conformer [a] | E | *ΔE* | Pop. | *ΔΔG* | Pop. | #ImFreq |
|---|---|---|---|---|---|---|
| 1 | −778.7983727 | 1.23 | 4.67 | 0.90 | 5.12 | 0 |
| 2 | −778.8003257 | 0.00 | 37 | 0.46 | 10.73 | 0 |
| 3 | −778.8002247 | 0.06 | 33.25 | 0.00 | 23.36 | 0 |
| 4 | −778.7989546 | 0.86 | 8.65 | 0.06 | 21.1 | 0 |
| 5 | −778.7989768 | 0.85 | 8.86 | 0.27 | 14.81 | 0 |
| 6 | −778.7969536 | 2.12 | 0 | 1.35 | 2.41 | 0 |
| 8 | −778.7977453 | 1.62 | 2.4 | 1.20 | 3.05 | 0 |
| 10 | −778.7973149 | 1.89 | 1.52 | 1.43 | 2.08 | 0 |
| 12 | −778.7955512 | 3 | 0 | 1.95 | 0.87 | 0 |

| | | | | | | |
|---|---|---|---|---|---|---|
| 13 | −778.7975471 | 1.74 | 1.95 | 1.11 | 3.57 | 0 |
| 14 | −778.7970899 | 2.03 | 0 | 0.96 | 4.6 | 0 |
| 15 | −778.7974147 | 1.83 | 1.69 | 0.74 | 6.66 | 0 |
| 16 | −778.7965866 | 2.35 | 0 | 1.58 | 1.63 | 0 |

[a] conformers are numbered according to their appearance during conformational search.

**Table S10.** Total (E, in Hartree) and relative energies (*ΔE*, *ΔΔG*, in kcal mol$^{-1}$), percentage populations (Pop.) and number of imaginary frequencies calculated at the IEFPCM($CHCl_3$)/B3LYP/6-311++G(d,p) level for low-energy conformers of **17**.

| Conformer [a] | E | *ΔE* | Pop. | *ΔΔG* | Pop. | #ImFreq |
|---|---|---|---|---|---|---|
| 1 | −778.794189 | 1.48 | 3.54 | 1.18 | 5.11 | 0 |
| 2 | −778.796516 | 0.02 | 41.66 | 0.42 | 18.45 | 0 |
| 3 | −778.796549 | 0.00 | 43.15 | 0.00 | 37.29 | 0 |
| 4 | −778.794863 | 1.06 | 7.23 | 0.15 | 28.79 | 0 |
| 5 | −778.794397 | 1.35 | 4.41 | 0.76 | 10.36 | 0 |

[a] conformers are numbered according to their appearance during conformational search.

**Table S11.** Total (E, in Hartree) and relative energies (*ΔE*, *ΔΔG*, in kcal mol$^{-1}$), percentage populations (Pop.) and number of imaginary frequencies calculated at the IEFPCM(MeCN)/B3LYP/6-311++G(d,p) level for low-energy conformers of **18**.

| Conformer [a] | E | *ΔE* | Pop. | *ΔΔG* | Pop. | #ImFreq |
|---|---|---|---|---|---|---|
| 1 | −857.4523288 | 0.07 | 14.22 | 0.46 | 5.35 | 0 |
| 2 | −857.4504841 | 1.23 | 2.01 | 1.16 | 1.65 | 0 |
| 3 | −857.4505381 | 1.19 | 2.13 | 0.57 | 4.46 | 0 |
| 4 | −857.4524365 | 0.00 | 15.94 | 0.52 | 4.85 | 0 |
| 5 | −857.4510023 | 0.90 | 3.49 | 0.73 | 3.38 | 0 |
| 6 | −857.4523622 | 0.05 | 14.73 | 0.39 | 5.99 | 0 |
| 7 | −857.4523523 | 0.05 | 14.58 | 0.04 | 10.98 | 0 |
| 8 | −857.451149 | 0.81 | 4.07 | 0.15 | 8.97 | 0 |
| 9 | −857.4512116 | 0.77 | 4.35 | 0.45 | 5.43 | 0 |
| 10 | −857.4489901 | 2.16 | 0 | 1.49 | 0.95 | 0 |
| 11 | −857.4511598 | 0.8 | 4.12 | 0 | 11.65 | 0 |
| 12 | −857.451166 | 0.8 | 4.15 | 0.43 | 5.59 | 0 |
| 13 | −857.4491445 | 2.07 | 0 | 1.52 | 0.9 | 0 |
| 16 | −857.4497658 | 1.68 | 0.94 | 1.13 | 1.72 | 0 |
| 17 | −857.4498376 | 1.63 | 1.01 | 0.97 | 2.27 | 0 |
| 20 | −857.44943 | 1.89 | 0.66 | 0.97 | 2.25 | 0 |
| 21 | −857.4495427 | 1.82 | 0.74 | 1.43 | 1.04 | 0 |
| 22 | −857.4471969 | 3.29 | 0 | 1.95 | 0.43 | 0 |
| 27 | −857.451166 | 0.80 | 4.15 | 0.43 | 5.59 | 0 |
| 28 | −857.4496868 | 1.73 | 0.86 | 1.50 | 0.92 | 0 |
| 29 | −857.4497668 | 1.68 | 0.94 | 1.20 | 1.54 | 0 |
| 30 | −857.4493103 | 1.96 | 0.58 | 1.70 | 0.66 | 0 |
| 31 | −857.4492873 | 1.98 | 0.57 | 1.58 | 0.81 | 0 |
| 32 | −857.4496886 | 1.72 | 0.87 | 1.52 | 0.89 | 0 |
| 33 | −857.4496396 | 1.76 | 0.82 | 1.01 | 2.13 | 0 |
| 35 | −857.4486711 | 2.36 | 0 | 1.72 | 0.63 | 0 |

[a] conformers are numbered according to their appearance during conformational search.

**Table S12.** Total (E, in Hartree) and relative energies ($\Delta E$, $\Delta\Delta G$, in kcal mol$^{-1}$), percentage populations (Pop.) and number of imaginary frequencies calculated at the IEFPCM($CHCl_3$)/B3LYP/6-311++G(d,p) level for low-energy conformers of **18**.

| Conformer [a] | E | $\Delta E$ | Pop. | $\Delta\Delta G$ | Pop. | #ImFreq |
|---|---|---|---|---|---|---|
| 2 | −857.446183 | 1.55 | 1.93 | 1.49 | 1.4 | 0 |
| 3 | −857.446291 | 1.48 | 2.16 | 0.65 | 5.74 | 0 |
| 4 | −857.448572 | 0.05 | 24.24 | 0.46 | 7.9 | 0 |
| 5 | −857.446742 | 1.20 | 3.48 | 0.74 | 4.96 | 0 |
| 6 | −857.448617 | 0.02 | 25.41 | 0.15 | 13.5 | 0 |
| 7 | −857.448652 | 0.00 | 26.38 | 0.00 | 18.31 | 0 |
| 8 | −857.44711 | 0.97 | 5.15 | 0.15 | 13.62 | 0 |
| 9 | −857.446612 | 1.28 | 3.04 | 0.67 | 5.26 | 0 |
| 10 | −857.44486 | 2.38 | 0 | 1.39 | 1.66 | 0 |
| 11 | −857.446566 | 1.31 | 2.89 | 0.34 | 9.97 | 0 |
| 12 | −857.447142 | 0.95 | 5.33 | 0.43 | 8.4 | 0 |
| 13 | −857.445012 | 2.28 | 0 | 1.49 | 1.39 | 0 |
| 16 | −857.445436 | 2.02 | 0 | 1.68 | 1.01 | 0 |
| 17 | −857.445394 | 2.04 | 0 | 1.24 | 2.14 | 0 |
| 20 | −857.444685 | 2.49 | 0 | 1.36 | 1.75 | 0 |
| 21 | −857.444737 | 2.46 | 0 | 1.91 | 0.68 | 0 |
| 28 | −857.444845 | 2.39 | 0 | 2.06 | 0 | 0 |
| 29 | −857.445005 | 2.29 | 0 | 1.69 | 1 | 0 |
| 32 | −857.444827 | 2.4 | 0 | 1.95 | 0.64 | 0 |
| 33 | −857.444786 | 2.43 | 0 | 1.33 | 1.83 | 0 |

[a] conformers are numbered according to their appearance during conformational search.

**Table S13.** Total (E, in Hartree) and relative energies ($\Delta E$, $\Delta\Delta G$, in kcal mol$^{-1}$), percentage populations (Pop.) and number of imaginary frequencies calculated at the IEFPCM(MeCN)/B3LYP/6-311++G(d,p) level for low-energy conformers of **19**.

| Conformer [a] | E | $\Delta E$ | Pop. | $\Delta\Delta G$ | Pop. | #ImFreq |
|---|---|---|---|---|---|---|
| 1 | −818.127403 | 0.39 | 15.74 | 0.78 | 9.6 | 0 |
| 2 | −818.128022 | 0.00 | 30.34 | 0.00 | 36.08 | 0 |
| 3 | −818.126227 | 1.13 | 4.53 | 0.94 | 7.35 | 0 |
| 4 | −818.126339 | 1.06 | 5.1 | 2.02 | 0 | 0 |
| 5 | −818.127208 | 0.51 | 12.81 | 1.33 | 3.81 | 0 |
| 6 | −818.124881 | 1.97 | 1.09 | 2.02 | 0 | 0 |
| 7 | −818.126291 | 1.09 | 4.85 | 1.19 | 4.86 | 0 |
| 8 | −818.125617 | 1.51 | 2.37 | 1.83 | 1.63 | 0 |
| 12 | −818.127129 | 0.56 | 11.78 | 0.30 | 21.65 | 0 |
| 13 | −818.126468 | 0.98 | 5.84 | 0.77 | 9.83 | 0 |
| 16 | −818.126421 | 1.00 | 5.56 | 1.15 | 5.18 | 0 |

[a] conformers are numbered according to their appearance during conformational search.

**Table S14.** Total (E, in Hartree) and relative energies ($\Delta E$, $\Delta\Delta G$, in kcal mol$^{-1}$), percentage populations (Pop.) and number of imaginary frequencies calculated at the IEFPCM($CHCl_3$)/B3LYP/6-311++G(d,p) level for low-energy conformers of **19**.

| Conformer [a] | E | $\Delta E$ | Pop. | $\Delta\Delta G$ | Pop. | #ImFreq |
|---|---|---|---|---|---|---|
| 1 | −818.123396 | 0.10 | 19.24 | 0.94 | 9.41 | 0 |
| 2 | −818.123552 | 0.00 | 22.71 | 0.00 | 46.19 | 0 |
| 3 | −818.122139 | 0.89 | 5.08 | 1.19 | 6.23 | 0 |

| | | | | | | |
|---|---|---|---|---|---|---|
| 4 | −818.122782 | 0.48 | 10.04 | 1.65 | 2.86 | 0 |
| 5 | −818.123502 | 0.03 | 21.53 | 1.13 | 6.81 | 0 |
| 6 | −818.120586 | 1.86 | 0.98 | 2.35 | 0 | 0 |
| 7 | −818.12162 | 1.21 | 2.93 | 1.37 | 4.57 | 0 |
| 8 | −818.120865 | 1.69 | 1.32 | 2.30 | 0 | 0 |
| 12 | −818.122776 | 0.49 | 9.97 | 0.71 | 13.98 | 0 |
| 13 | −818.121781 | 1.11 | 3.47 | 1.06 | 7.74 | 0 |
| 16 | −818.121556 | 1.25 | 2.74 | 1.80 | 2.21 | 0 |

[a] conformers are numbered according to their appearance during conformational search.

**Table S15.** Total (E, in Hartree) and relative energies ($\Delta E$, $\Delta\Delta G$, in kcal mol$^{-1}$), percentage populations (Pop.) and number of imaginary frequencies calculated at the IEFPCM(MeCN)/B3LYP/6-311++G(d,p) level for low-energy conformers of **20**.

| Conformer [a] | E | $\Delta E$ | Pop. | $\Delta\Delta G$ | Pop. | #ImFreq |
|---|---|---|---|---|---|---|
| 1 | −857.4530357 | 1.48 | 2.45 | 1.68 | 2.17 | 0 |
| 4 | −857.4548673 | 0.33 | 17.04 | 0.49 | 16.4 | 0 |
| 5 | −857.4542218 | 0.74 | 8.6 | 1.00 | 6.93 | 0 |
| 17 | −857.4529805 | 1.51 | 2.31 | 1.25 | 4.52 | 0 |
| 20 | −857.4531357 | 1.42 | 2.72 | 1.53 | 2.79 | 0 |
| 24 | −857.4532572 | 1.34 | 3.09 | 1.60 | 2.49 | 0 |
| 26 | −857.4540028 | 0.87 | 6.82 | 1.32 | 4.01 | 0 |
| 33 | −857.4553935 | 0.00 | 29.76 | 0.00 | 37.2 | 0 |
| 38 | −857.454734 | 0.41 | 14.79 | 0.65 | 12.36 | 0 |
| 41 | −857.4545692 | 0.52 | 12.42 | 0.71 | 11.13 | 0 |

[a] conformers are numbered according to their appearance during conformational search.

**Table S16.** Total (E, in Hartree) and relative energies ($\Delta E$, $\Delta\Delta G$, in kcal mol$^{-1}$), percentage populations (Pop.) and number of imaginary frequencies calculated at the IEFPCM($CHCl_3$)/B3LYP/6-311++G(d,p) level for low-energy conformers of **20**.

| Conformer [a] | E | $\Delta E$ | Pop. | $\Delta\Delta G$ | Pop. | #ImFreq |
|---|---|---|---|---|---|---|
| 1 | −857.4495131 | 0.98 | 1.99 | 5.2 | 1.43 | 0 |
| 3 | −857.4504411 | 0.40 | 0.34 | 13.91 | 23.01 | 0 |
| 5 | −857.4502584 | 0.51 | 0.99 | 11.46 | 7.7 | 0 |
| 17 | −857.4489162 | 1.36 | 1.23 | 2.76 | 5.14 | 0 |
| 20 | −857.4484538 | 1.65 | 1.92 | 1.69 | 1.6 | 0 |
| 24 | −857.4483962 | 1.68 | 1.86 | 1.59 | 1.77 | 0 |
| 26 | −857.4502805 | 0.50 | 1.25 | 11.73 | 4.94 | 0 |
| 33 | −857.4510777 | 0.00 | 0.00 | 27.3 | 40.82 | 0 |
| 38 | −857.4502134 | 0.54 | 1.66 | 10.93 | 2.45 | 0 |
| 41 | −857.4504082 | 0.42 | 0.77 | 13.43 | 11.13 | 0 |

[a] conformers are numbered according to their appearance during conformational search.

**Table S17.** Calculated at the IEFPCM($CHCl_3$)/B3LYP/*aug*-cc-pVTZ level optical rotations for alcohol **13**.

| Conformer [a] | 589 nm | 578 nm | 546 nm | 436 nm |
|---|---|---|---|---|
| 1 | −473 | −496 | −573 | −1065 |
| 3 | 455 | 477 | 551 | 1027 |
| 4 | −430 | −462 | −535 | −1011 |
| 6 | 445 | 468 | 543 | 1039 |
| 14 | −20 | −20 | −19 | 2 |

| | | | | |
|---|---|---|---|---|
| 16 | −1 | −1 | −1 | 2 |
| 18 | 66 | 70 | 83 | 181 |
| 20 | 137 | 144 | 167 | 325 |
| 26 | 206 | 216 | 245 | 411 |
| 29 | −140 | −146 | −169 | −312 |
| 32 | −4 | −3 | −1 | 23 |
| 33 | 111 | 116 | 130 | 209 |
| 35 | 132 | 138 | 159 | 288 |
| 39 | 95 | 100 | 116 | 217 |
| 40 | −57 | −59 | −68 | −116 |
| 43 | −136 | −142 | −162 | −274 |
| 44 | −154 | −161 | −186 | −342 |
| 46 | −535 | −562 | −653 | −1258 |
| 51 | −78 | −82 | −95 | −181 |
| 52 | 21 | 23 | 28 | 66 |
| 53 | −30 | −31 | −33 | −24 |
| 54 | 419 | 440 | 507 | 943 |
| 60 | −9 | −9 | −8 | 5 |

[a] conformers are numbered according to their appearance during conformational search.

**Table 18.** Calculated at the IEFPCM($CHCl_3$)/B3LYP/*aug*-cc-pVTZ level optical rotations for alcohol **14.**

| Conformer [a] | 589 nm | 578 nm | 546 nm | 436 nm |
|---|---|---|---|---|
| 1 | 367 | 386 | 446 | 839 |
| 2 | 595 | 624 | 720 | 1323 |
| 3 | 355 | 373 | 433 | 840 |
| 4 | 594 | 624 | 721 | 1346 |
| 5 | −33 | −35 | −41 | −81 |
| 6 | −308 | −322 | −371 | −673 |
| 7 | −496 | −521 | −606 | −1164 |
| 8 | −680 | −714 | −826 | −1553 |
| 9 | 100 | 104 | 117 | 183 |
| 10 | −135 | −141 | −159 | −255 |
| 11 | 148 | 156 | 182 | 355 |
| 12 | 121 | 126 | 145 | 256 |
| 13 | −151 | −158 | −181 | −326 |
| 14 | 50 | 52 | 60 | 109 |
| 15 | −153 | −161 | −187 | −356 |
| 16 | −240 | −251 | −288 | −513 |
| 17 | −129 | −135 | −155 | −276 |
| 18 | 98 | 102 | 117 | 198 |
| 19 | −149 | −156 | −177 | −299 |
| 20 | −464 | −487 | −563 | −1057 |
| 21 | −677 | −710 | −818 | −1507 |
| 22 | 7 | 8 | 8 | 9 |
| 23 | −258 | −271 | −311 | −560 |
| 24 | −433 | −455 | −526 | −985 |
| 25 | −152 | −158 | −179 | −292 |
| 26 | 101 | 106 | 123 | 229 |
| 27 | 133 | 140 | 163 | 321 |
| 28 | −48 | −50 | −55 | −68 |
| 29 | 218 | 229 | 266 | 504 |

| | | | | |
|---|---|---|---|---|
| 30 | 142 | 149 | 172 | 323 |
| 31 | −394 | −414 | −481 | −922 |
| 32 | −140 | −147 | −167 | −283 |
| 33 | −638 | −669 | −772 | −1416 |
| 34 | −623 | −653 | −755 | −1400 |
| 35 | −69 | −72 | −81 | −122 |
| 36 | 187 | 196 | 227 | 431 |
| 37 | −380 | −399 | −460 | −850 |
| 38 | −576 | −604 | −695 | −1262 |
| 39 | 367 | 385 | 445 | 835 |
| 40 | 599 | 628 | 724 | 1325 |
| 41 | 371 | 390 | 453 | 869 |
| 42 | 600 | 629 | 726 | 1349 |

[a] conformers are numbered according to their appearance during conformational search.

**Table S19.** Calculated at the IEFPCM($CHCl_3$)/B3LYP/*aug*-cc-pVTZ level optical rotations for alcohol **15.**

| Conformer [a] | 589 nm | 578 nm | 546 nm | 436 nm |
|---|---|---|---|---|
| 2 | 400 | 420 | 486 | 912 |
| 4 | −393 | −417 | −479 | −915 |
| 11 | 383 | 403 | 468 | 898 |
| 18 | 54 | 57 | 68 | 149 |
| 21 | −13 | −13 | −12 | 10 |
| 25 | −131 | −137 | −157 | −282 |
| 26 | 191 | 200 | 228 | 406 |
| 27 | −66 | −69 | −79 | −139 |
| 28 | 201 | 211 | 243 | 453 |
| 34 | −388 | −408 | −474 | −910 |
| 39 | −396 | −415 | −480 | −904 |
| 44 | −93 | −97 | −112 | −201 |
| 45 | −32 | −34 | −38 | −64 |
| 46 | −165 | −172 | −196 | −337 |
| 49 | −176 | −185 | −213 | −389 |

[a] conformers are numbered according to their appearance during conformational search.

**Table S20.** Calculated at the IEFPCM($CHCl_3$)/B3LYP/*aug*-cc-pVTZ level optical rotations for alcohol **16.**

| Conformer [a] | 589 nm | 578 nm | 546 nm | 436 nm |
|---|---|---|---|---|
| 2 | 372 | 390 | 451 | 851 |
| 9 | 350 | 368 | 428 | 826 |
| 15 | −22 | −23 | −23 | −14 |
| 16 | 52 | 55 | 66 | 143 |
| 22 | −116 | −121 | −139 | −246 |
| 23 | 220 | 231 | 264 | 471 |
| 24 | 238 | 248 | 288 | 535 |
| 25 | −48 | −50 | −57 | −97 |
| 35 | −350 | −368 | −428 | −826 |
| 38 | −360 | −378 | −438 | −827 |
| 39 | −199 | −208 | −238 | −417 |
| 40 | −79 | −83 | −95 | −168 |
| 43 | −204 | −214 | −247 | −454 |

| | | | | |
|---|---|---|---|---|
| 46 | 329 | 345 | 398 | 738 |
| 48 | −186 | −195 | −226 | −421 |

[a] conformers are numbered according to their appearance during conformational search.

**Table S21.** Calculated at the IEFPCM($CHCl_3$)/B3LYP/*aug*-cc-pVTZ level optical rotations for alcohol **17.**

| Conformer[a] | 589 nm | 578 nm | 546 nm | 436 nm |
|---|---|---|---|---|
| 1 | 436 | 458 | 529 | 985 |
| 2 | −403 | −423 | −489 | −911 |
| 3 | 55 | 58 | 68 | 137 |
| 4 | −187 | −196 | −226 | −422 |
| 5 | −55 | −57 | −63 | −90 |

[a] conformers are numbered according to their appearance during conformational search.

**Table S22.** Calculated at the IEFPCM($CHCl_3$)/B3LYP/*aug*-cc-pVTZ level optical rotations for alcohol **18**.

| Conformer [a] | 589 nm | 578 nm | 546 nm | 436 nm |
|---|---|---|---|---|
| 2 | 354 | 372 | 470 | 811 |
| 3 | 594 | 623 | 718 | 1322 |
| 4 | −596 | −625 | −721 | −1323 |
| 5 | 306 | 322 | 372 | 700 |
| 6 | 134 | 140 | 162 | 301 |
| 7 | −163 | −170 | −194 | −334 |
| 8 | −54 | −57 | −68 | −140 |
| 9 | −185 | −193 | −220 | −371 |
| 10 | 97 | 101 | 113 | 177 |
| 11 | 103 | 109 | 127 | 249 |
| 12 | −330 | −346 | −398 | −733 |
| 13 | −145 | −153 | −178 | −338 |
| 16 | −472 | −496 | −575 | −1096 |
| 17 | −692 | −726 | −839 | −1561 |
| 20 | 371 | 390 | 453 | 872 |
| 21 | 598 | 627 | 725 | 1357 |
| 29 | 587 | 616 | 710 | 1301 |
| 32 | −155 | −161 | −183 | −304 |
| 33 | 124 | 130 | 151 | 289 |

[a] conformers are numbered according to their appearance during conformational search.

**Table S23.** Calculated at the IEFPCM($CHCl_3$)/B3LYP/*aug*-cc-pVTZ level optical rotations for alcohol **19**.

| Conformer [a] | 589 nm | 578 nm | 546 nm | 436 nm |
|---|---|---|---|---|
| 1 | 370 | 388 | 449 | 839 |
| 2 | −41 | −43 | −47 | −66 |
| 3 | −168 | −176 | −203 | −376 |
| 4 | −330 | −346 | −401 | −753 |
| 5 | 11 | 12 | 14 | 34 |
| 6 | 173 | 181 | 207 | 367 |
| 7 | 388 | 408 | 474 | 911 |
| 8 | −211 | −222 | −256 | −474 |
| 12 | −101 | −106 | −121 | −208 |

| | | | | |
|---|---|---|---|---|
| 13 | 353 | 371 | 428 | 793 |
| 16 | −2 | −1 | 0.5 | 20 |

[a] conformers are numbered according to their appearance during conformational search.

**Table S24.** Calculated at the IEFPCM($CHCl_3$)/B3LYP/*aug*-cc-pVTZ level optical rotations for alcohol **20**.

| Conformer [a] | 589 nm | 578 nm | 546 nm | 436 nm |
|---|---|---|---|---|
| 1 | −275 | −289 | 334 | −632 |
| 3 | −43 | −45 | −50 | −73 |
| 5 | 343 | 361 | 417 | 783 |
| 17 | −152 | −159 | −184 | −339 |
| 20 | 363 | 382 | 443 | 858 |
| 24 | −2 | −2 | −1 | 18 |
| 26 | 35 | 37 | 43 | 88 |
| 33 | −77 | −81 | −92 | −162 |
| 38 | −145 | −152 | −175 | −325 |
| 41 | 288 | 302 | 348 | 643 |

[a] conformers are numbered according to their appearance during conformational search.

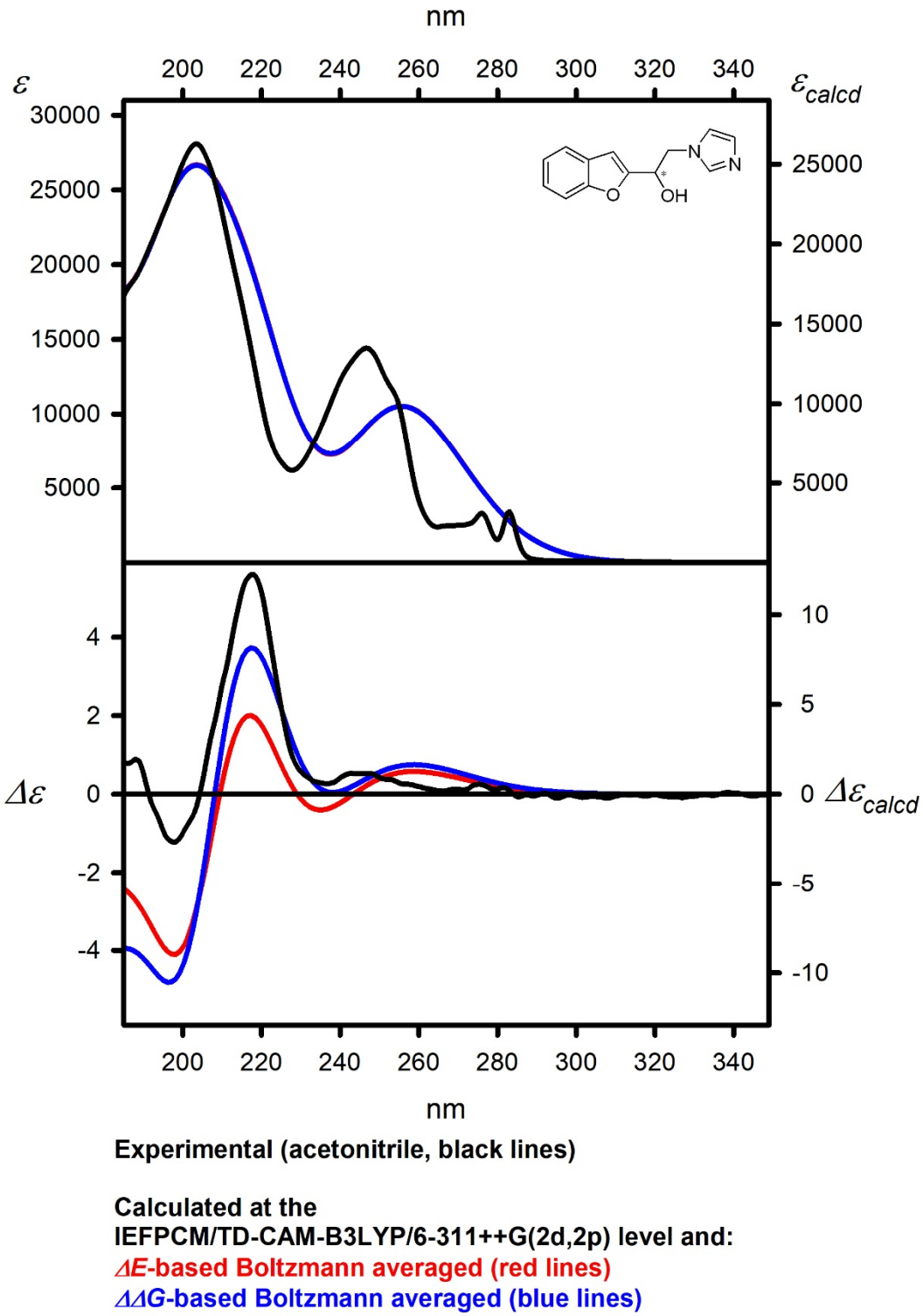


**Figure 25.** UV (upper panel) and ECD (lower panel) spectra of alcohol **13**, measured in acetonitrile (black lines), and calculated at the IEFPCM/TD-CAM-B3LYP/6-311++G(2p,2d) level and $\Delta E$- (red lines) and $\Delta\Delta G$-based Boltzmann averaged (blue lines). Wavelengths were corrected to match experimental UV maximum.

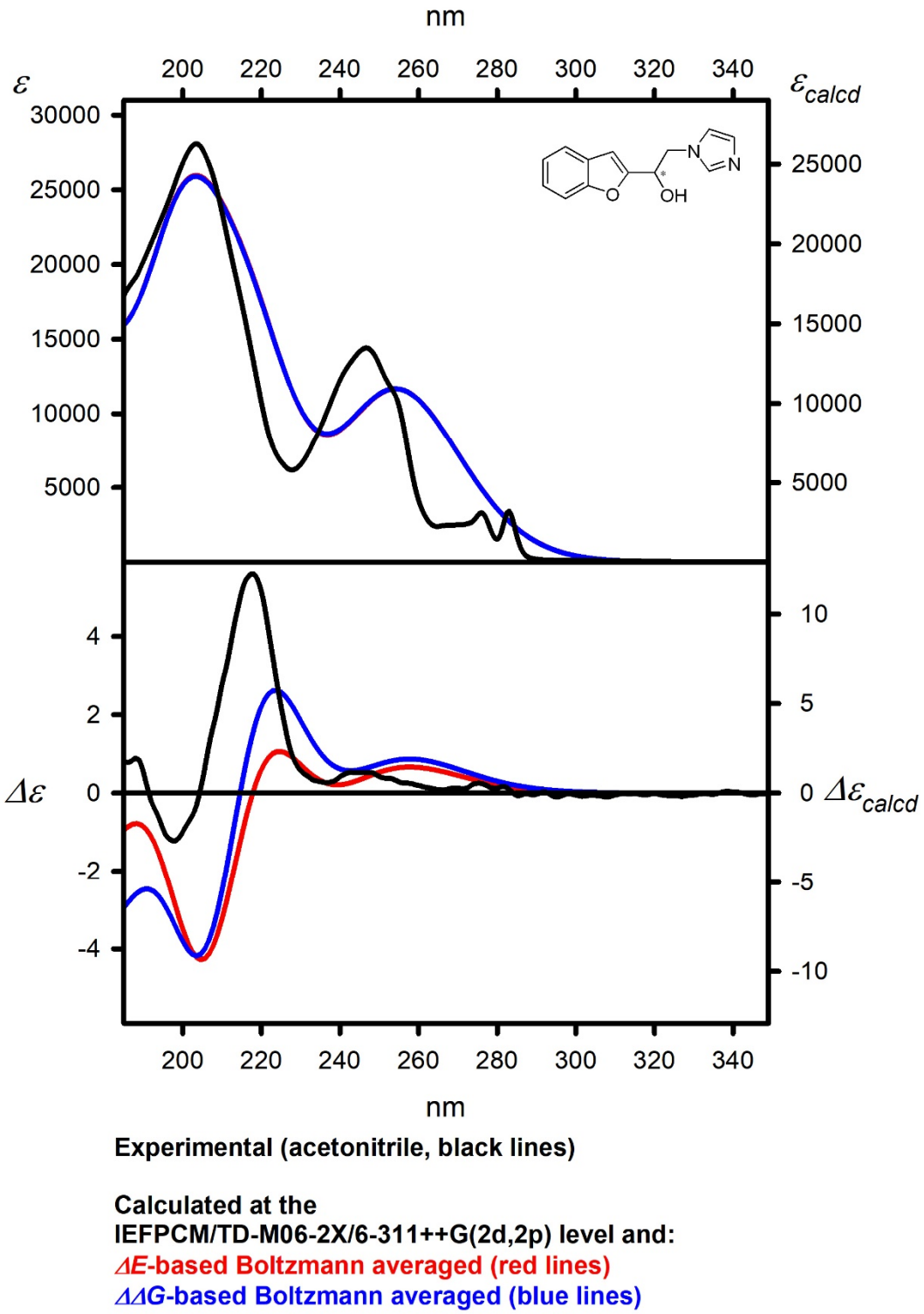


**Figure S26.** UV (upper panel) and ECD (lower panel) spectra of alcohol **13**, measured in acetonitrile (black lines), and calculated at the IEFPCM/TD-M06-2X/6-311++G(2p,2d) level and $\Delta E$- (red lines) and $\Delta\Delta G$-based Boltzmann averaged (blue lines). Wavelengths were corrected to match experimental UV maximum.

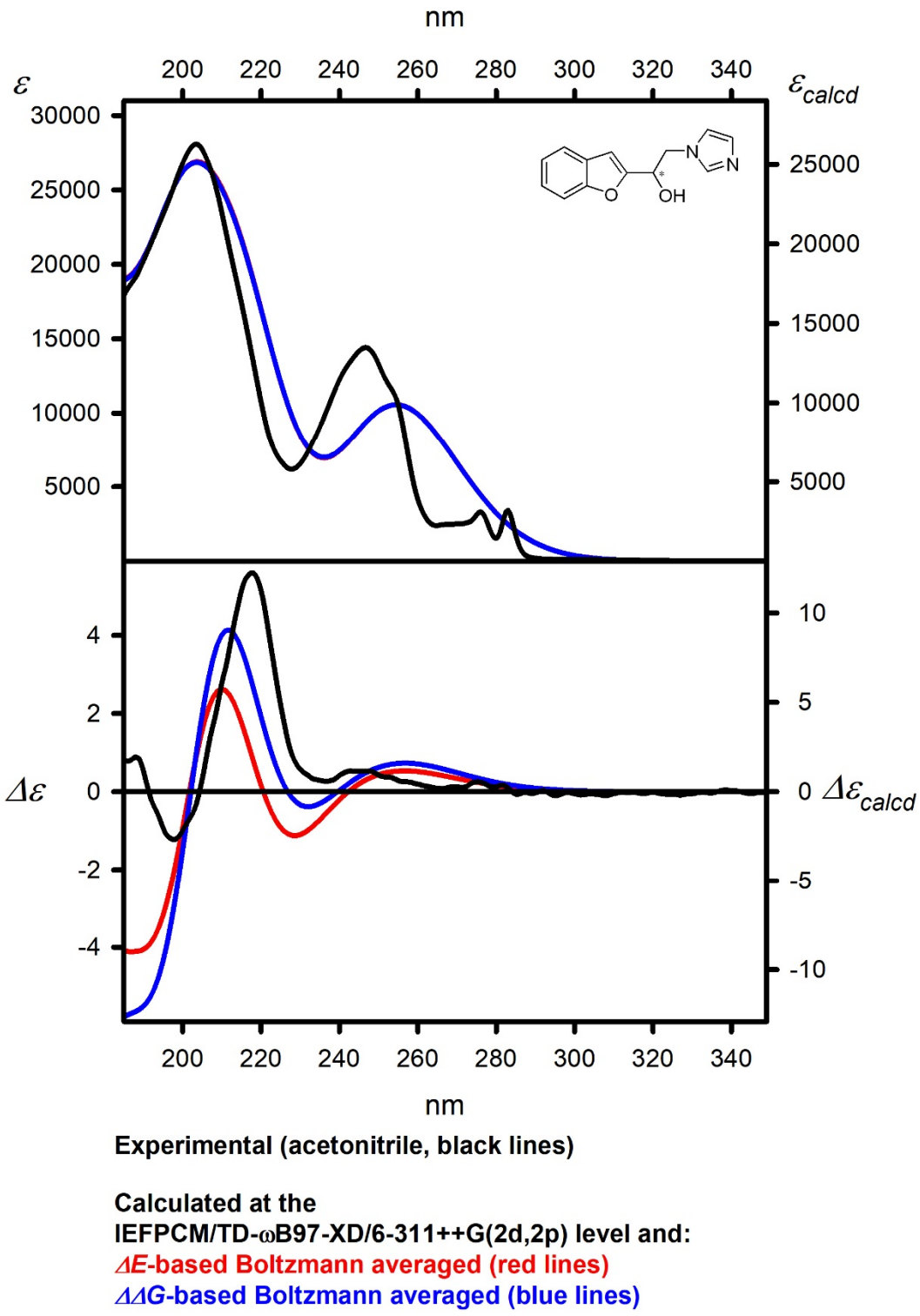


**Figure S27.** UV (upper panel) and ECD (lower panel) spectra of alcohol **13**, measured in acetonitrile (black lines), and calculated at the IEFPCM/TD-$\omega$B97-XD/6-311++G(2p,2d) level and $\Delta E$- (red lines) and $\Delta\Delta G$-based Boltzmann averaged (blue lines). Wavelengths were corrected to match experimental UV maximum.

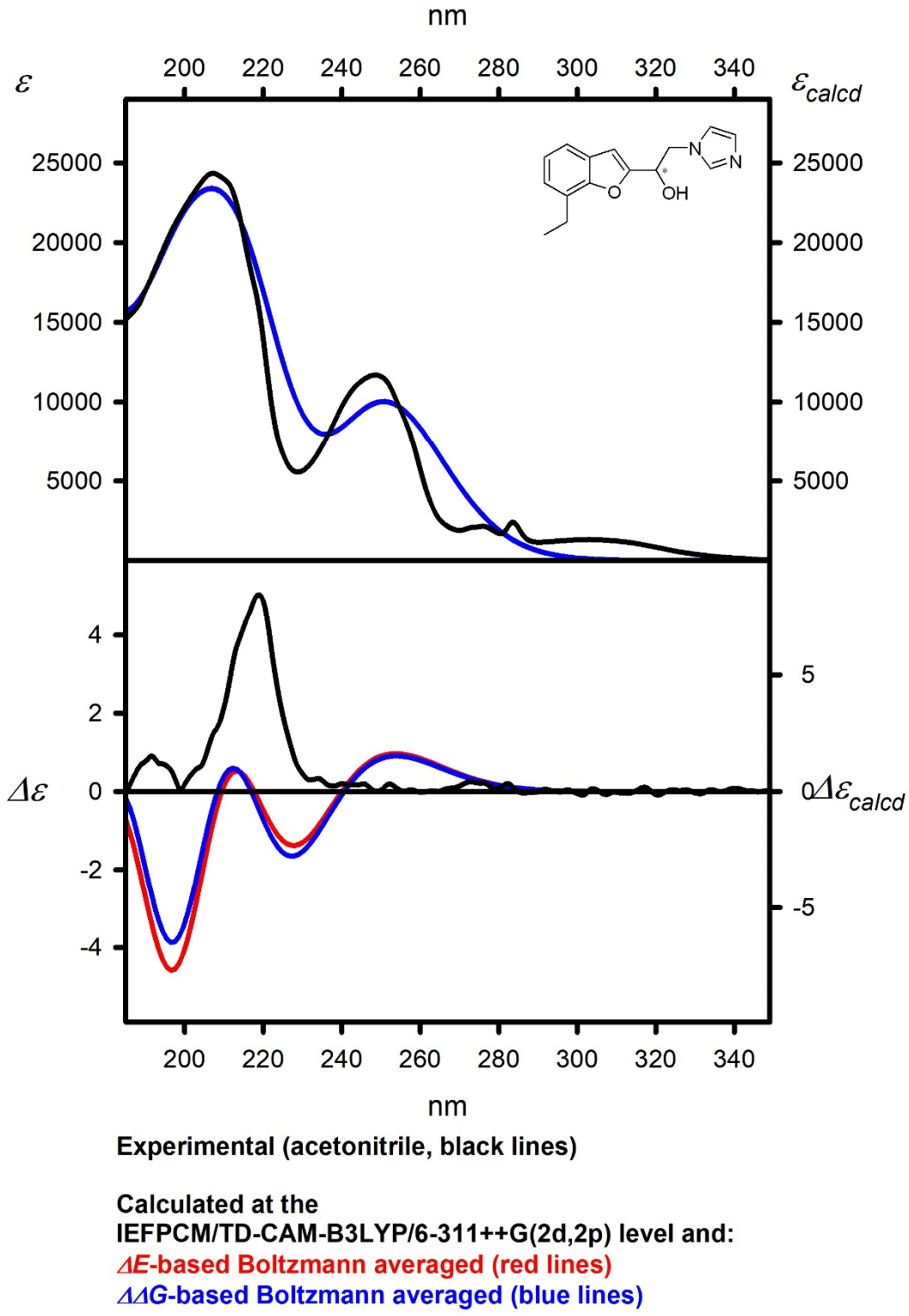


**Figure S28.** UV (upper panel) and ECD (lower panel) spectra of alcohol **14**, measured in acetonitrile (black lines), and calculated at the IEFPCM/TD-CAM-B3LYP/6-311++G(2p,2d) level and $\Delta E$- (red lines) and $\Delta\Delta G$-based Boltzmann averaged (blue lines). Wavelengths were corrected to match experimental UV maximum.

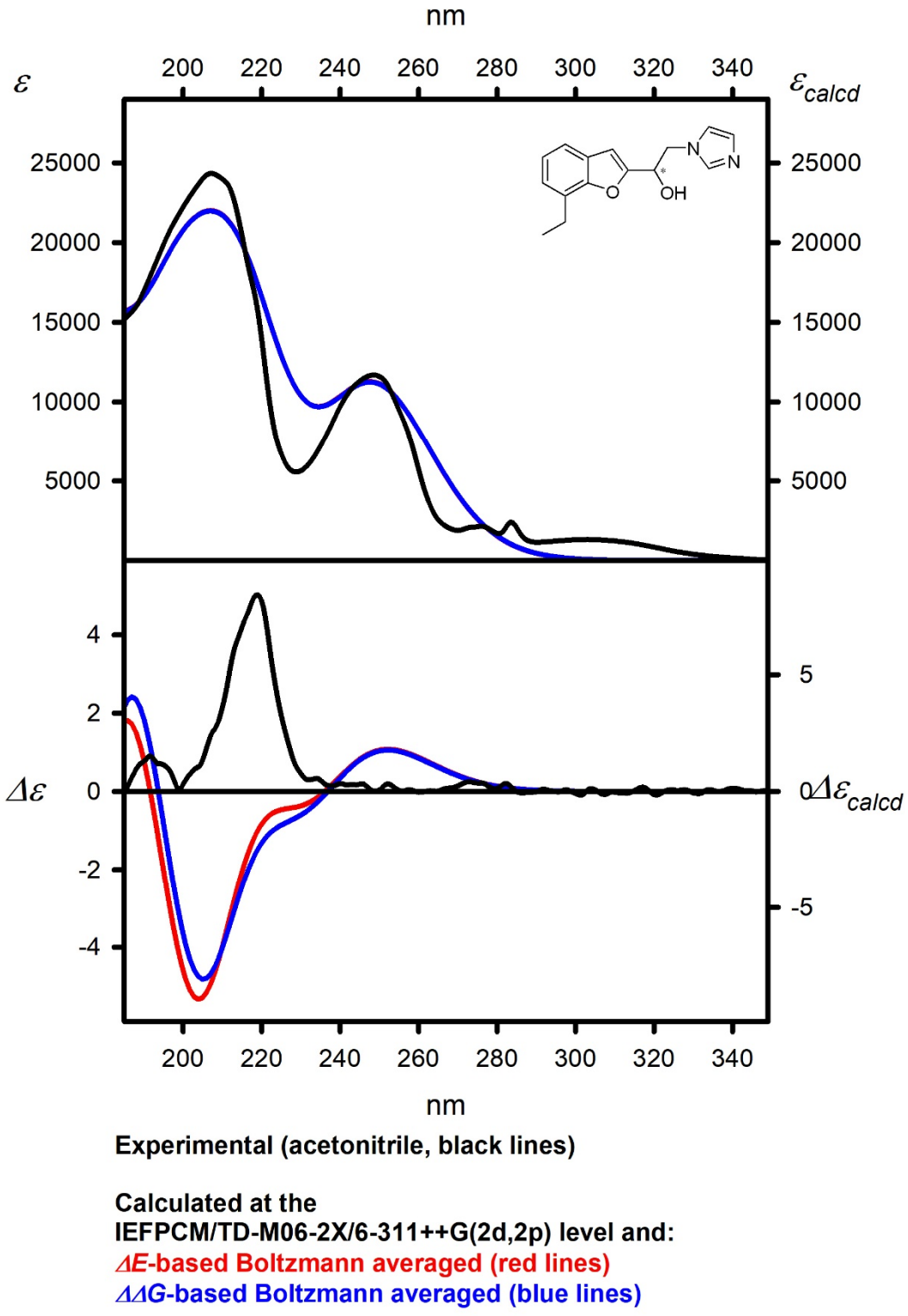


**Figure S29.** UV (upper panel) and ECD (lower panel) spectra of alcohol **14**, measured in acetonitrile (black lines), and calculated at the IEFPCM/TD-M06-2X/6-311++G(2p,2d) level and *ΔE*- (red lines) and *ΔΔG*-based Boltzmann averaged (blue lines). Wavelengths were corrected to match experimental UV maximum.

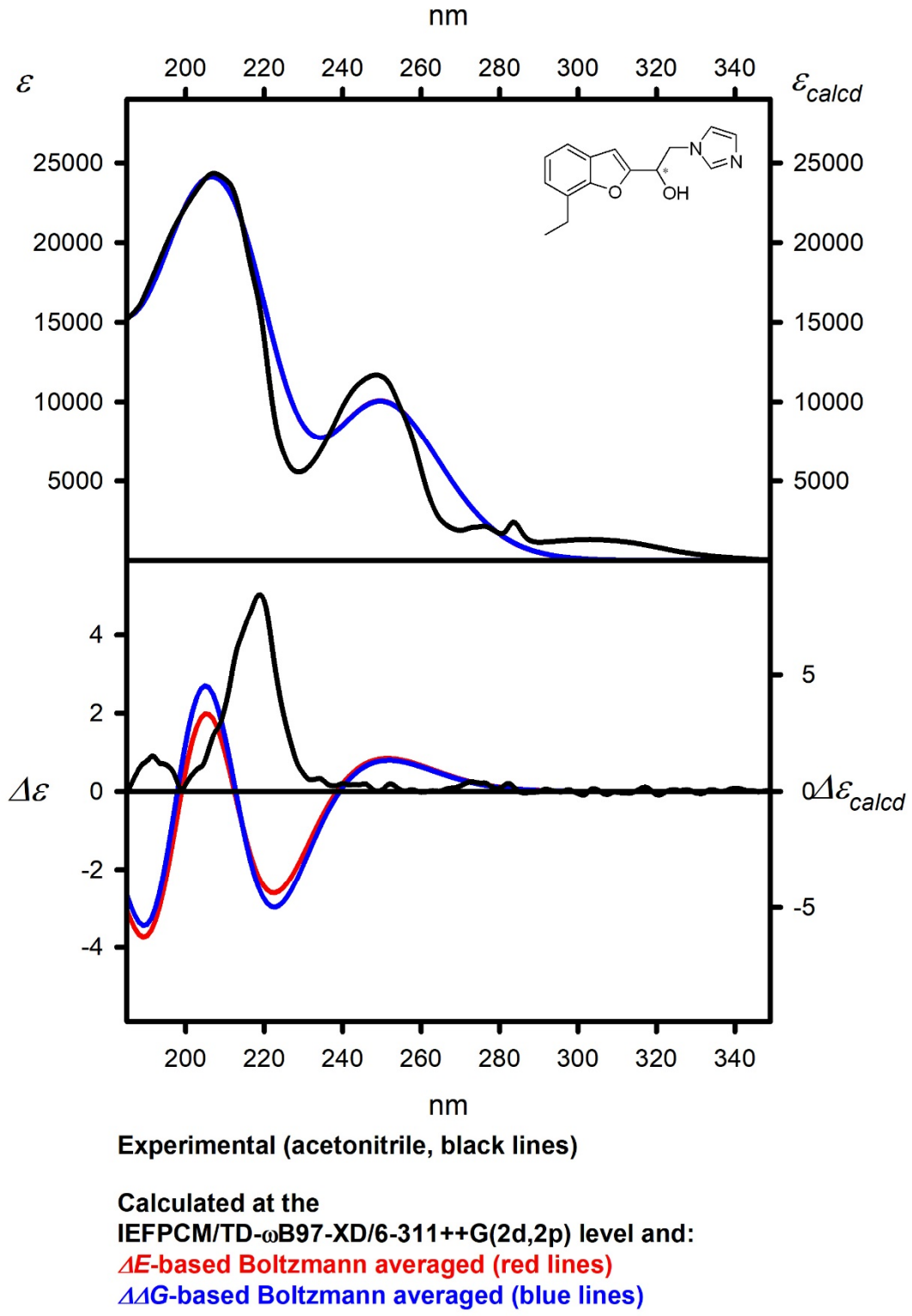


**Figure S30.** UV (upper panel) and ECD (lower panel) spectra of alcohol **14**, measured in acetonitrile (black lines), and calculated at the IEFPCM/TD-*ω*B97-XD/6-311++G(2p,2d) level and *ΔE*- (red lines) and *ΔΔG*-based Boltzmann averaged (blue lines). Wavelengths were corrected to match experimental UV maximum.

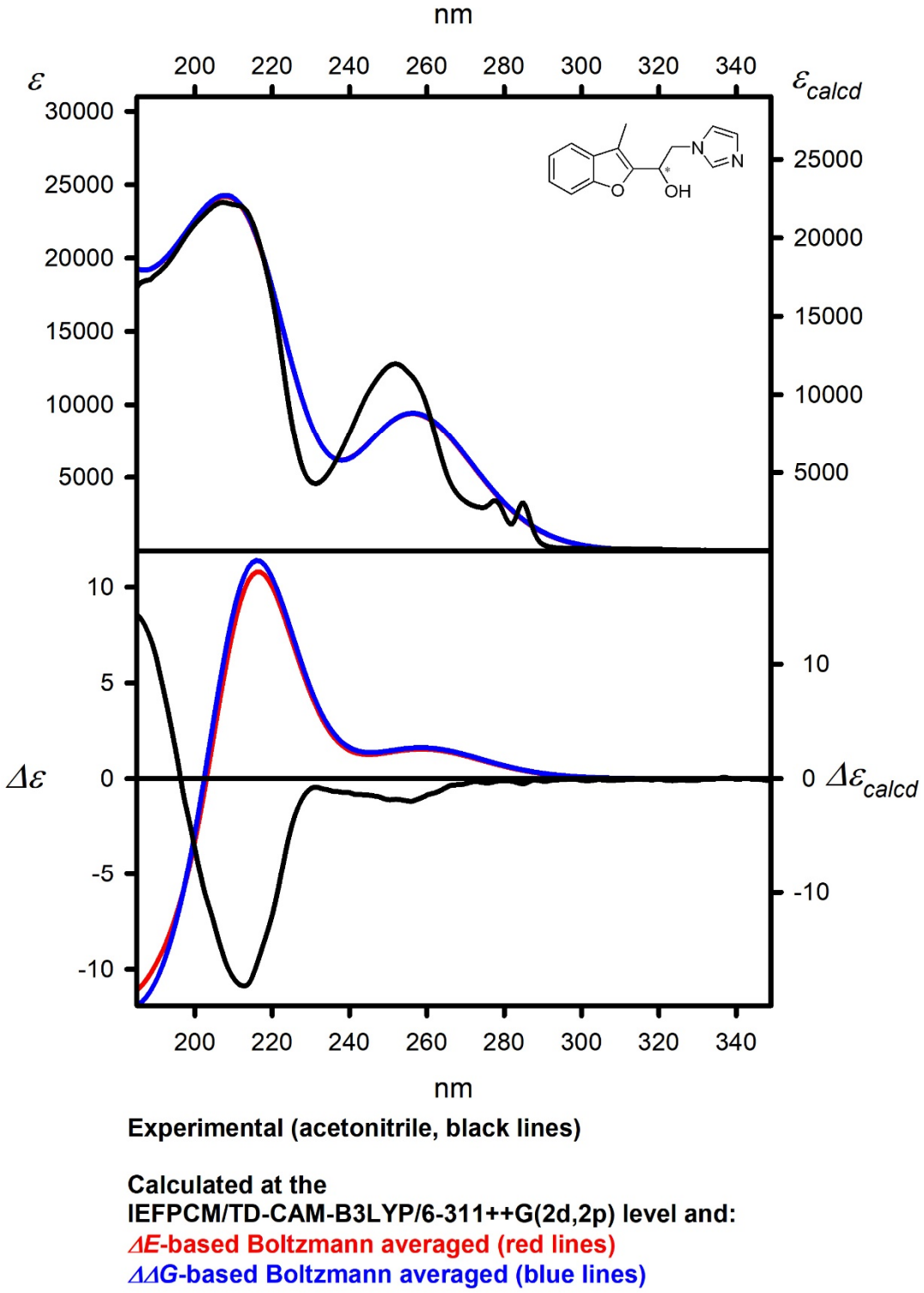


**Figure S31.** UV (upper panel) and ECD (lower panel) spectra of alcohol **15**, measured in acetonitrile (black lines), and calculated at the IEFPCM/TD-CAM-B3LYP/6-311++G(2p,2d) level and *ΔE*- (red lines) and *ΔΔG*-based Boltzmann averaged (blue lines). Wavelengths were corrected to match experimental UV maximum.

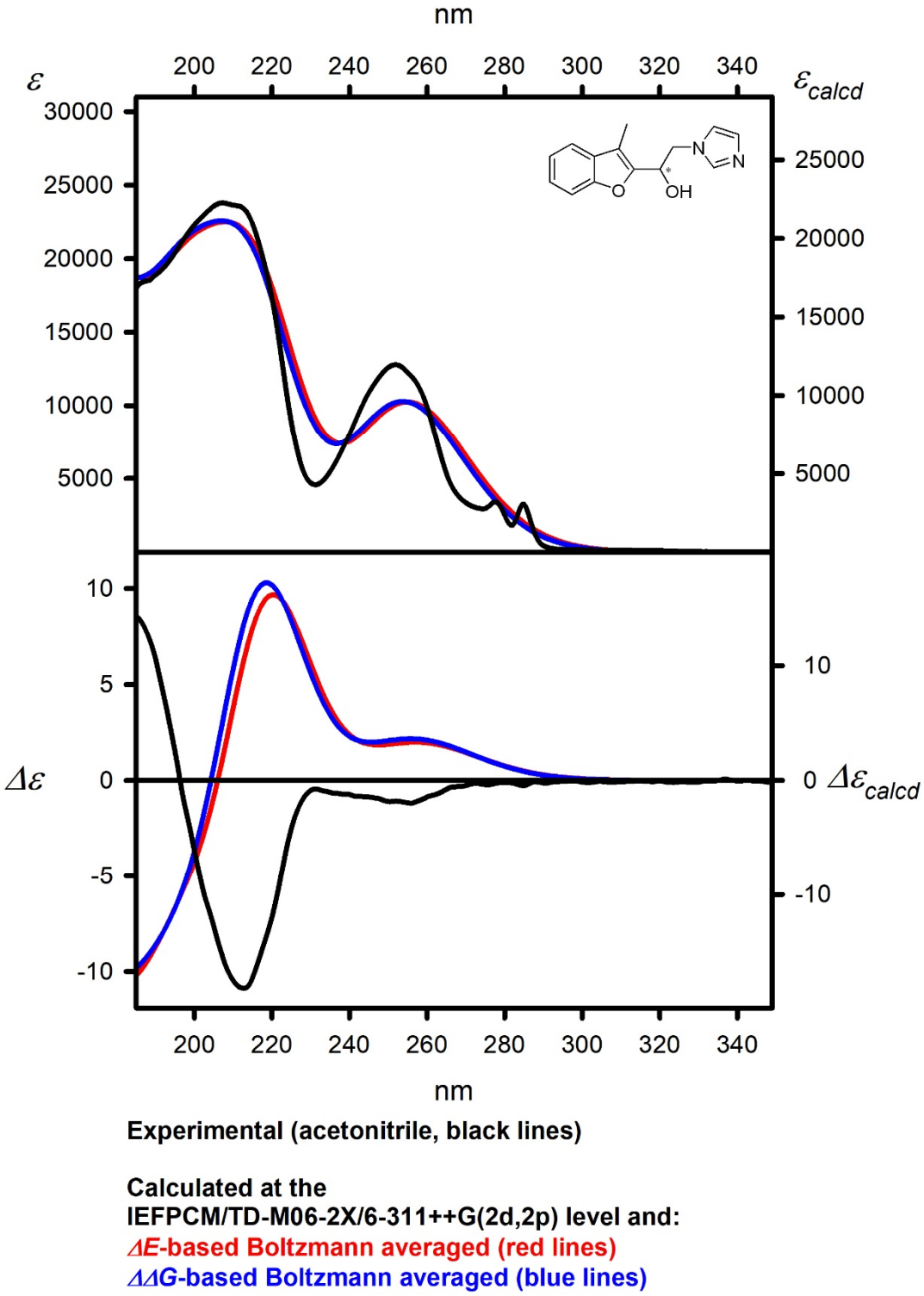


**Figure S32.** UV (upper panel) and ECD (lower panel) spectra of alcohol **15**, measured in acetonitrile (black lines), and calculated at the IEFPCM/TD-M06-2X/6-311++G(2p,2d) level and $\Delta E$- (red lines) and $\Delta\Delta G$-based Boltzmann averaged (blue lines). Wavelengths were corrected to match experimental UV maximum.

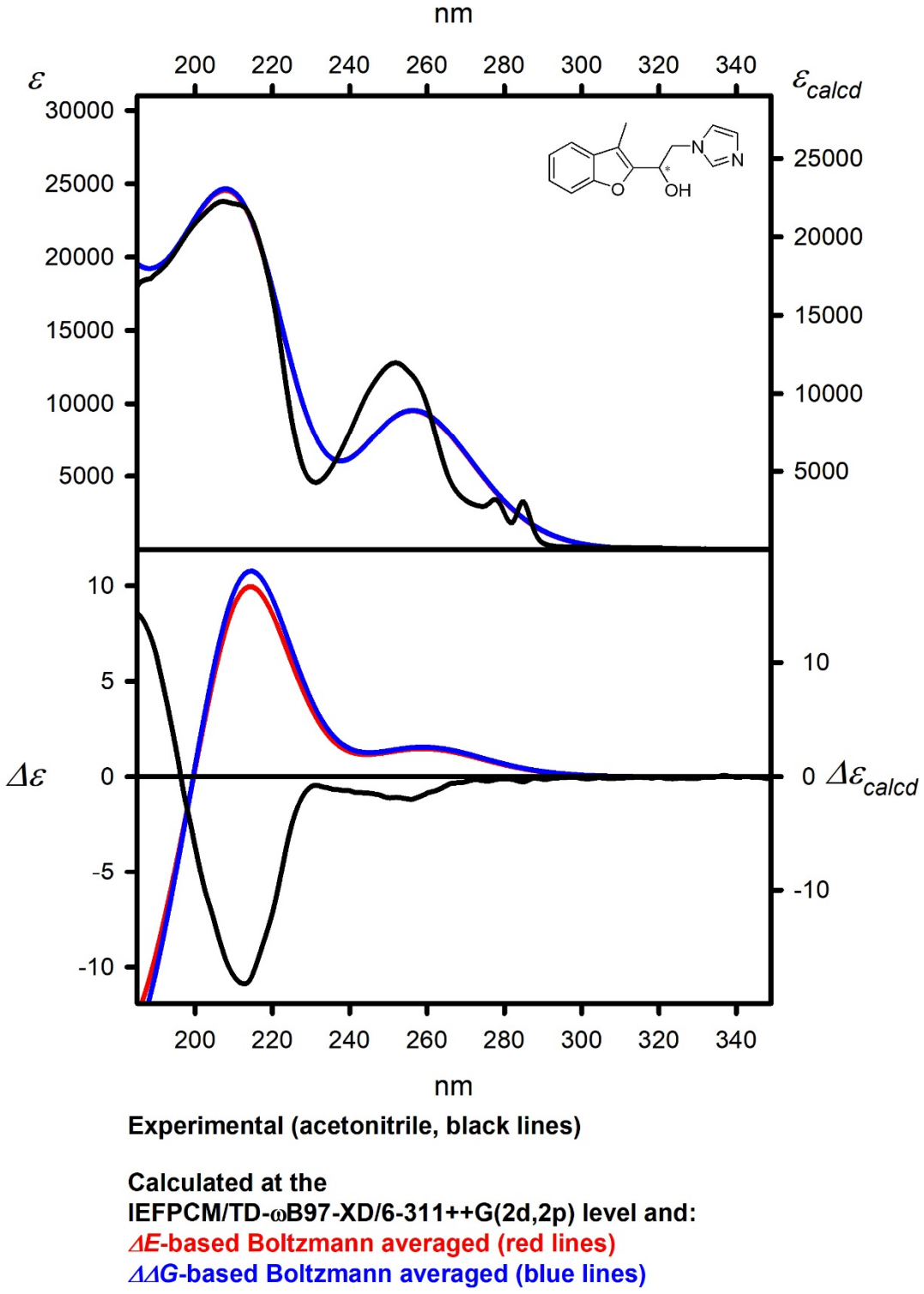


**Figure S33.** UV (upper panel) and ECD (lower panel) spectra of alcohol **15**, measured in acetonitrile (black lines), and calculated at the IEFPCM/TD-*ω*B97-XD/6-311++G(2p,2d) level and *ΔE*- (red lines) and *ΔΔG*-based Boltzmann averaged (blue lines). Wavelengths were corrected to match experimental UV maximum.

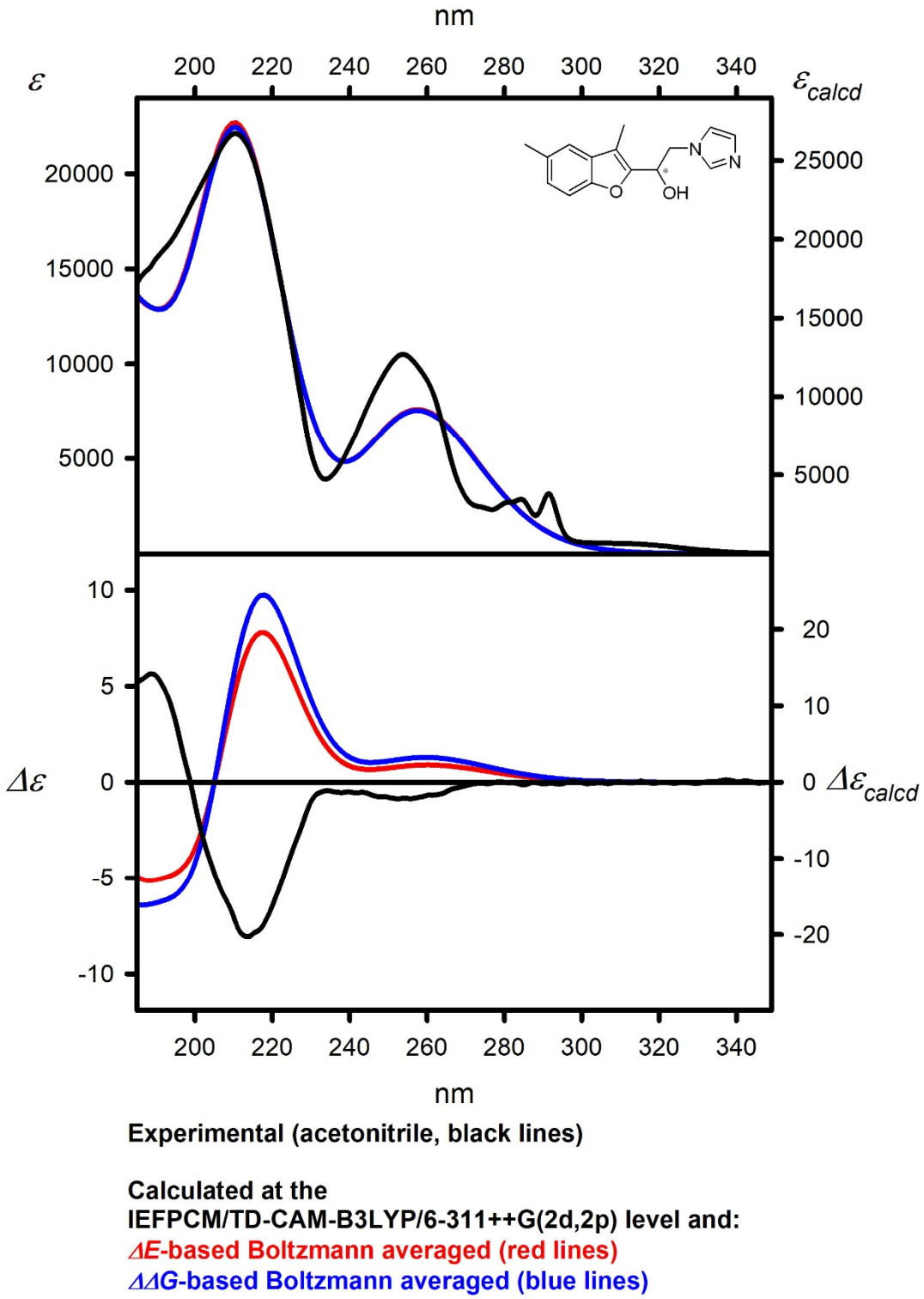


**Figure S34.** UV (upper panel) and ECD (lower panel) spectra of alcohol **16**, measured in acetonitrile (black lines), and calculated at the IEFPCM/TD-CAM-B3LYP/6-311++G(2p,2d) level and $\Delta E$- (red lines) and $\Delta\Delta G$-based Boltzmann averaged (blue lines). Wavelengths were corrected to match experimental UV maximum.

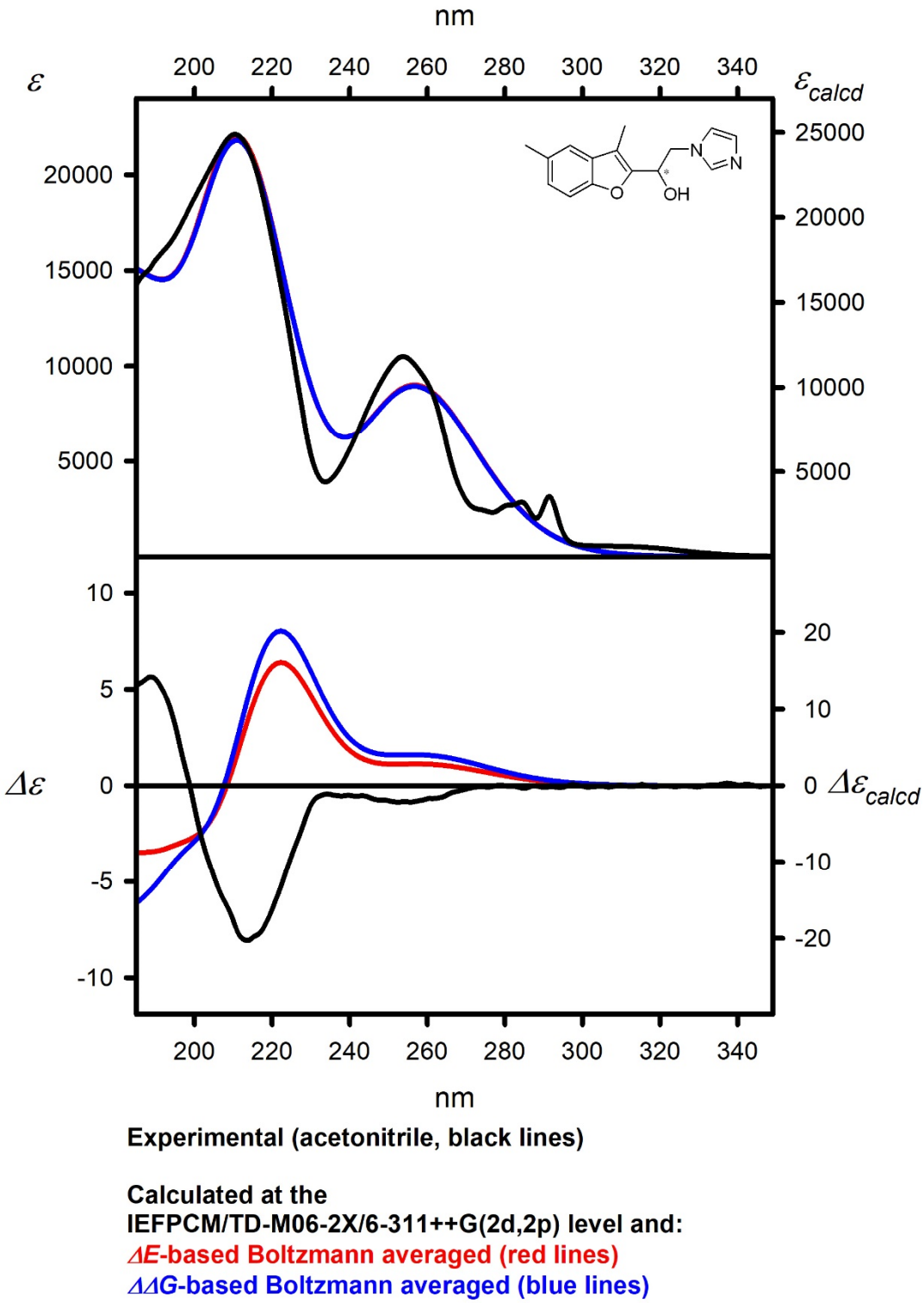


**Figure S35.** UV (upper panel) and ECD (lower panel) spectra of alcohol **16**, measured in acetonitrile (black lines), and calculated at the IEFPCM/TD-M06-2X/6-311++G(2p,2d) level and $\Delta E$- (red lines) and $\Delta\Delta G$-based Boltzmann averaged (blue lines). Wavelengths were corrected to match experimental UV maximum.

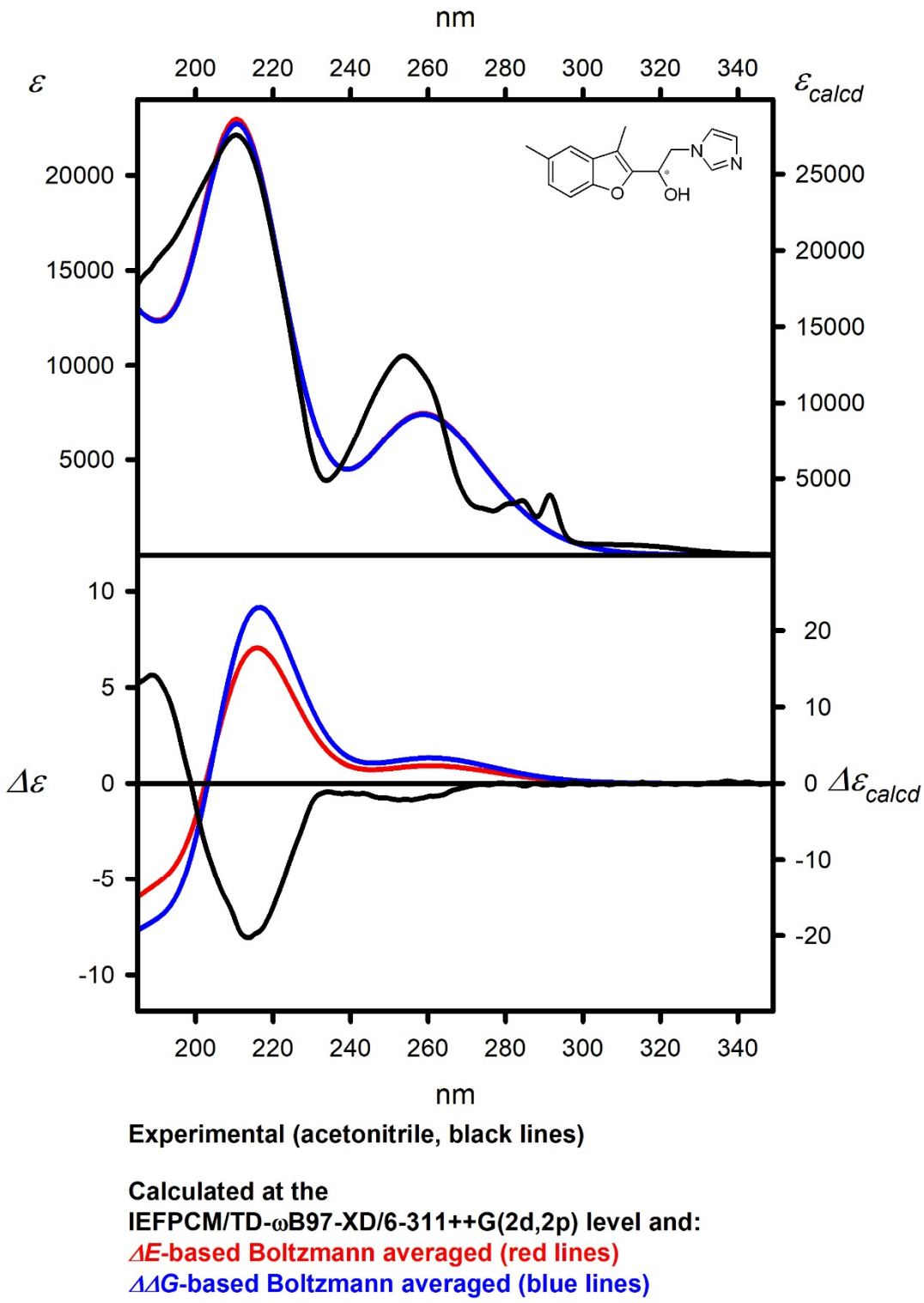


**Figure S36.** UV (upper panel) and ECD (lower panel) spectra of alcohol **16**, measured in acetonitrile (black lines), and calculated at the IEFPCM/TD-*ω*B97-XD/6-311++G(2p,2d) level and *ΔE*- (red lines) and *ΔΔG*-based Boltzmann averaged (blue lines). Wavelengths were corrected to match experimental UV maximum.

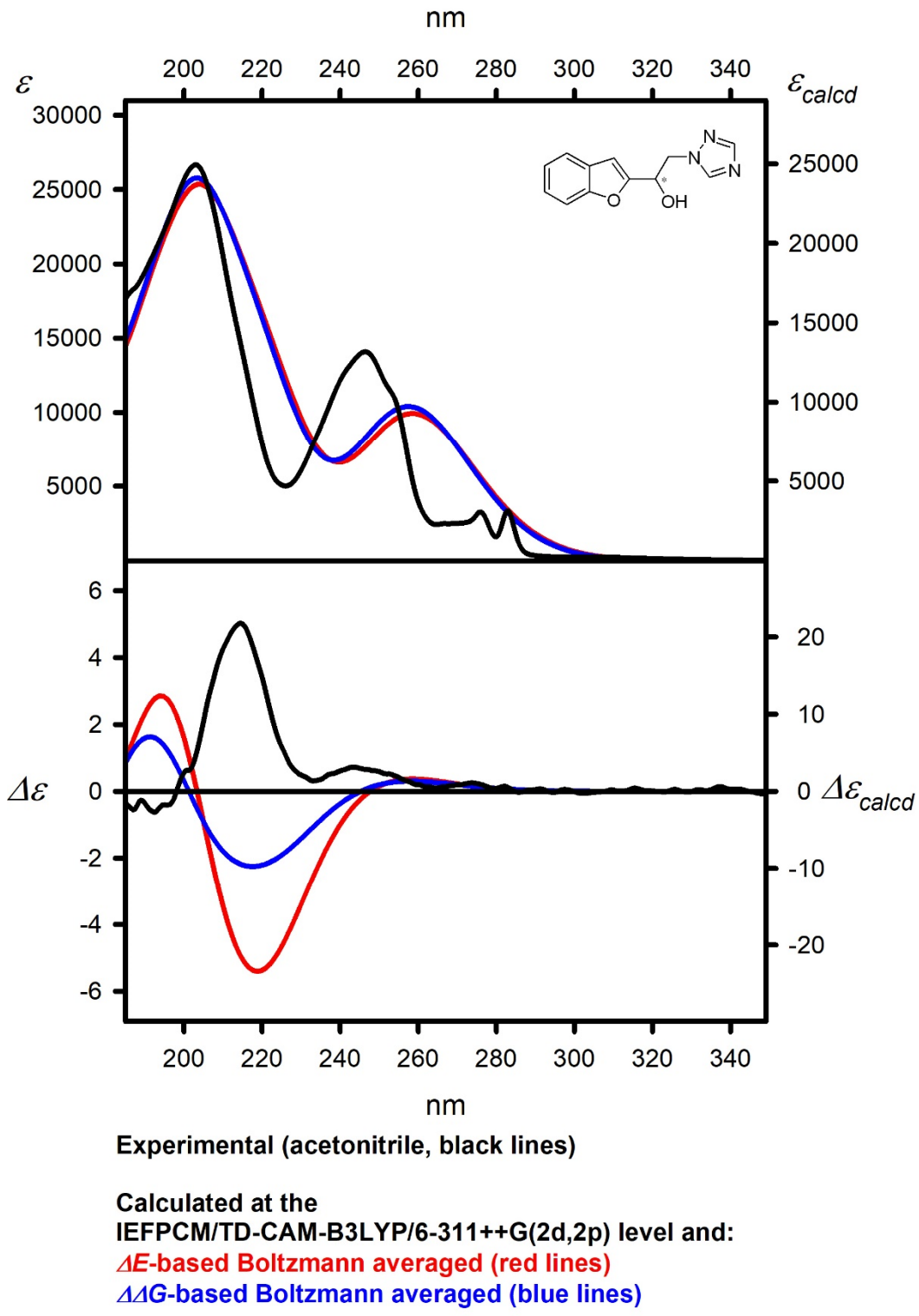


**Figure S37.** UV (upper panel) and ECD (lower panel) spectra of alcohol **17**, measured in acetonitrile (black lines), and calculated at the IEFPCM/TD-CAM-B3LYP/6-311++G(2p,2d) level and $\Delta E$- (red lines) and $\Delta\Delta G$-based Boltzmann averaged (blue lines). Wavelengths were corrected to match experimental UV maximum.

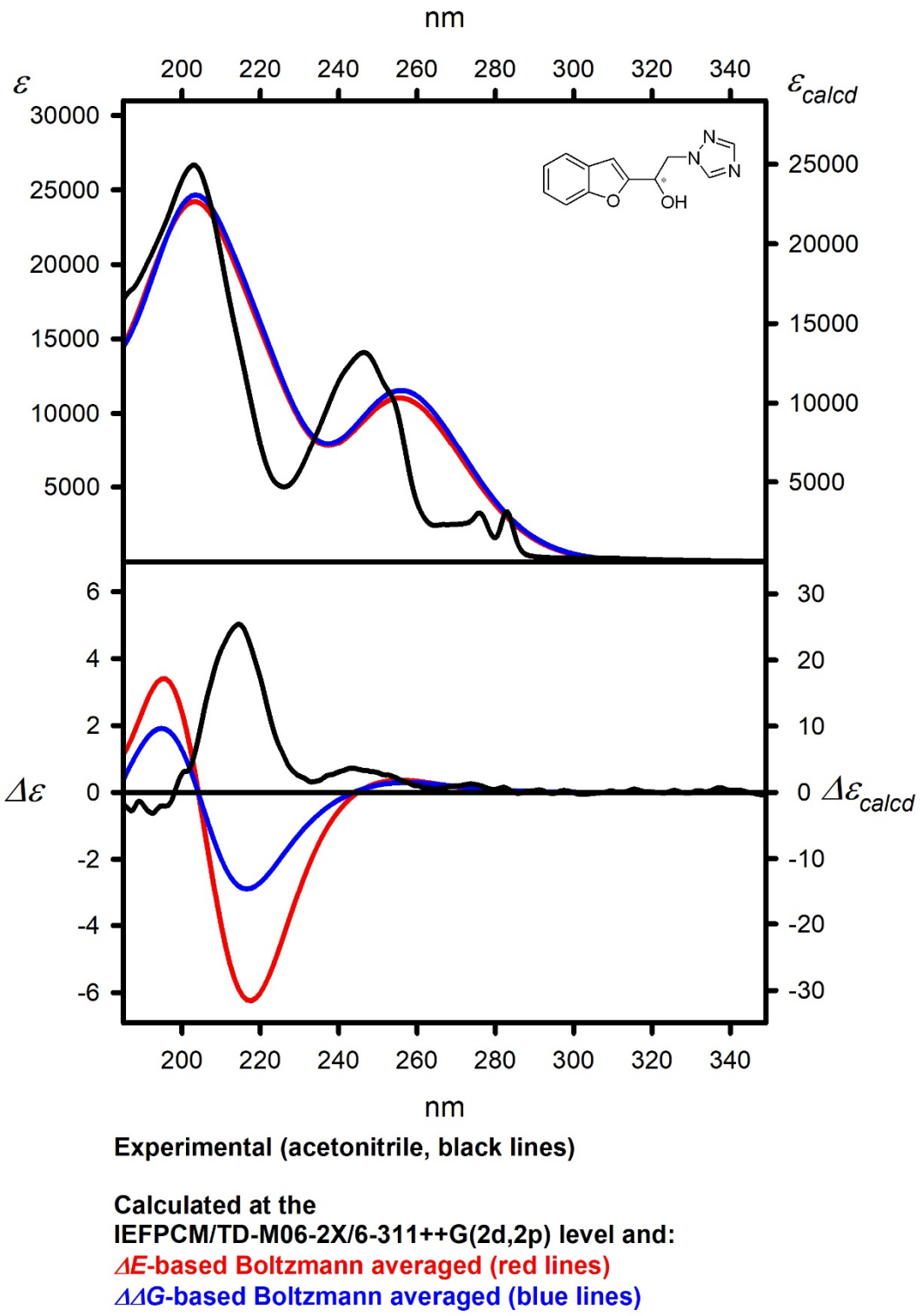


**Figure S38.** UV (upper panel) and ECD (lower panel) spectra of alcohol **17**, measured in acetonitrile (black lines), and calculated at the IEFPCM/TD-M06-2X/6-311++G(2p,2d) level and *ΔE*- (red lines) and *ΔΔG*-based Boltzmann averaged (blue lines). Wavelengths were corrected to match experimental UV maximum.

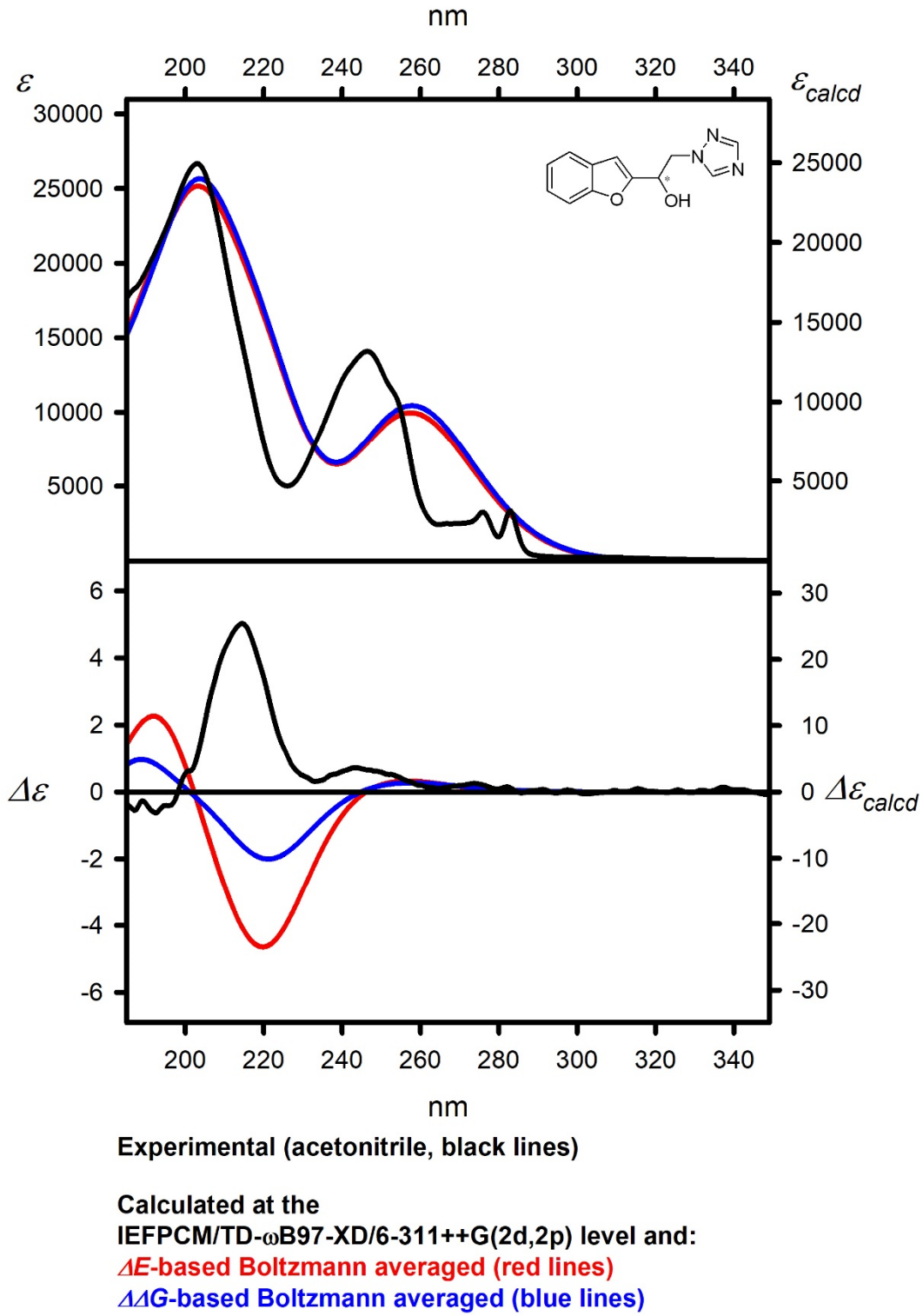


**Figure S39.** UV (upper panel) and ECD (lower panel) spectra of alcohol **17**, measured in acetonitrile (black lines), and calculated at the IEFPCM/TD-*ω*B97-XD/6-311++G(2p,2d) level and *ΔE*- (red lines) and *ΔΔG*-based Boltzmann averaged (blue lines). Wavelengths were corrected to match experimental UV maximum.

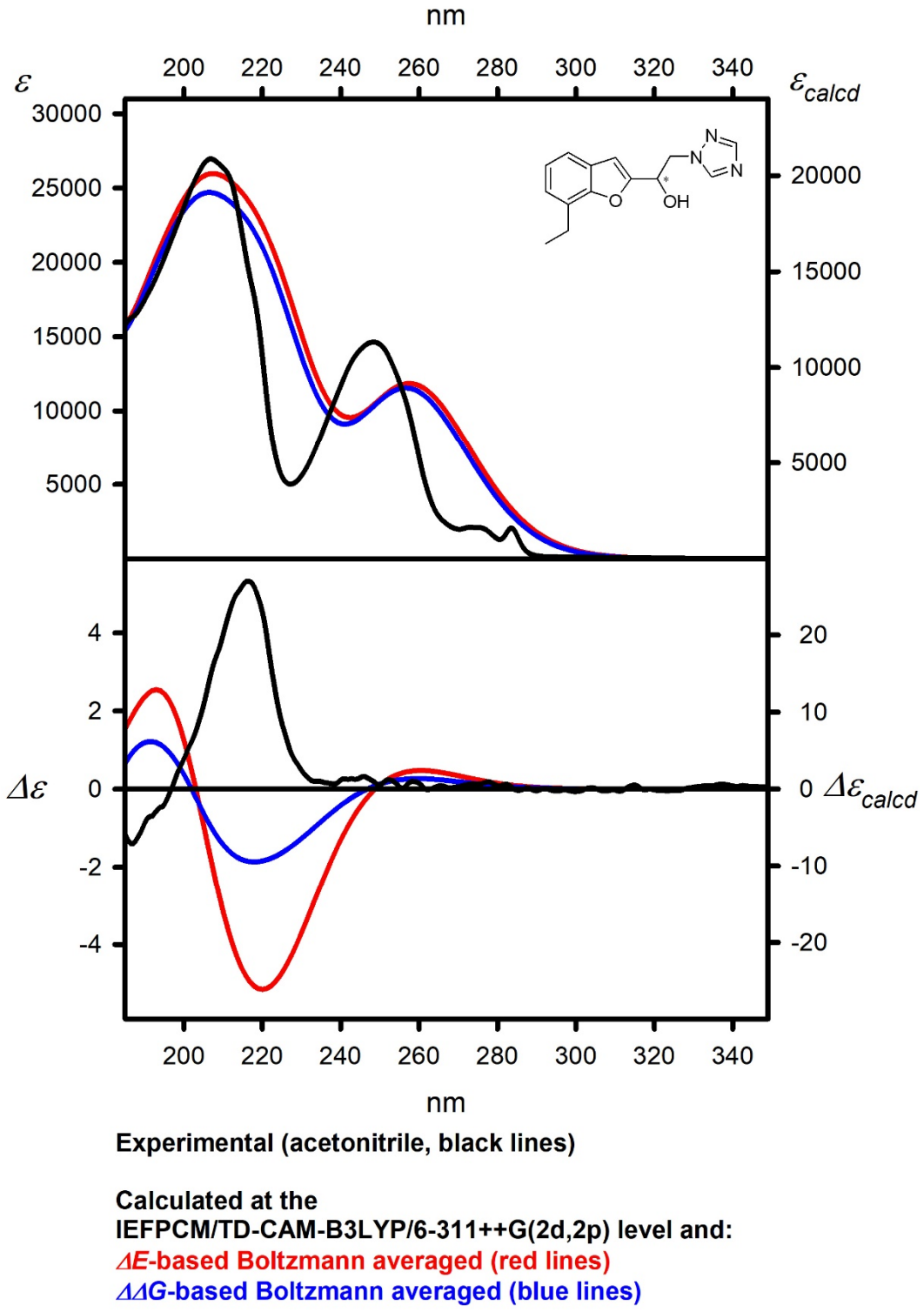


**Figure S40.** UV (upper panel) and ECD (lower panel) spectra of alcohol **18**, measured in acetonitrile (black lines), and calculated at the IEFPCM/TD-CAM-B3LYP/6-311++G(2p,2d) level and $\Delta E$- (red lines) and $\Delta\Delta G$-based Boltzmann averaged (blue lines). Wavelengths were corrected to match experimental UV maximum.

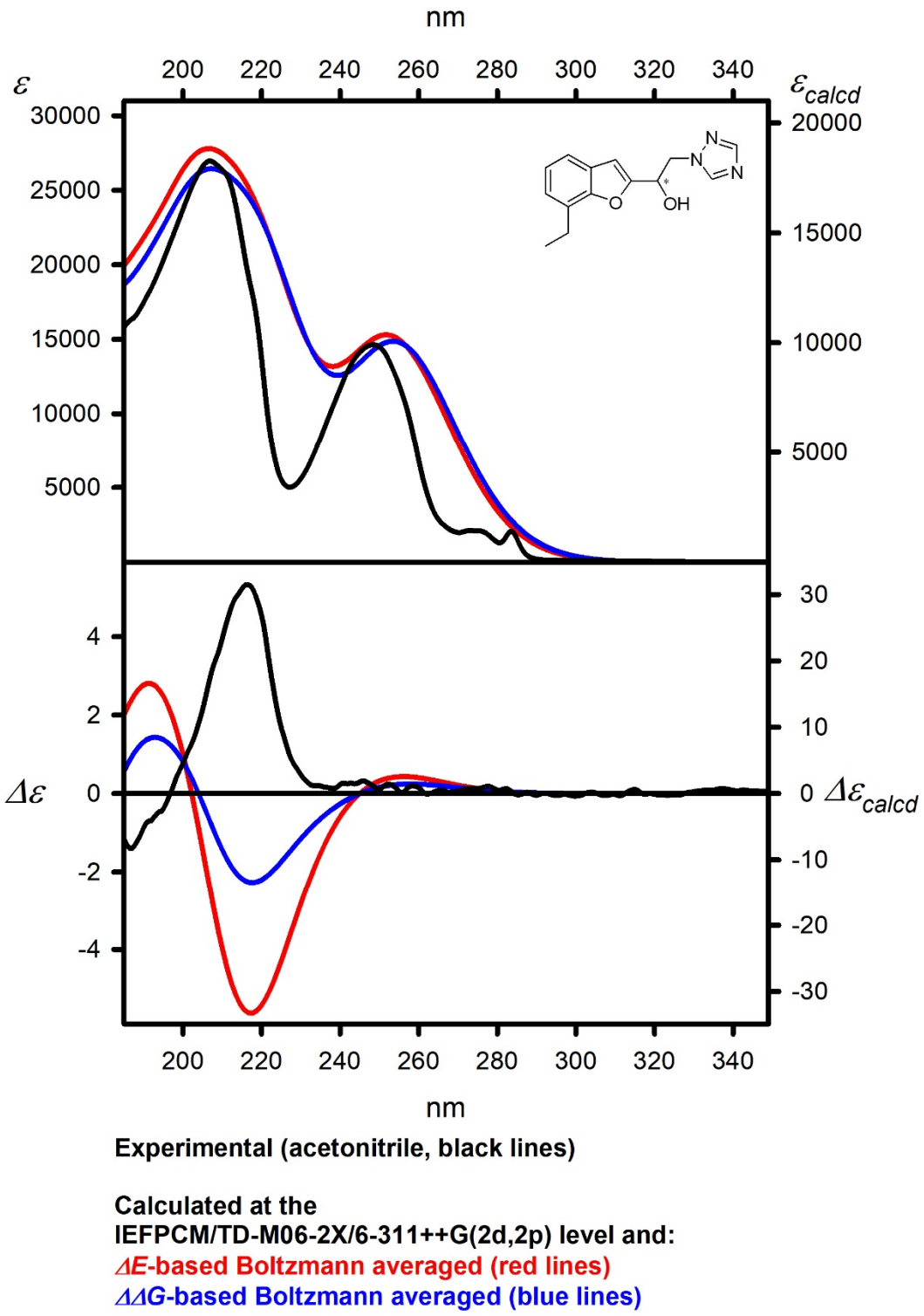


**Figure S41.** UV (upper panel) and ECD (lower panel) spectra of alcohol **18**, measured in acetonitrile (black lines), and calculated at the IEFPCM/TD-M06-2X/6-311++G(2p,2d) level and $\Delta E$- (red lines) and $\Delta\Delta G$-based Boltzmann averaged (blue lines). Wavelengths were corrected to match experimental UV maximum.

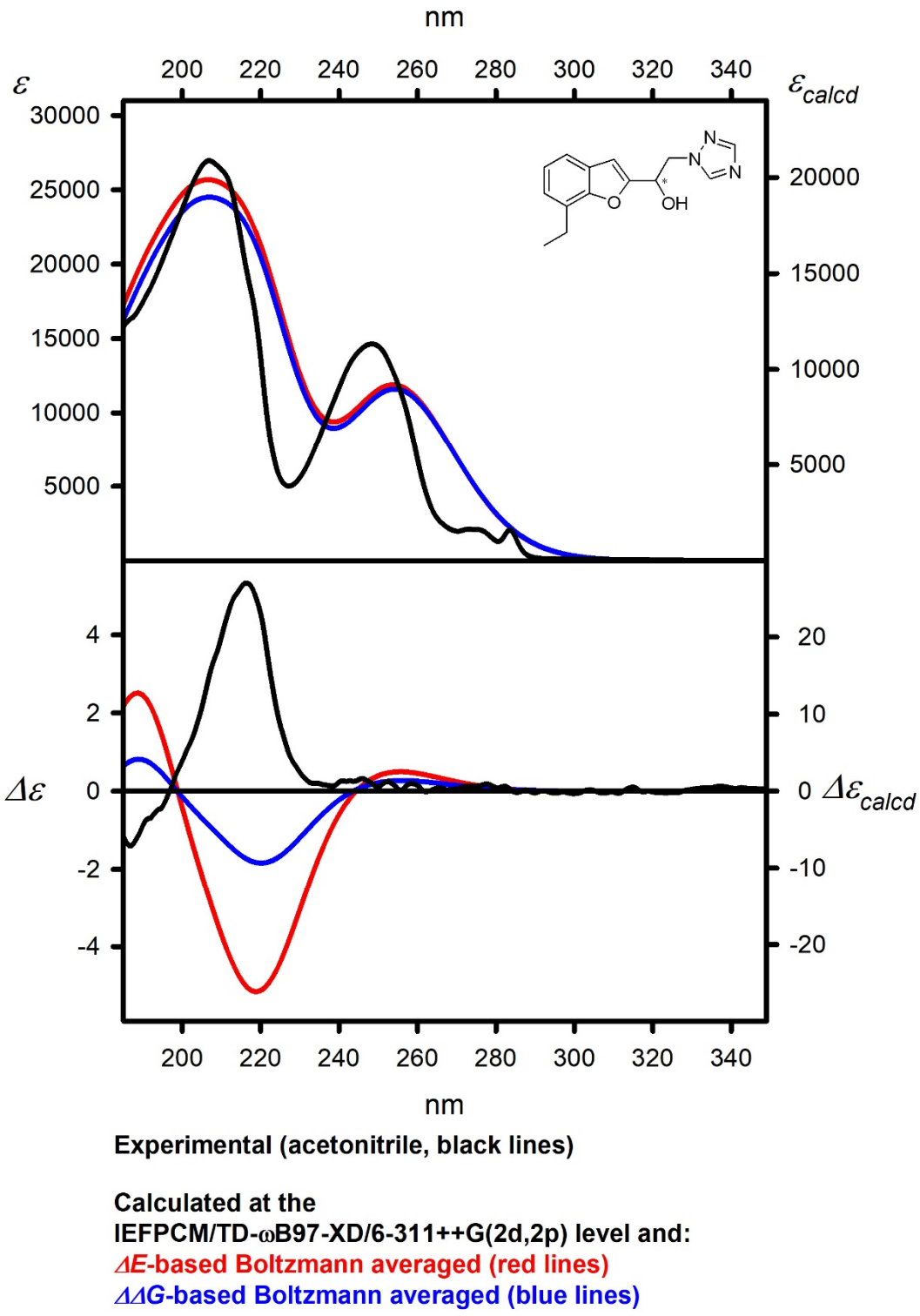


**Figure S42.** UV (upper panel) and ECD (lower panel) spectra of alcohol **18**, measured in acetonitrile (black lines), and calculated at the IEFPCM/TD-*ω*B97-XD/6-311++G(2p,2d) level and *ΔE*- (red lines) and *ΔΔG*-based Boltzmann averaged (blue lines). Wavelengths were corrected to match experimental UV maximum.

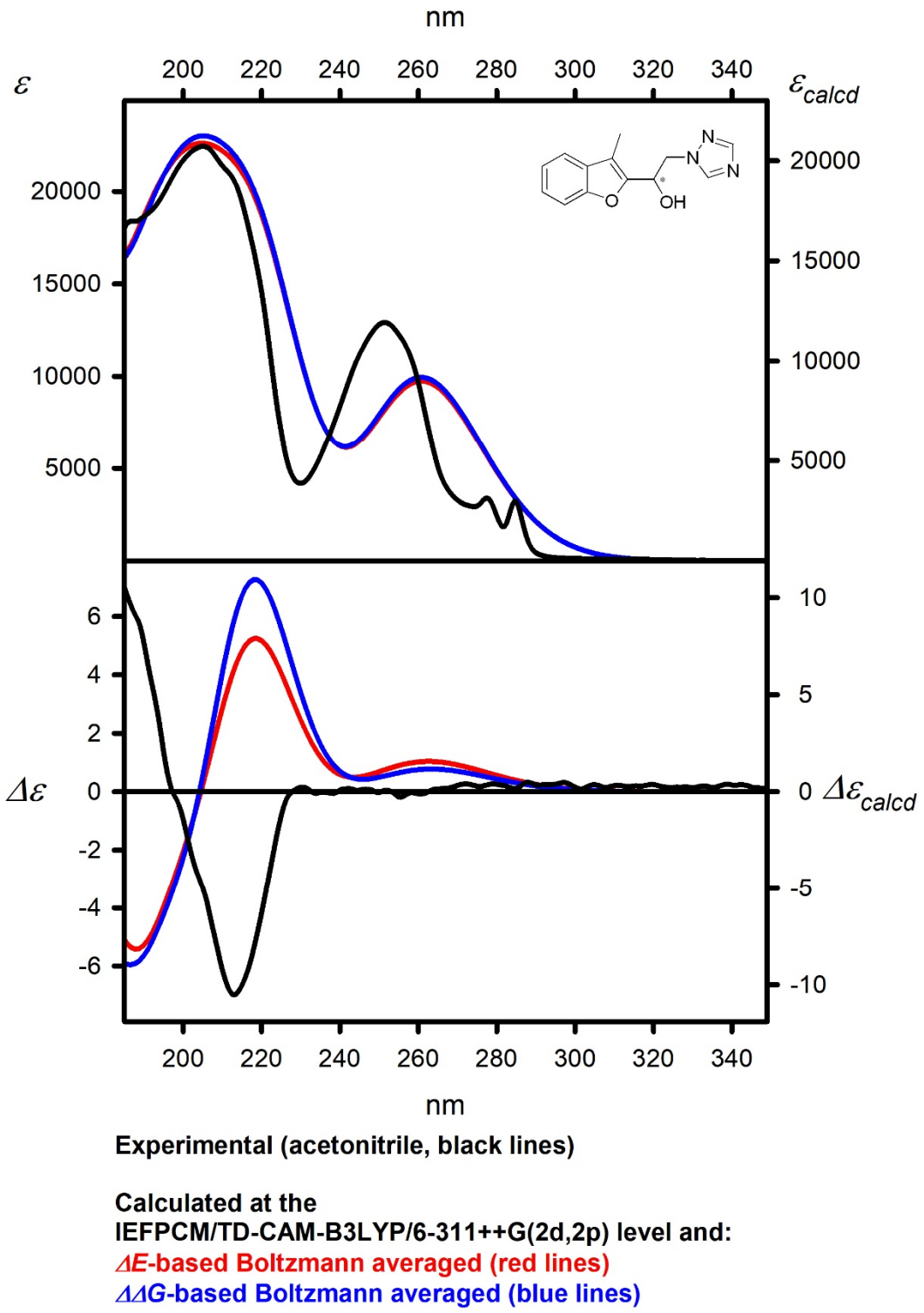


**Figure S43.** UV (upper panel) and ECD (lower panel) spectra of alcohol **19**, measured in acetonitrile (black lines), and calculated at the IEFPCM/TD-CAM-B3LYP/6-311++G(2p,2d) level and *ΔE*- (red lines) and *ΔΔG*-based Boltzmann averaged (blue lines). Wavelengths were corrected to match experimental UV maximum.

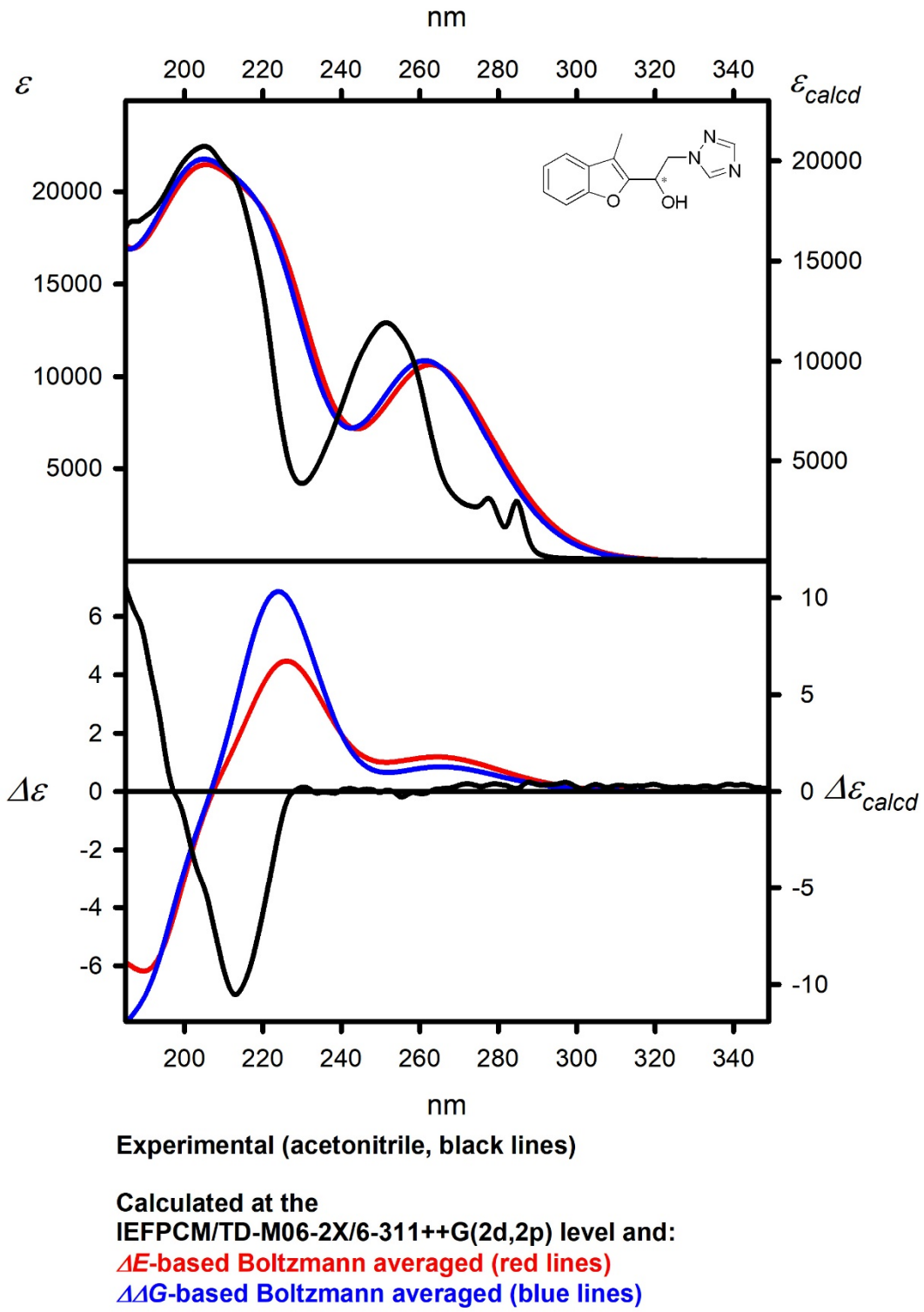


**Figure S44.** UV (upper panel) and ECD (lower panel) spectra of alcohol **19**, measured in acetonitrile (black lines), and calculated at the IEFPCM/TD-M06-2X/6-311++G(2p,2d) level and $\Delta E$- (red lines) and $\Delta\Delta G$-based Boltzmann averaged (blue lines). Wavelengths were corrected to match experimental UV maximum.

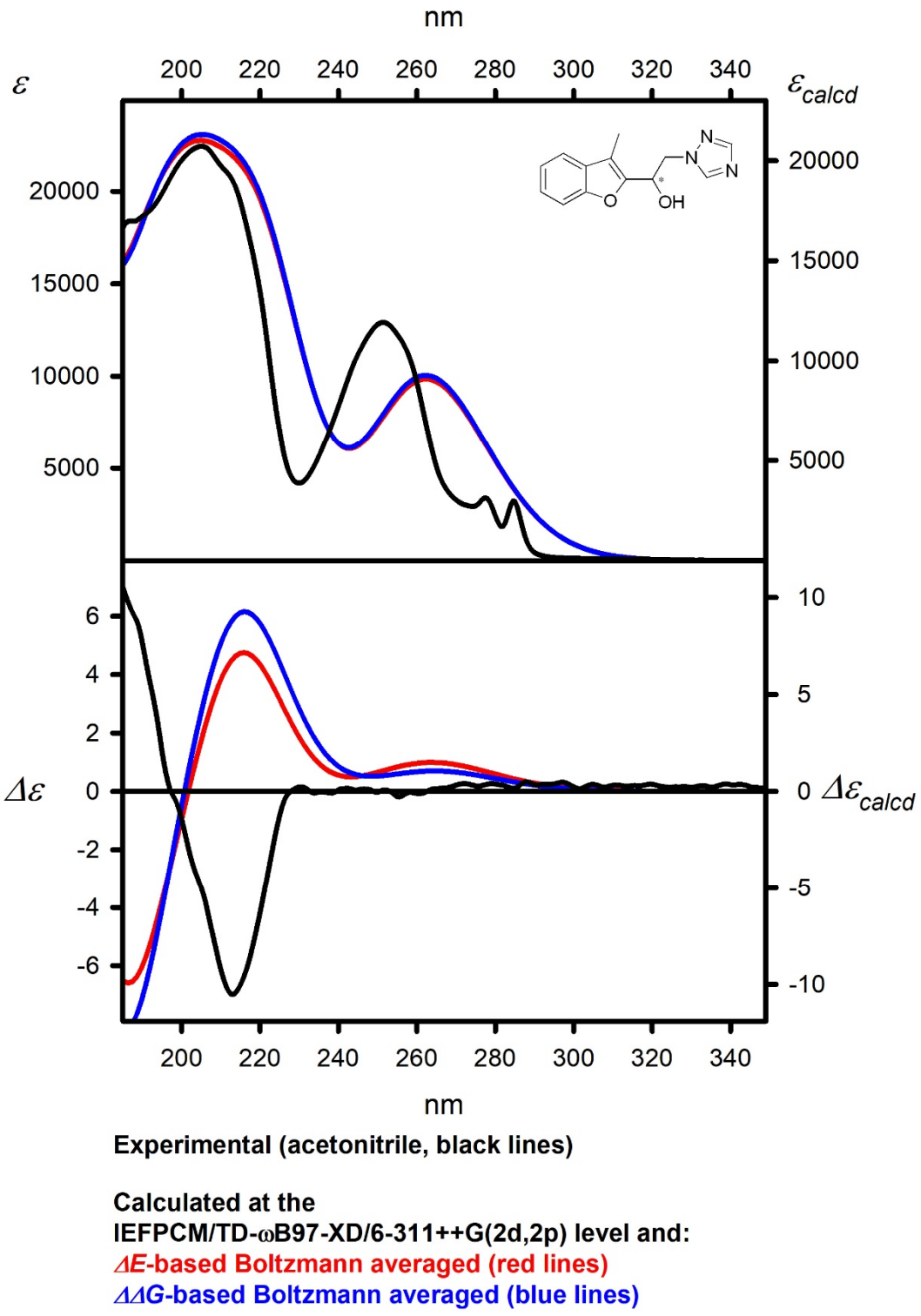


**Figure S45.** UV (upper panel) and ECD (lower panel) spectra of alcohol **19**, measured in acetonitrile (black lines), and calculated at the IEFPCM/TD-*ω*B97-XD/6-311++G(2p,2d) level and *ΔE*- (red lines) and *ΔΔG*-based Boltzmann averaged (blue lines). Wavelengths were corrected to match experimental UV maximum.

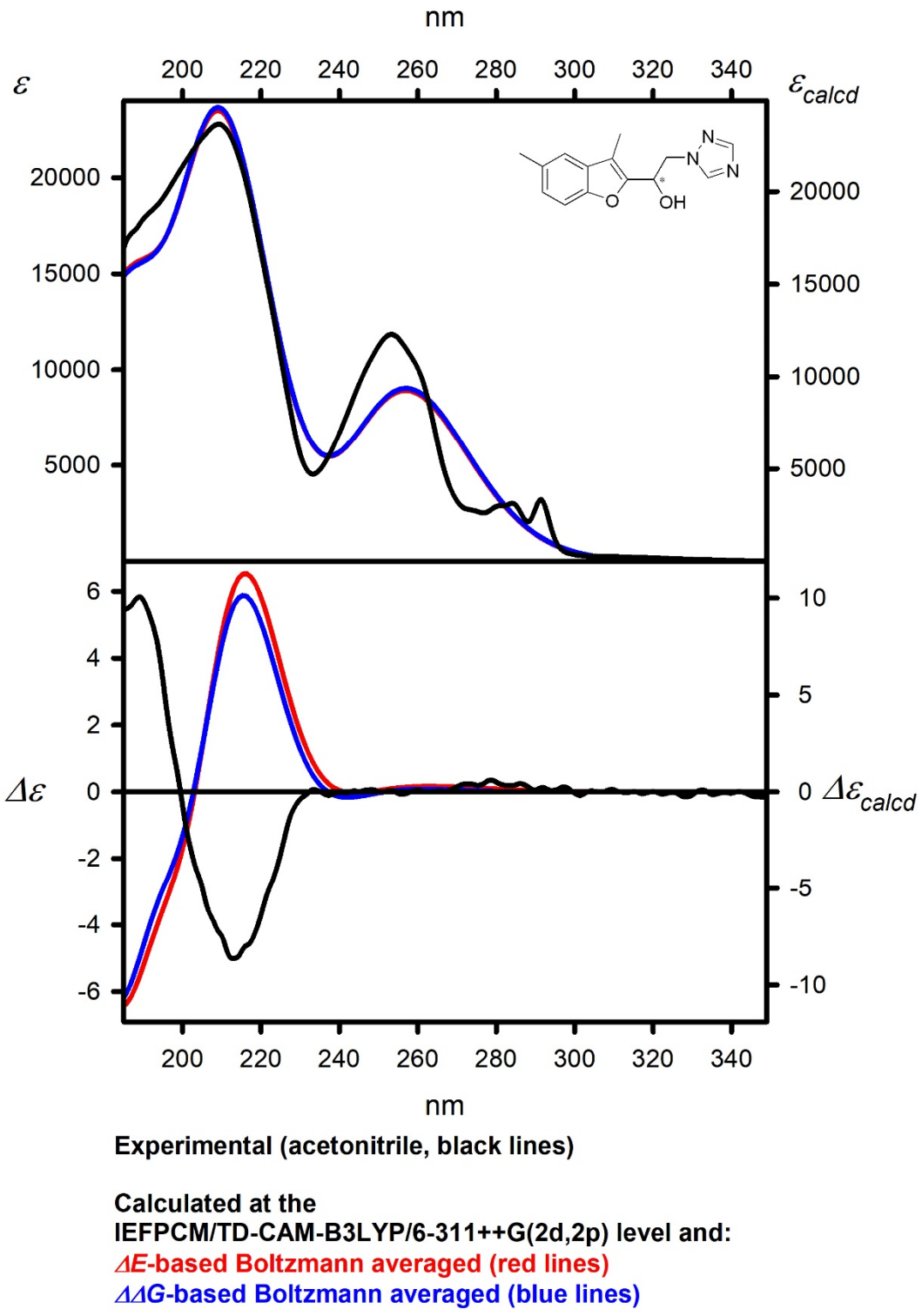


**Figure S46.** UV (upper panel) and ECD (lower panel) spectra of alcohol **20**, measured in acetonitrile (black lines), and calculated at the IEFPCM/TD-CAM-B3LYP/6-311++G(2p,2d) level and *ΔE*- (red lines) and *ΔΔG*-based Boltzmann averaged (blue lines). Wavelengths were corrected to match experimental UV maximum.

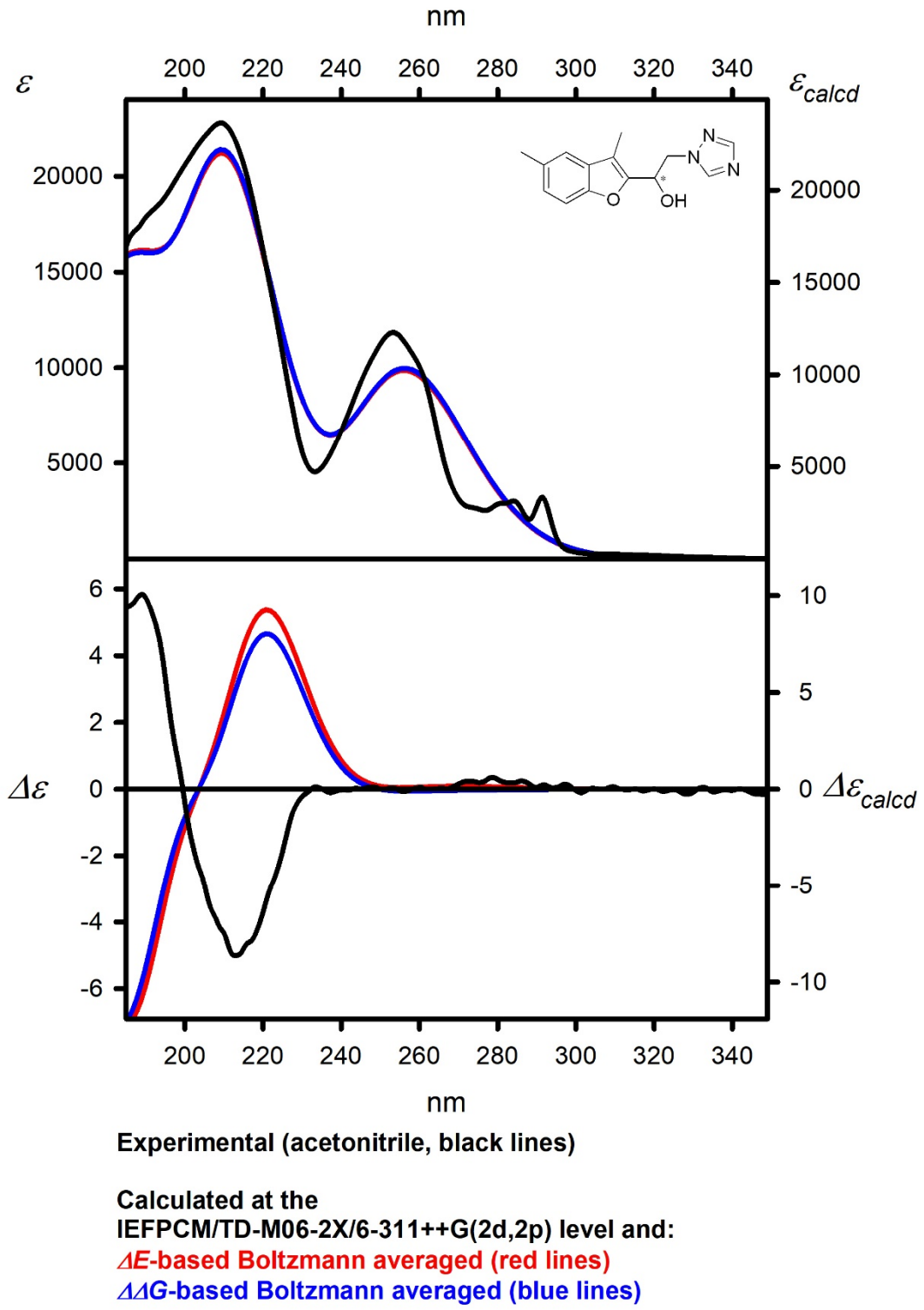


**Figure S47.** UV (upper panel) and ECD (lower panel) spectra of alcohol **20**, measured in acetonitrile (black lines), and calculated at the IEFPCM/TD-M06-2X/6-311++G(2p,2d) level and $\Delta E$- (red lines) and $\Delta\Delta G$-based Boltzmann averaged (blue lines). Wavelengths were corrected to match experimental UV maximum.

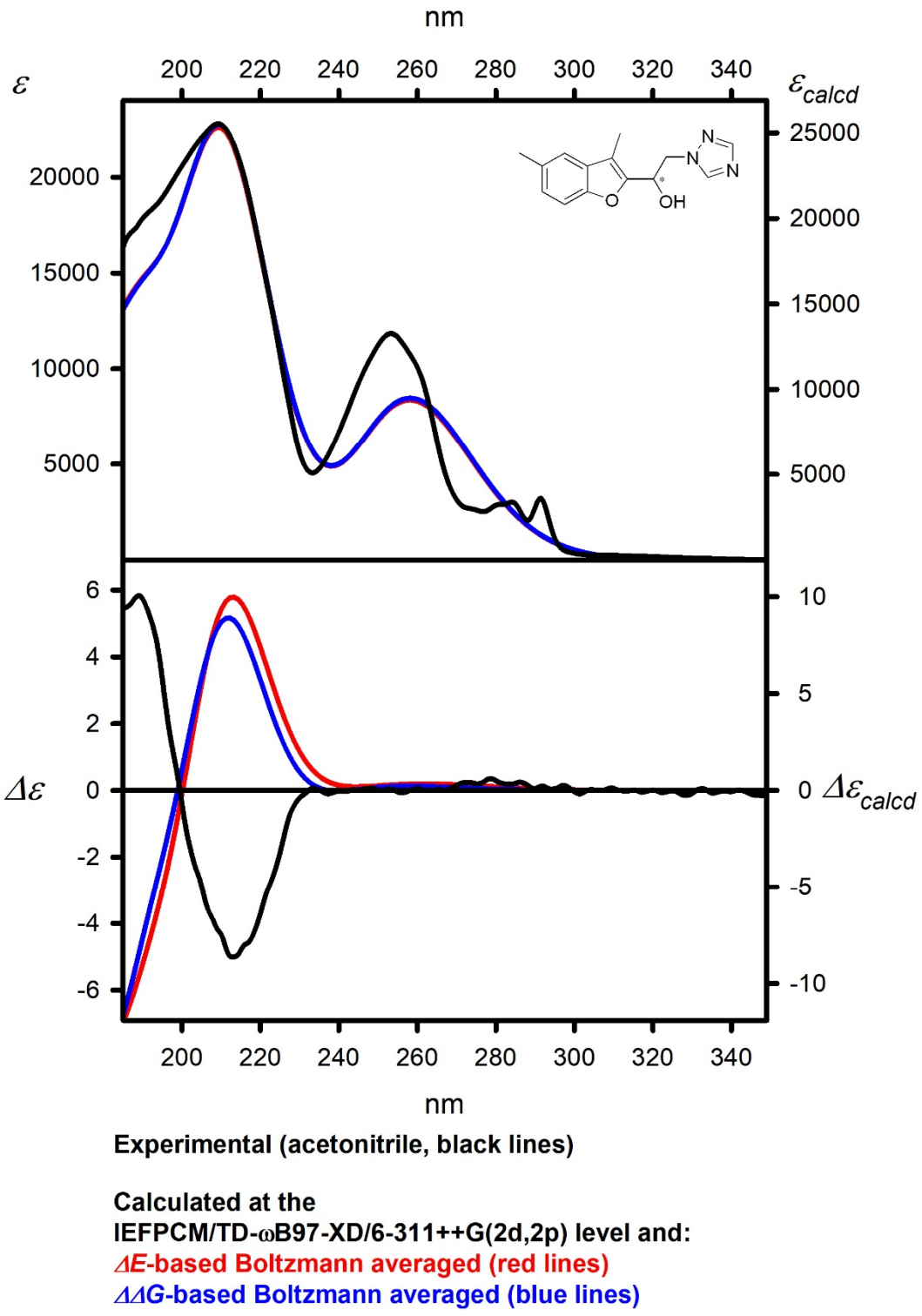


**Figure S48.** UV (upper panel) and ECD (lower panel) spectra of alcohol **20**, measured in acetonitrile (black lines), and calculated at the IEFPCM/TD-*ω*B97-XD/6-311++G(2p,2d) level and *ΔE*- (red lines) and *ΔΔG*-based Boltzmann averaged (blue lines). Wavelengths were corrected to match experimental UV maximum.

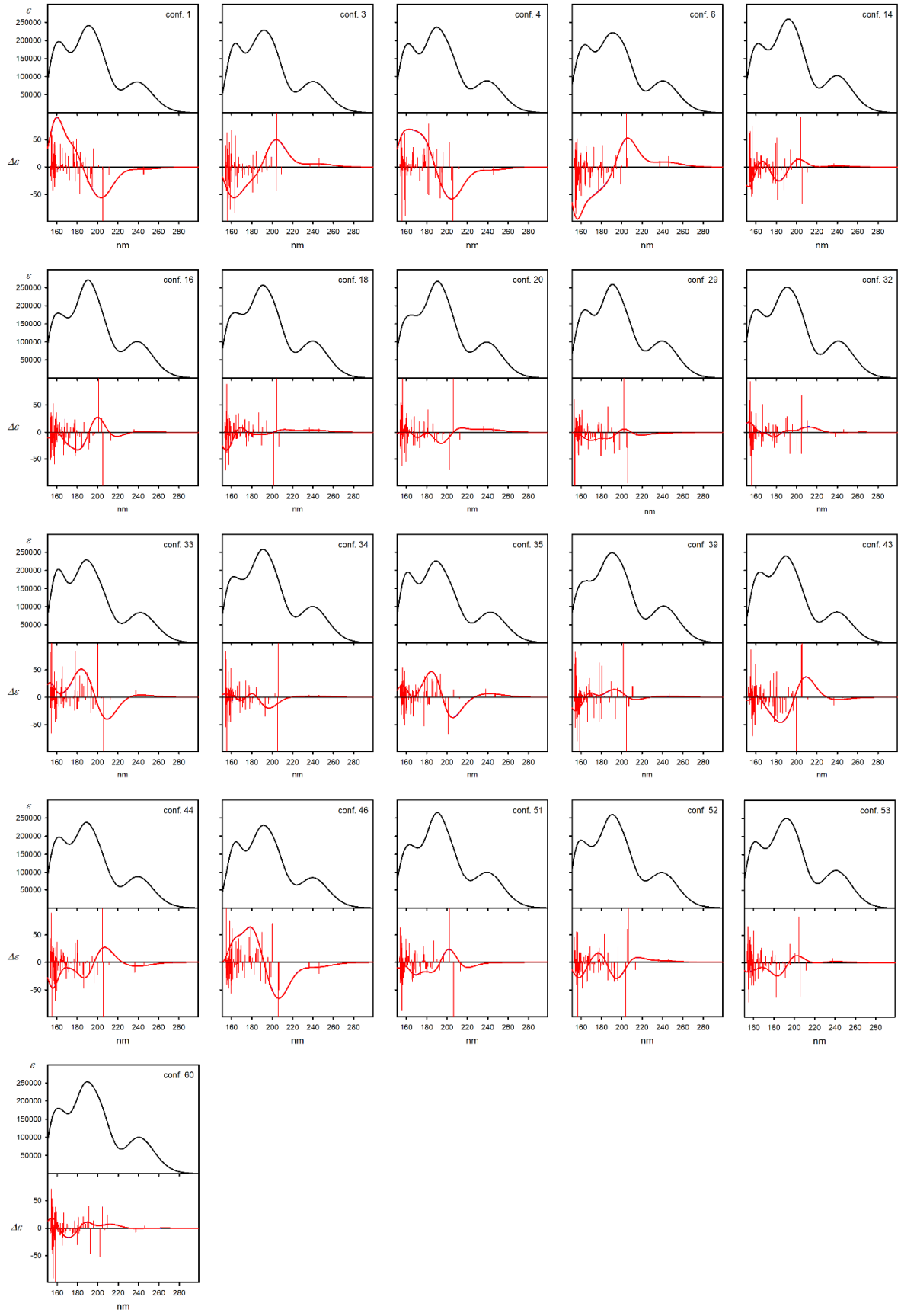


**Figure S49.** UV (upper panels) and ECD (lower panels) spectra calculated at the IEFPCM/TD-CAM-B3LYP/6-311++G(2d,2p) level for individual low-energy conformers of **13**. Wavelengths were not corrected.

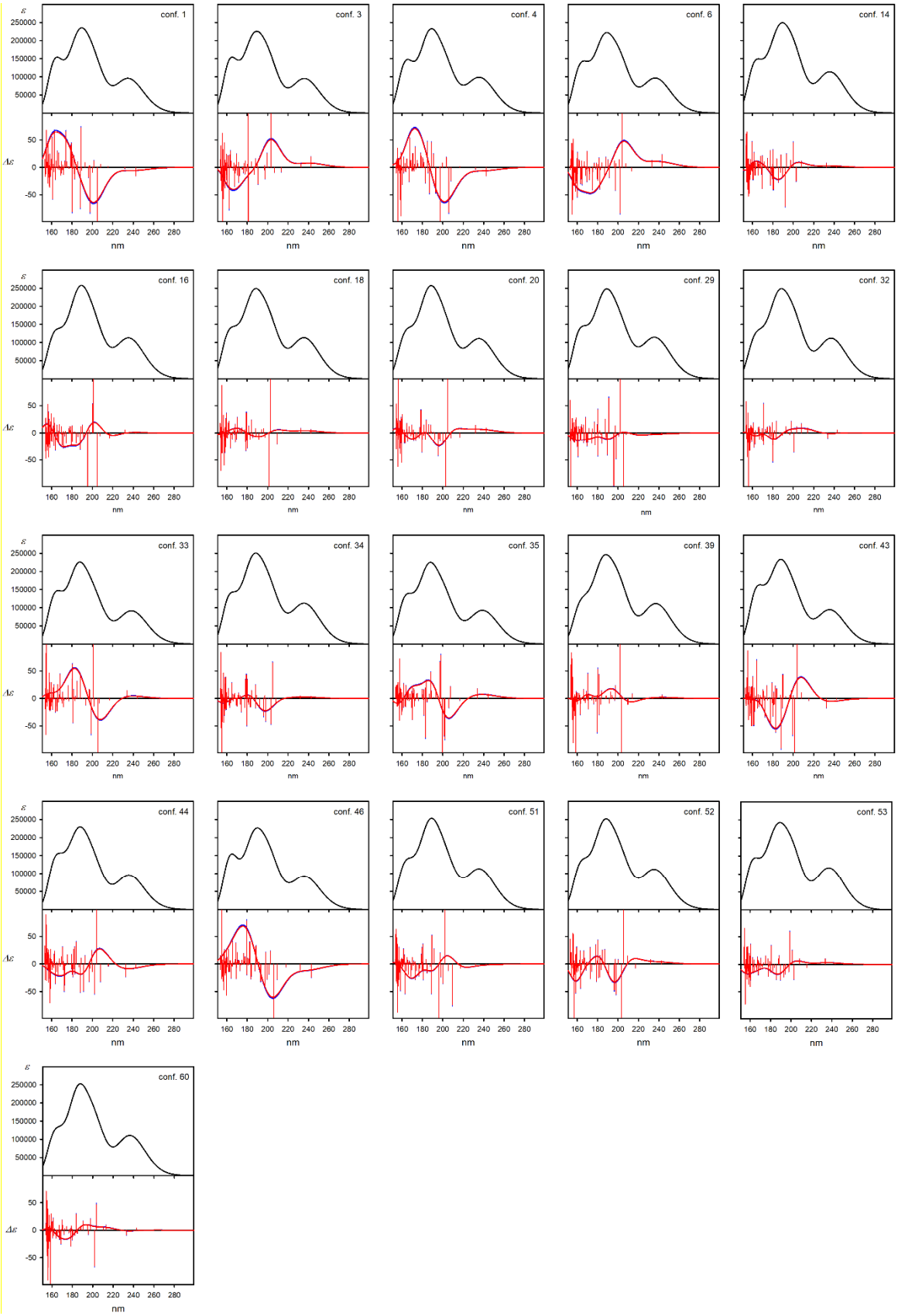


**Figure S50.** UV (upper panels) and ECD (lower panels) spectra calculated at the IEFPCM/TD-M06-2X/6-311++G(2d,2p) level for individual low-energy conformers of **13**. Wavelengths were not corrected.

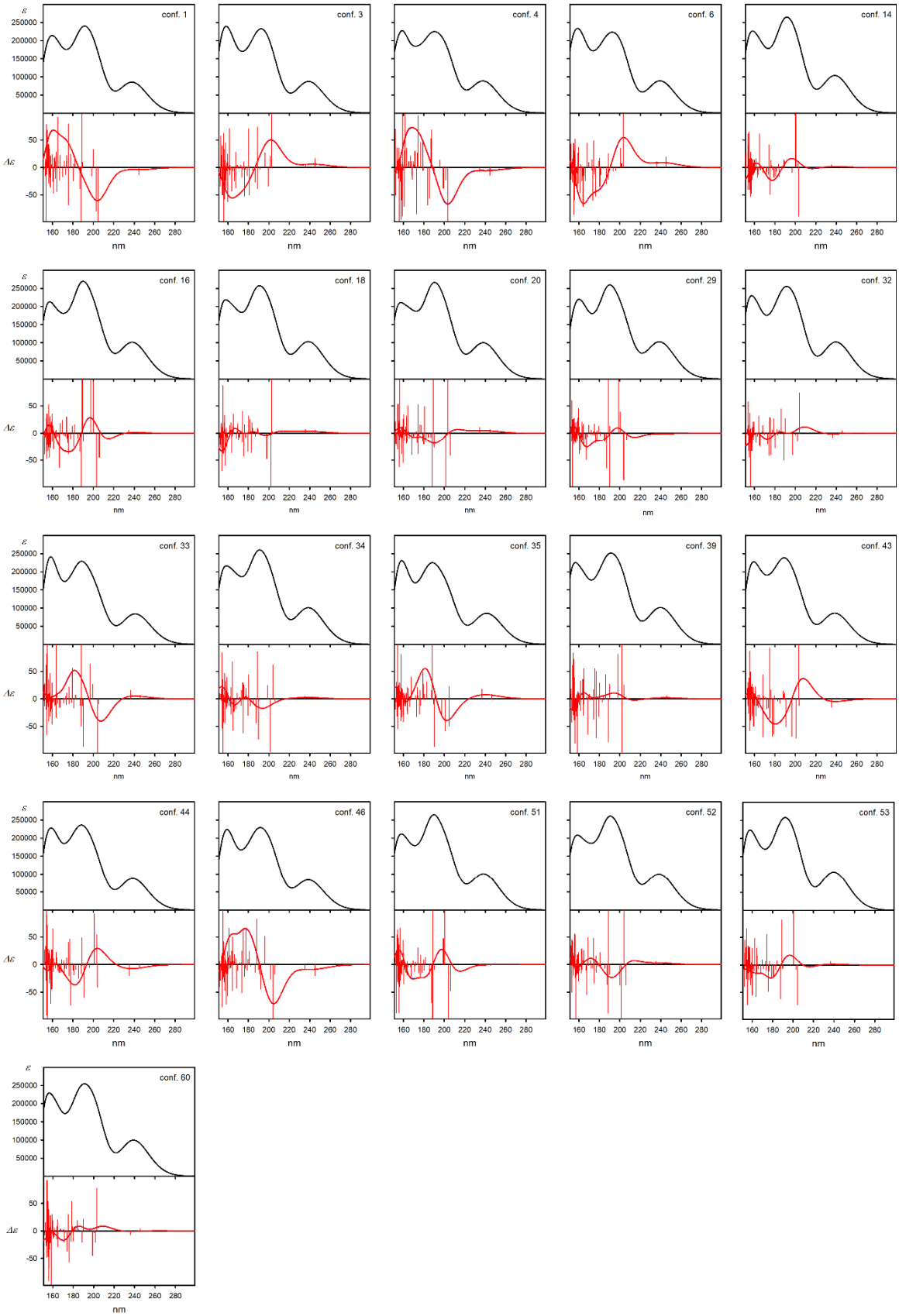


**Figure S51.** UV (upper panels) and ECD (lower panels) spectra calculated at the IEFPCM/TD-$\omega$B97-XD/6-311++G(2d,2p) level for individual low-energy conformers of **13**. Wavelengths were not corrected.

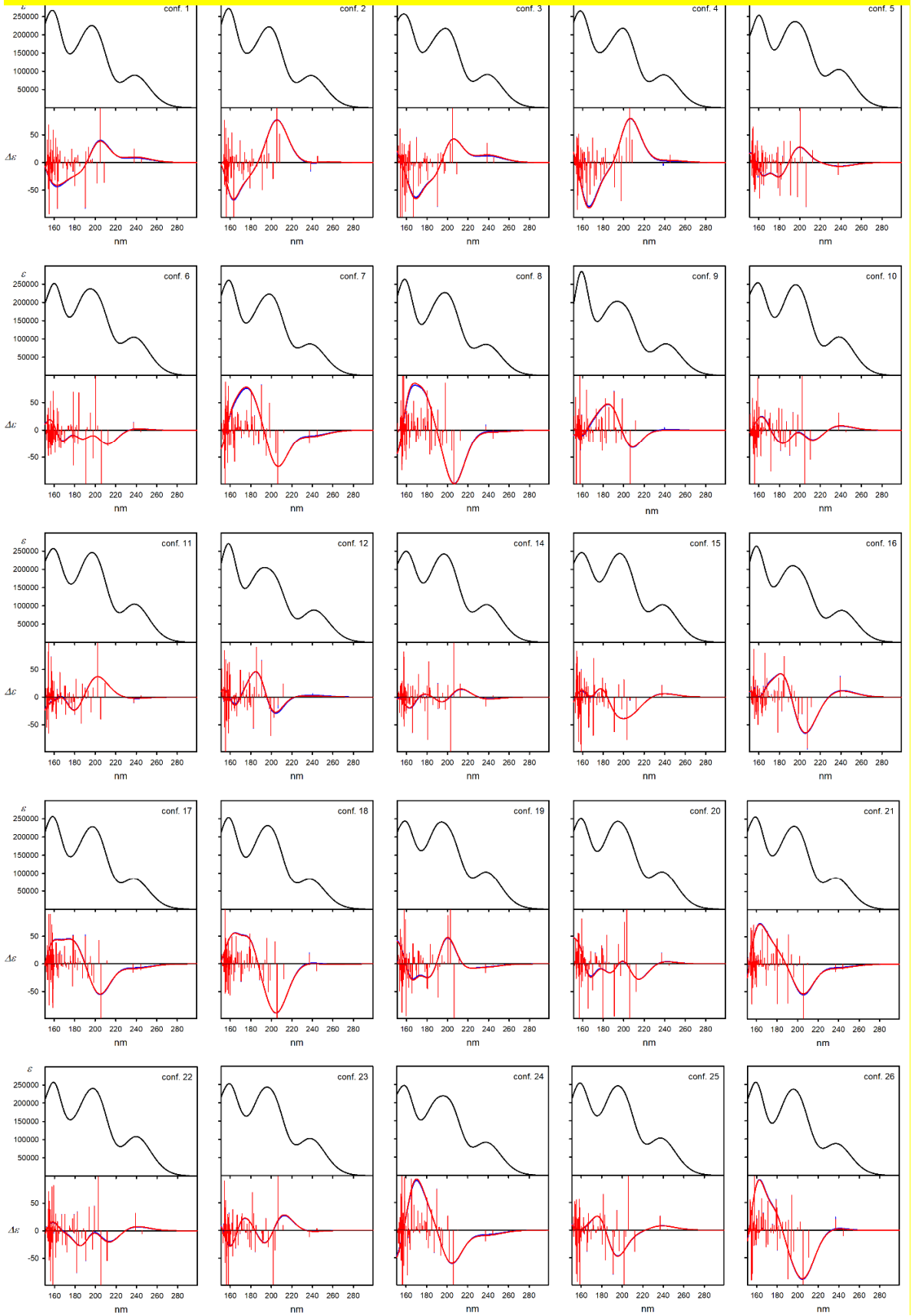


**Figure S52.** UV (upper panels) and ECD (lower panels) spectra calculated at the IEFPCM/TD-CAM-B3LYP/6-311++G(2d,2p) level for individual low-energy conformers of **14**. Wavelengths were not corrected.

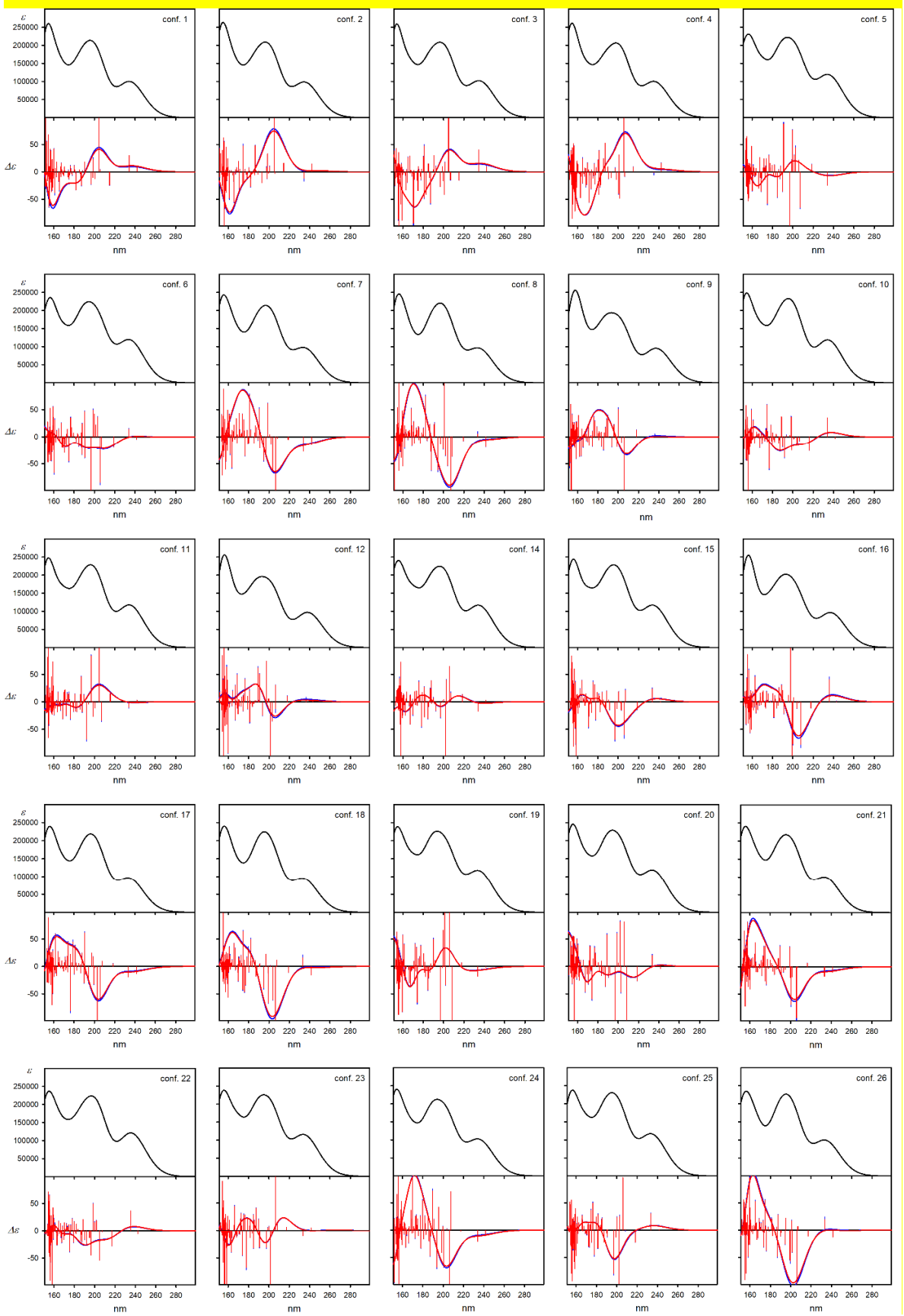
conf. 1
conf. 2
conf. 3
conf. 4
conf. 5
conf. 6
conf. 7
conf. 8
conf. 9
conf. 10
conf. 11
conf. 12
conf. 14
conf. 15
conf. 16
conf. 17
conf. 18
conf. 19
conf. 20
conf. 21
conf. 22
conf. 23
conf. 24
conf. 25
conf. 26
ε
Δε
nm

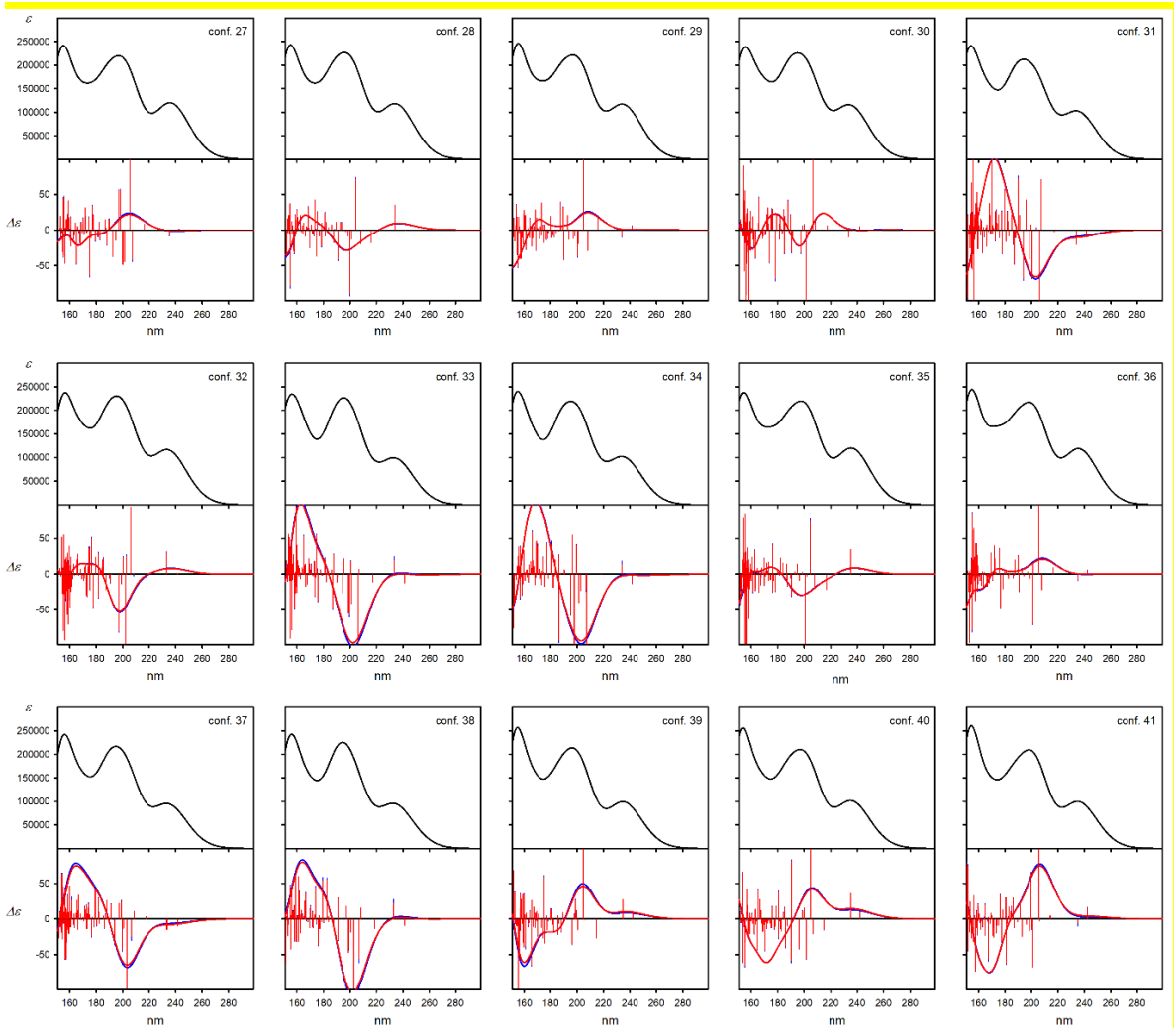


**Figure S53.** UV (upper panels) and ECD (lower panels) spectra calculated at the IEFPCM/TD-M06-2X/6-311++G(2d,2p) level for individual low-energy conformers of **14**. Wavelengths were not corrected.

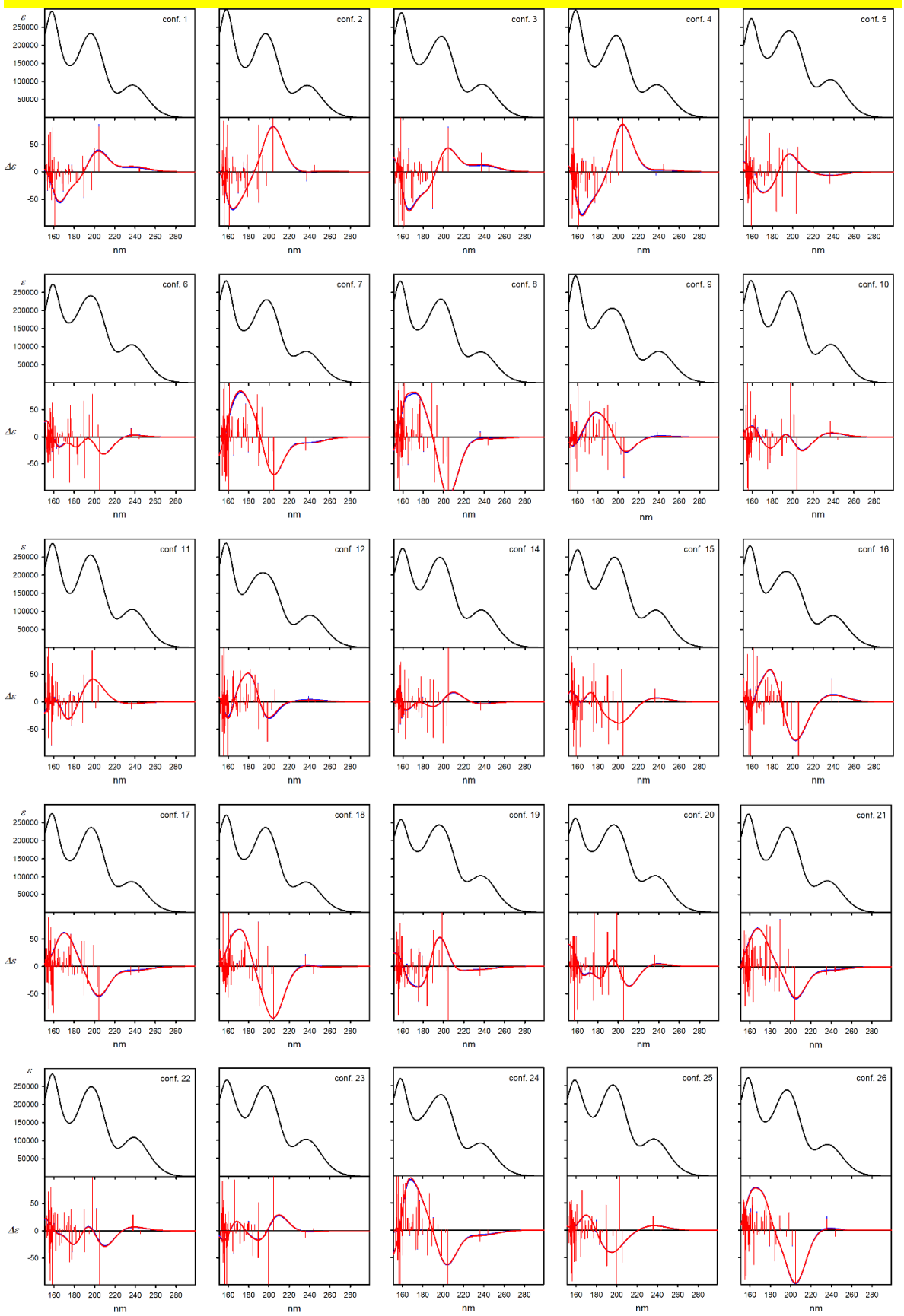
conf. 1
conf. 2
conf. 3
conf. 4
conf. 5
conf. 6
conf. 7
conf. 8
conf. 9
conf. 10
conf. 11
conf. 12
conf. 14
conf. 15
conf. 16
conf. 17
conf. 18
conf. 19
conf. 20
conf. 21
conf. 22
conf. 23
conf. 24
conf. 25
conf. 26
ε
Δε
nm

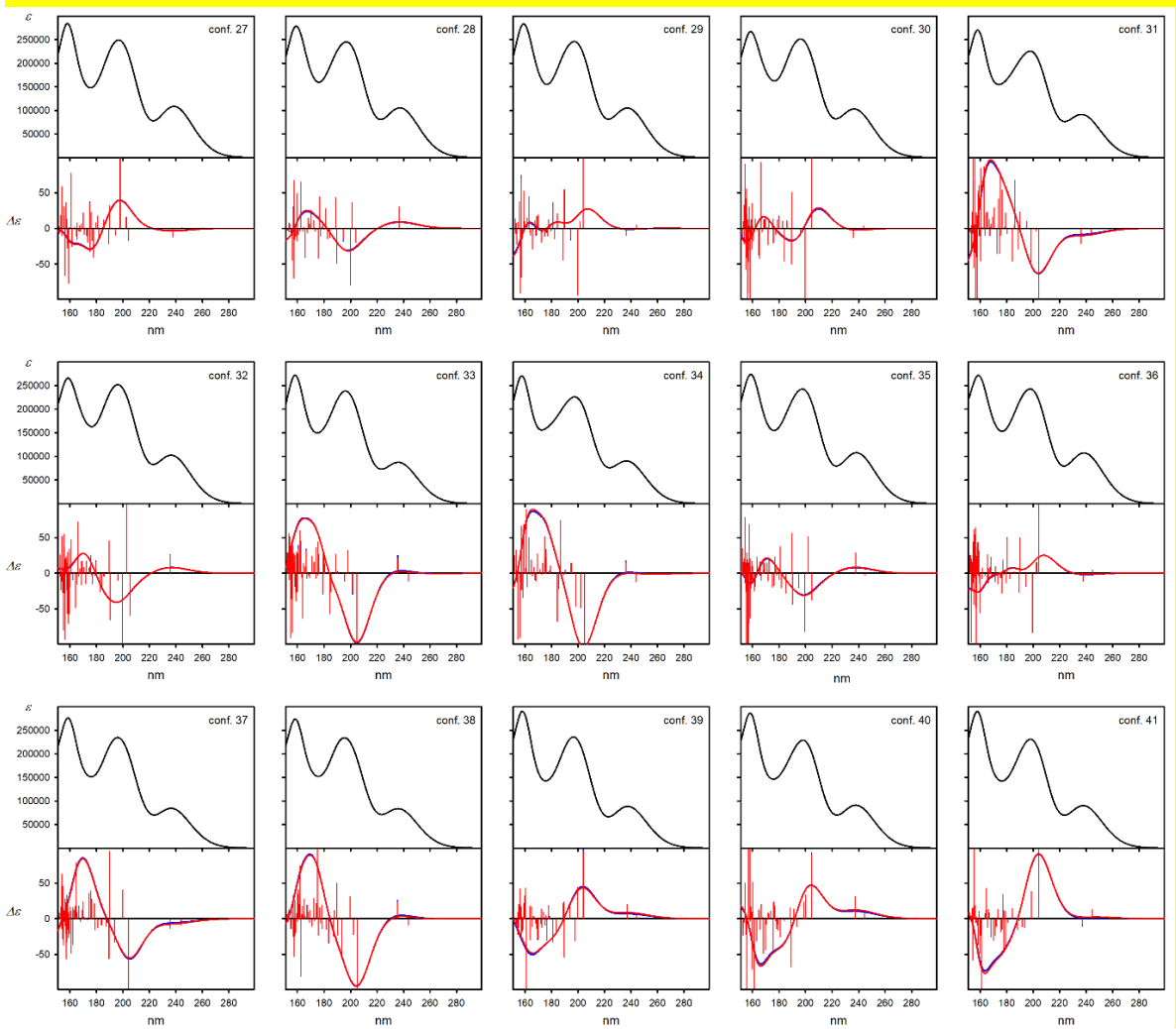


**Figure S54.** UV (upper panels) and ECD (lower panels) spectra calculated at the IEFPCM/TD-ωB97-XD/6-311++G(2d,2p) level for individual low-energy conformers of **14**. Wavelengths were not corrected.

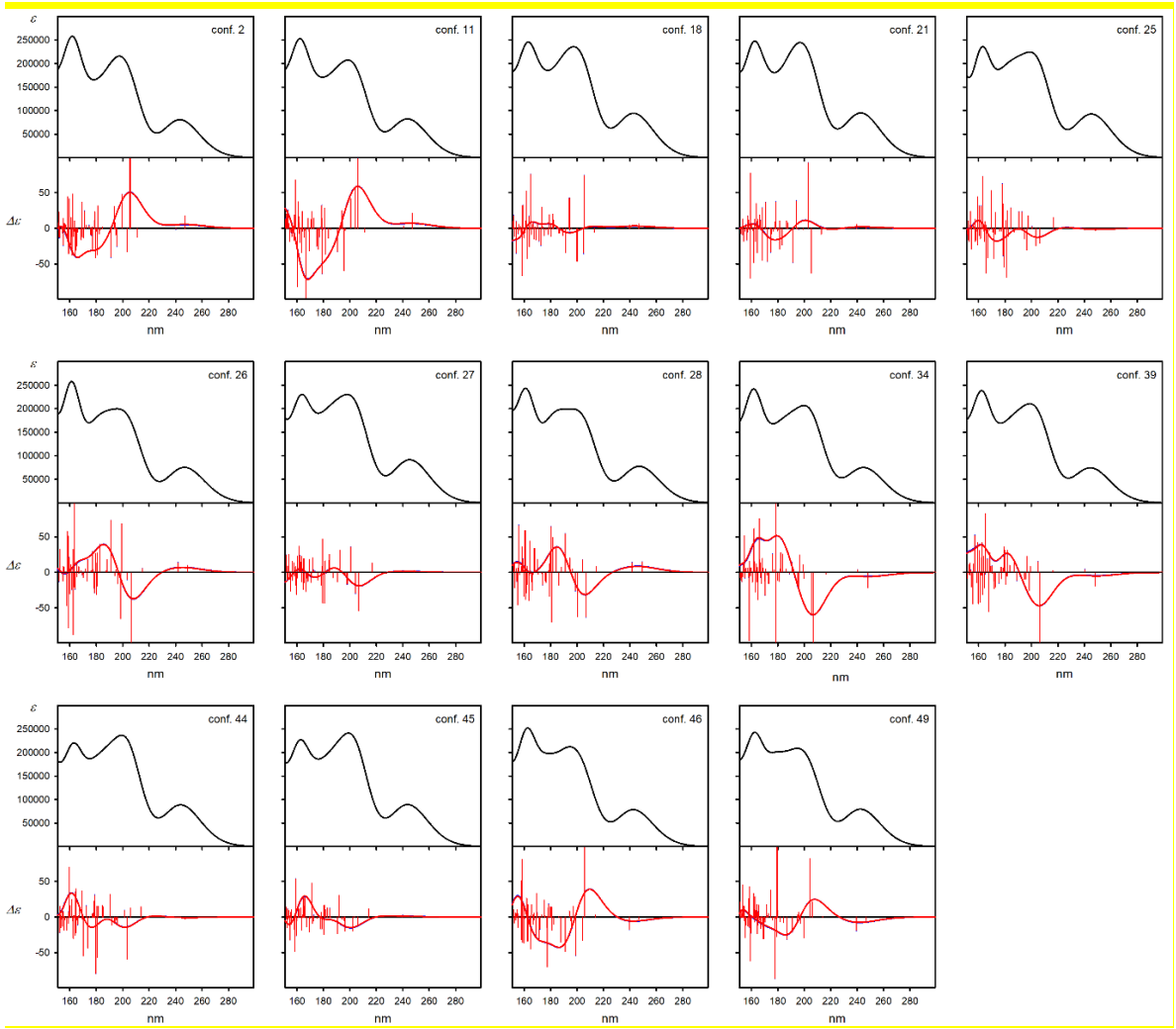


**Figure S55.** UV (upper panels) and ECD (lower panels) spectra calculated at the IEFPCM/TD-CAM-B3LYP/6-311++G(2d,2p) level for individual low-energy conformers of **15**. Wavelengths were not corrected.

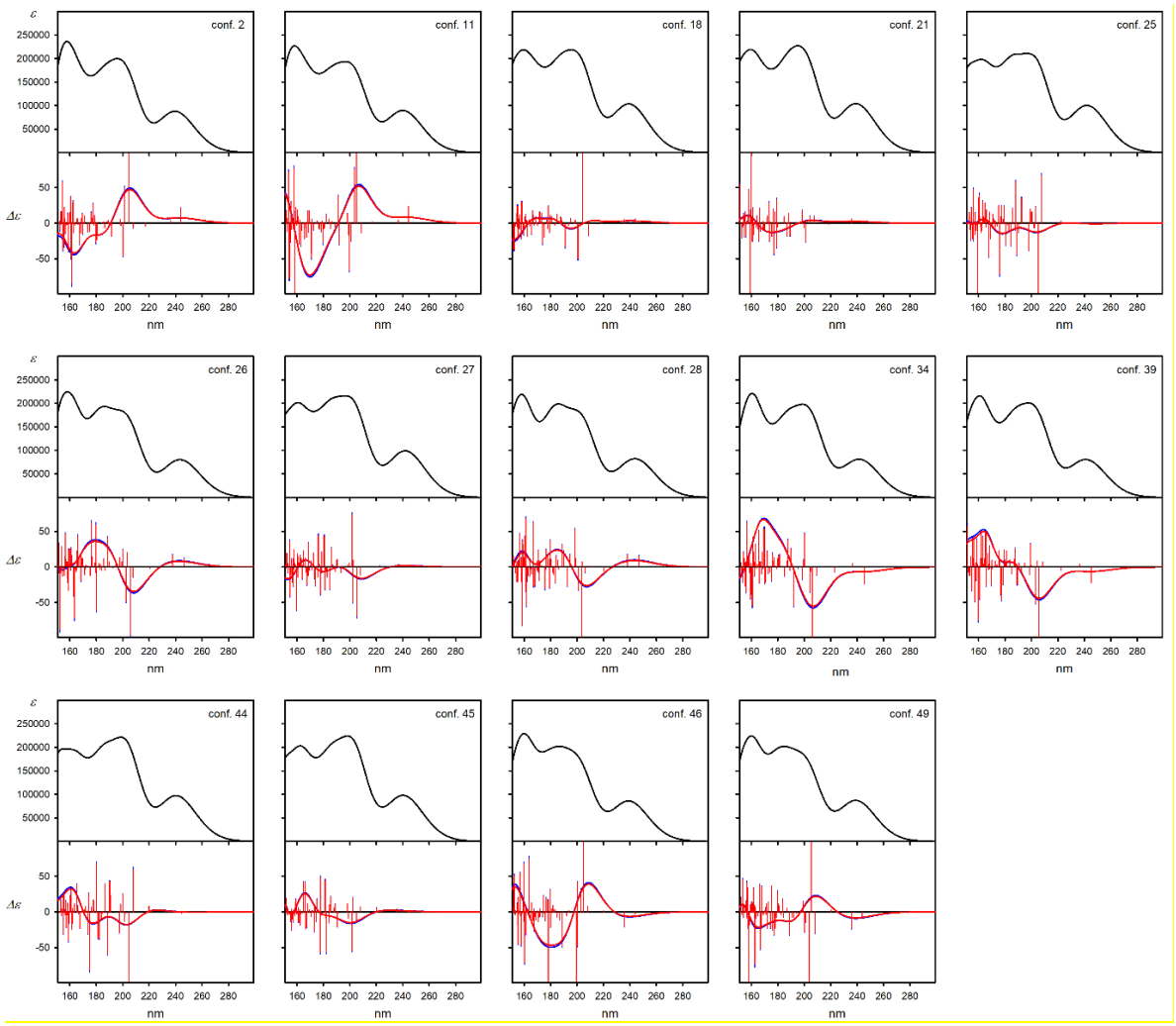


**Figure S56.** UV (upper panels) and ECD (lower panels) spectra calculated at the IEFPCM/TD-M06-2X/6-311++G(2d,2p) level for individual low-energy conformers of **15**. Wavelengths were not corrected.

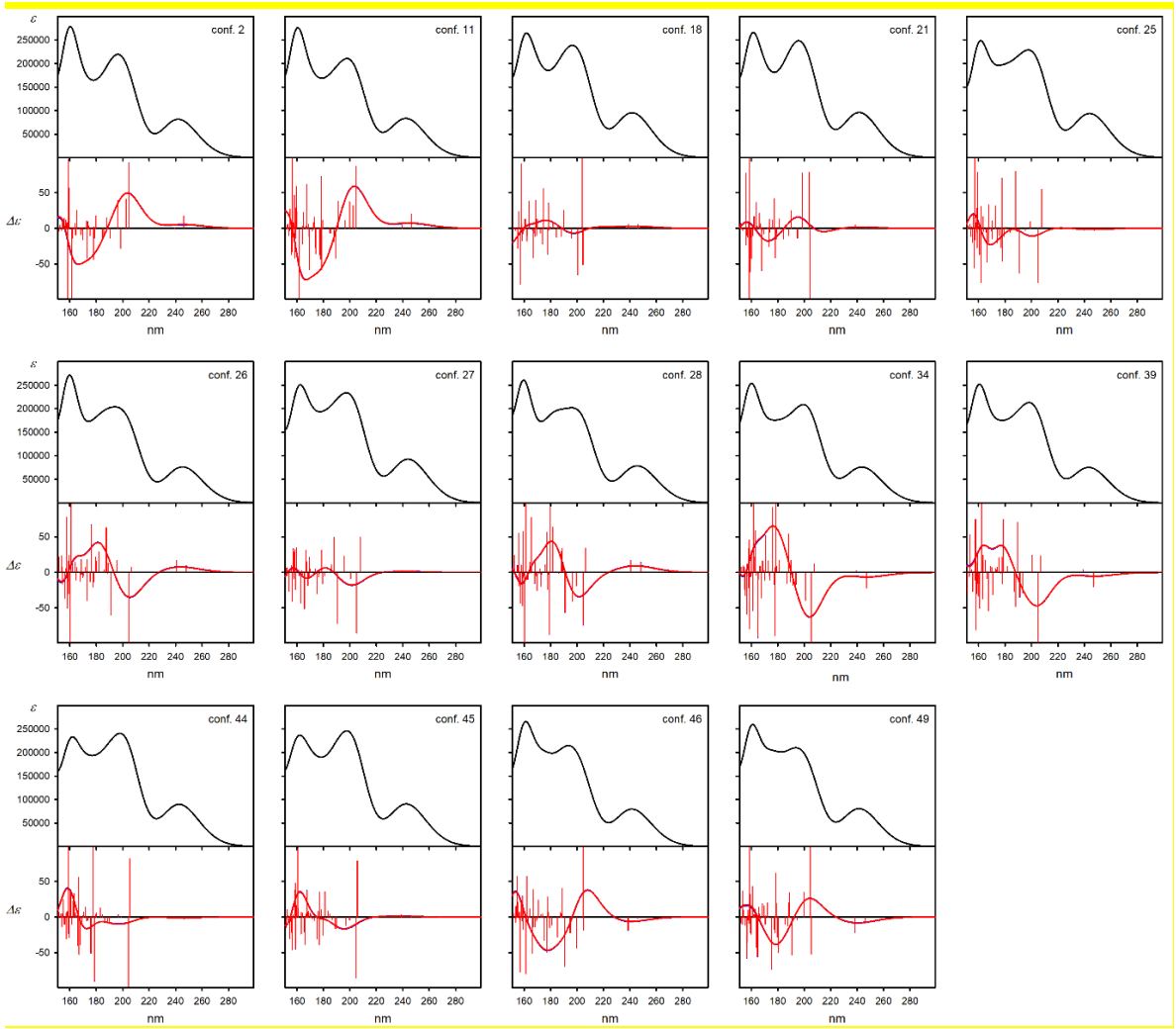


**Figure S57.** UV (upper panels) and ECD (lower panels) spectra calculated at the IEFPCM/TD-$\omega$B97-XD/6-311++G(2d,2p) level for individual low-energy conformers of **15**. Wavelengths were not corrected.

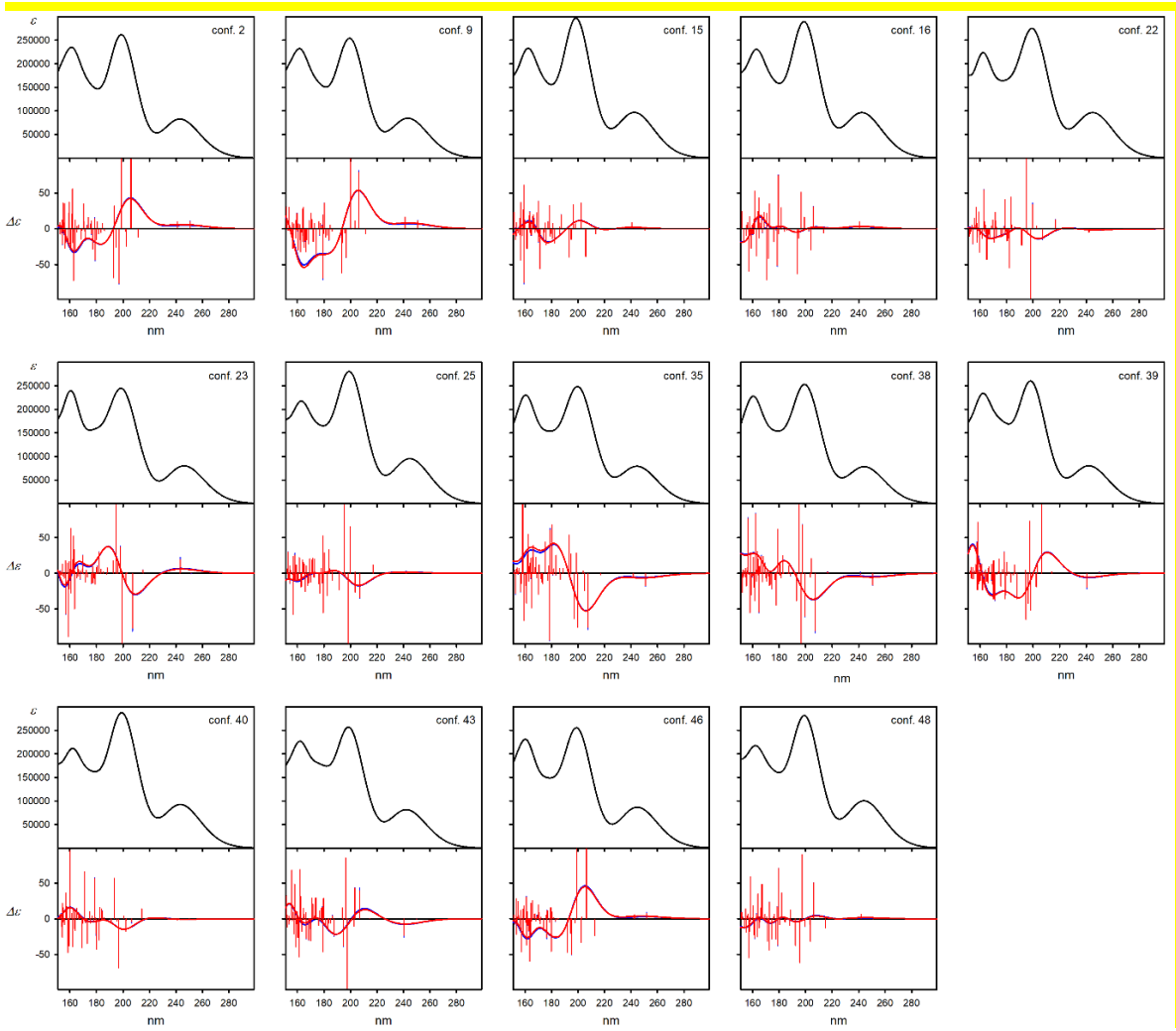


**Figure S58.** UV (upper panels) and ECD (lower panels) spectra calculated at the IEFPCM/TD-CAM-B3LYP/6-311++G(2d,2p) level for individual low-energy conformers of **16**. Wavelengths were not corrected.

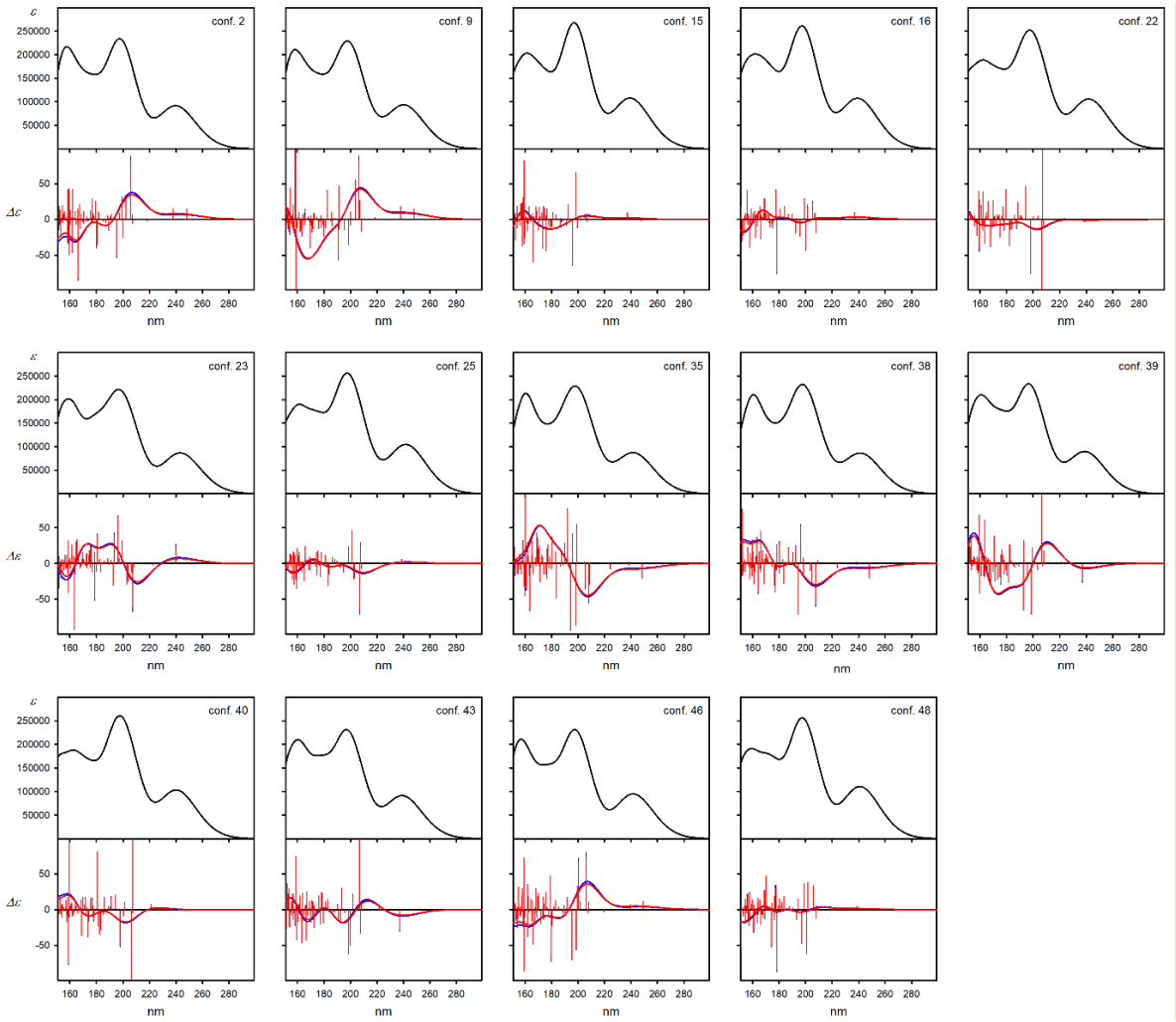


**Figure S59.** UV (upper panels) and ECD (lower panels) spectra calculated at the IEFPCM/TD-M06-2X/6-311++G(2d,2p) level for individual low-energy conformers of **16**. Wavelengths were not corrected.

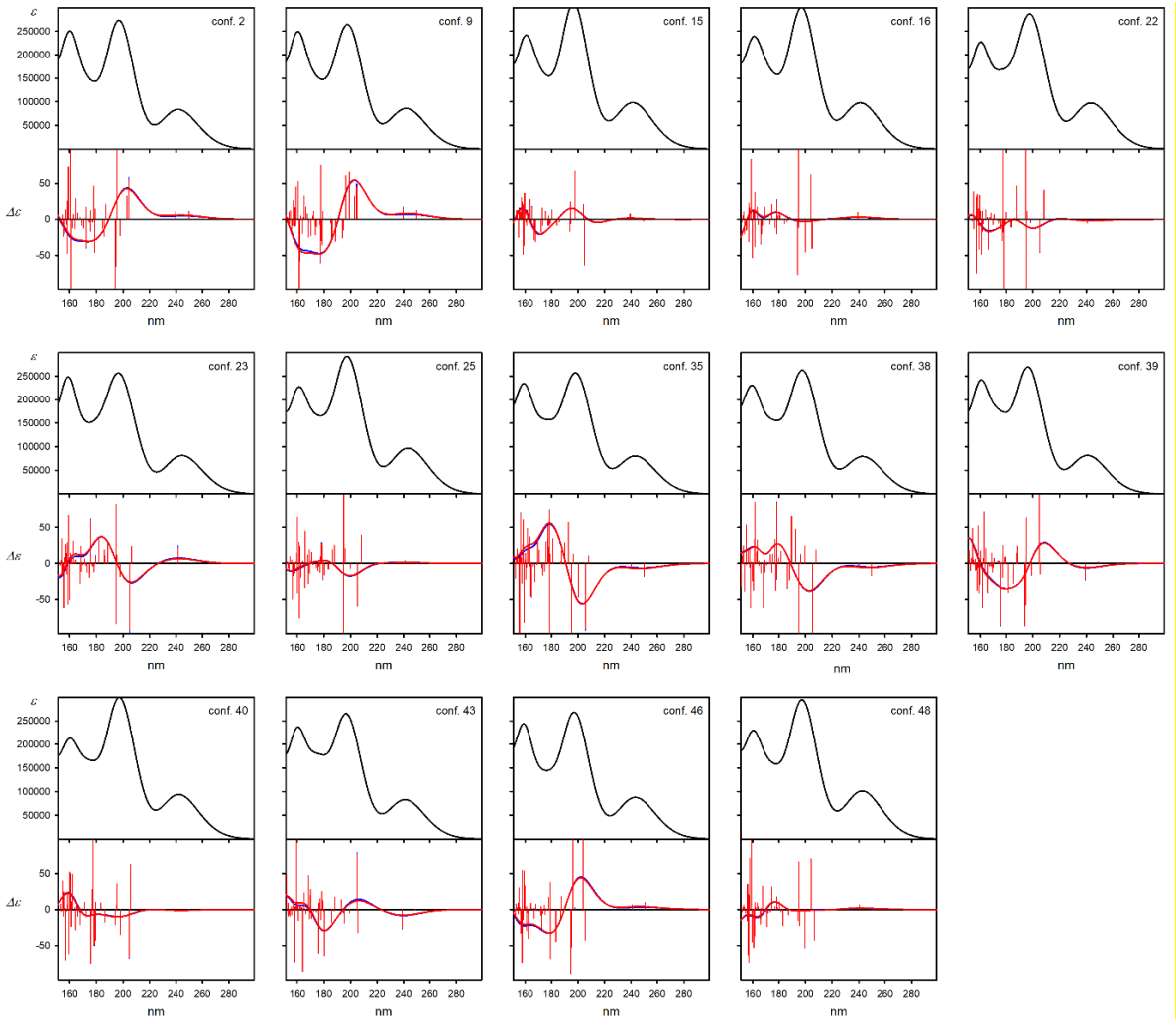


**Figure S60.** UV (upper panels) and ECD (lower panels) spectra calculated at the IEFPCM/TD-$\omega$B97-XD/6-311++G(2d,2p) level for individual low-energy conformers of **16**. Wavelengths were not corrected.

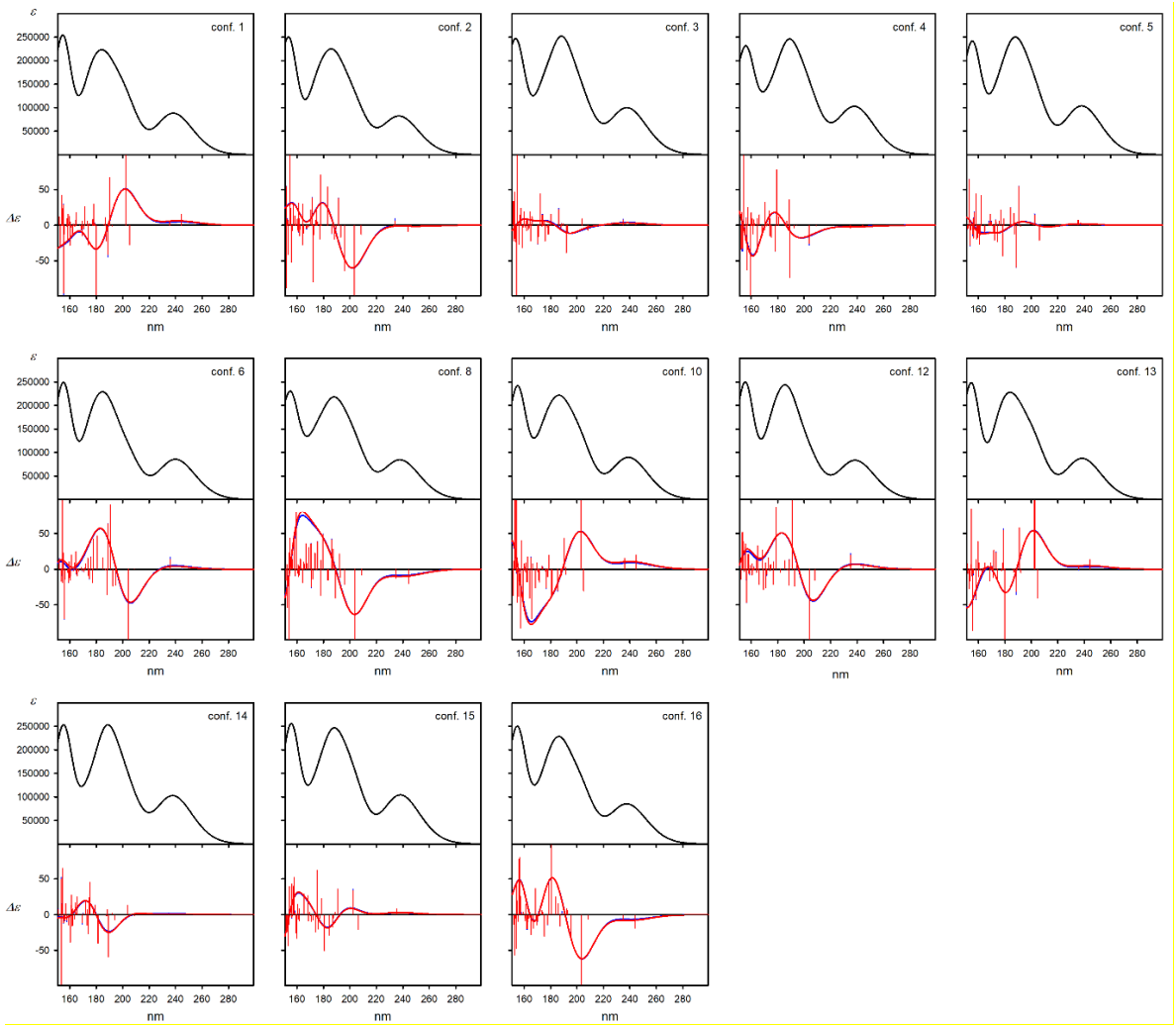


**Figure S61.** UV (upper panels) and ECD (lower panels) spectra calculated at the IEFPCM/TD-CAM-B3LYP/6-311++G(2d,2p) level for individual low-energy conformers of **17**. Wavelengths were not corrected.

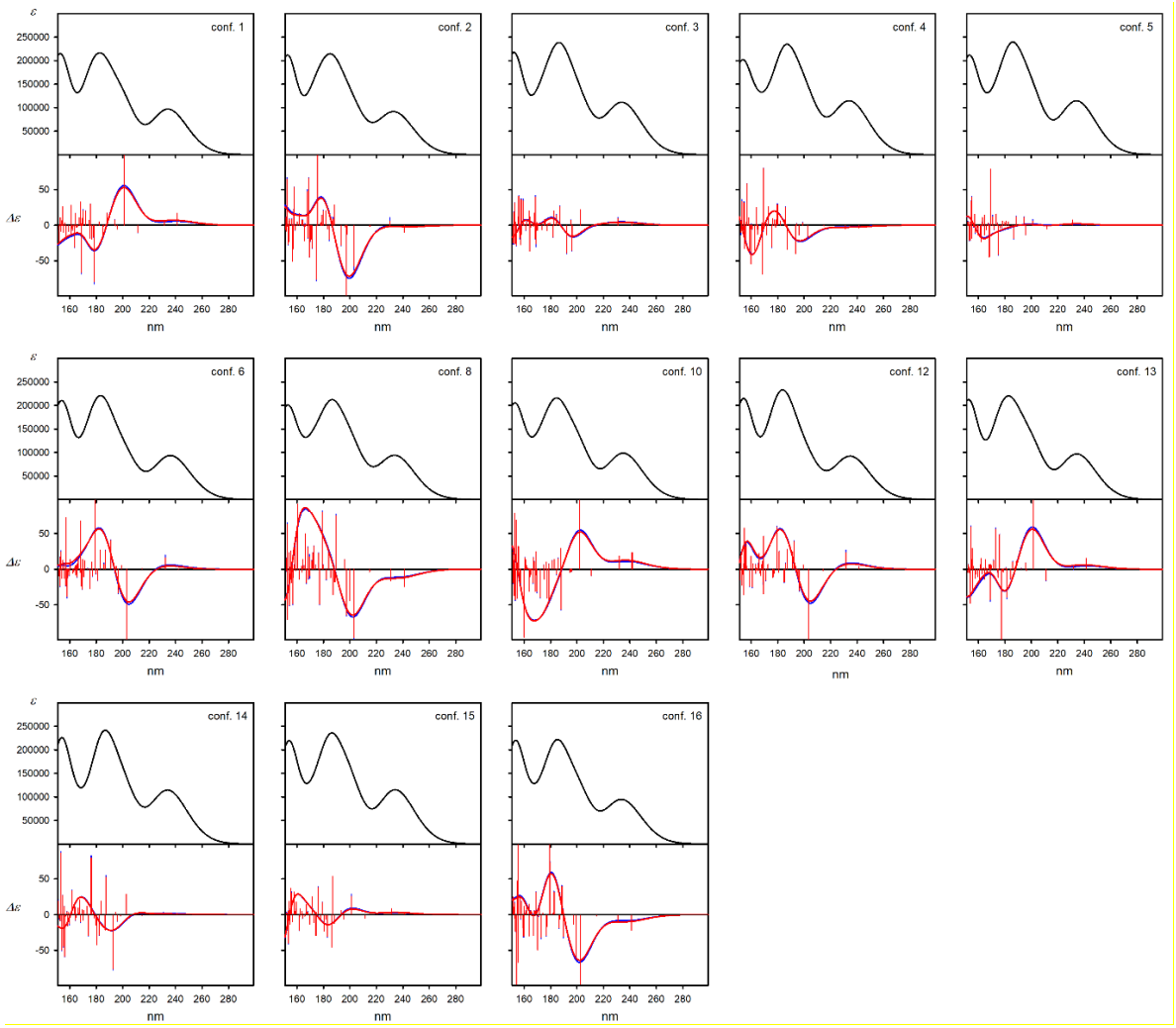


**Figure S62.** UV (upper panels) and ECD (lower panels) spectra calculated at the IEFPCM/TD-M06-2X/6-311++G(2d,2p) level for individual low-energy conformers of **17**. Wavelengths were not corrected.

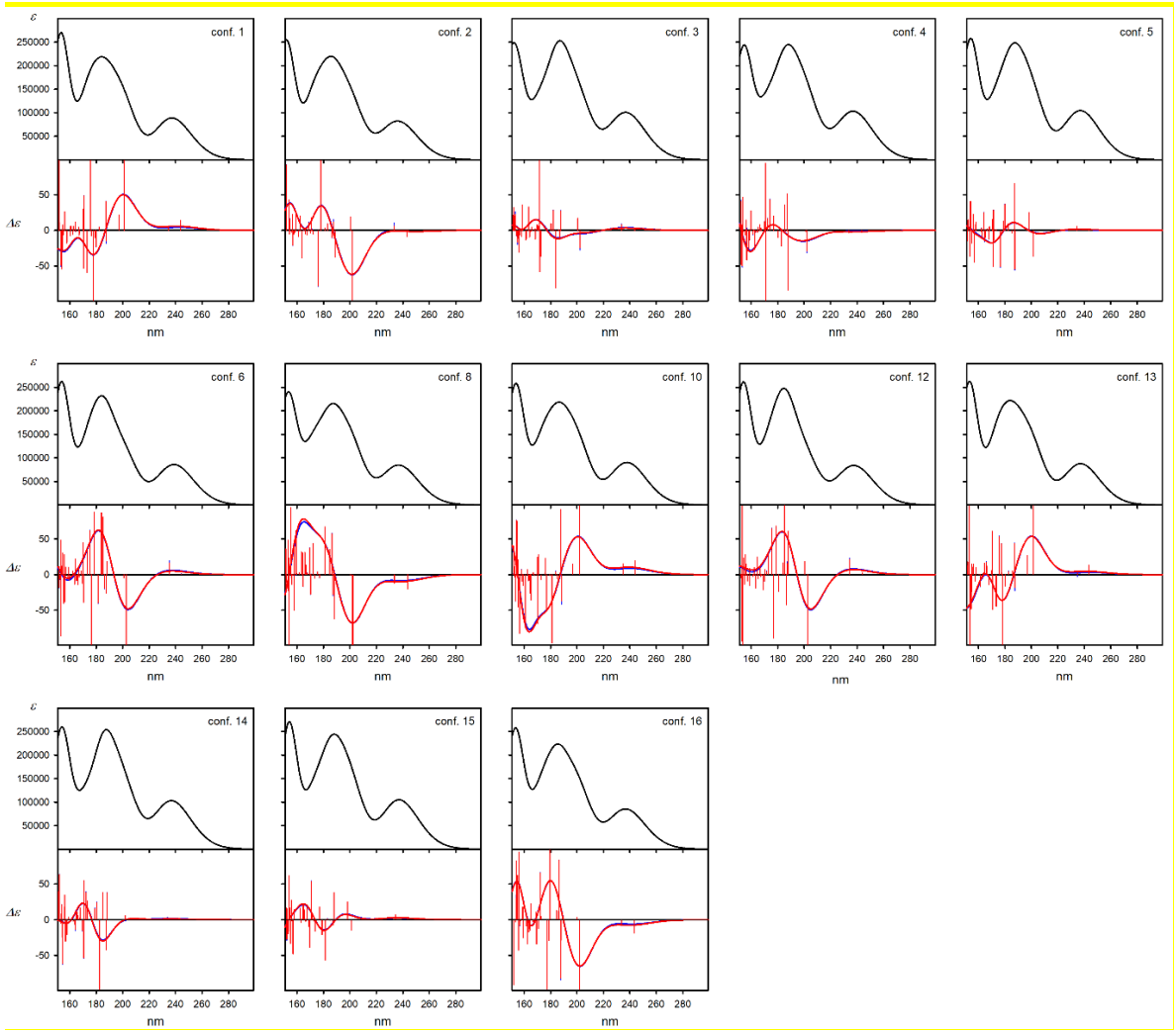


**Figure S63.** UV (upper panels) and ECD (lower panels) spectra calculated at the IEFPCM/TD-ωB97-XD/6-311++G(2d,2p) level for individual low-energy conformers of **17**. Wavelengths were not corrected.

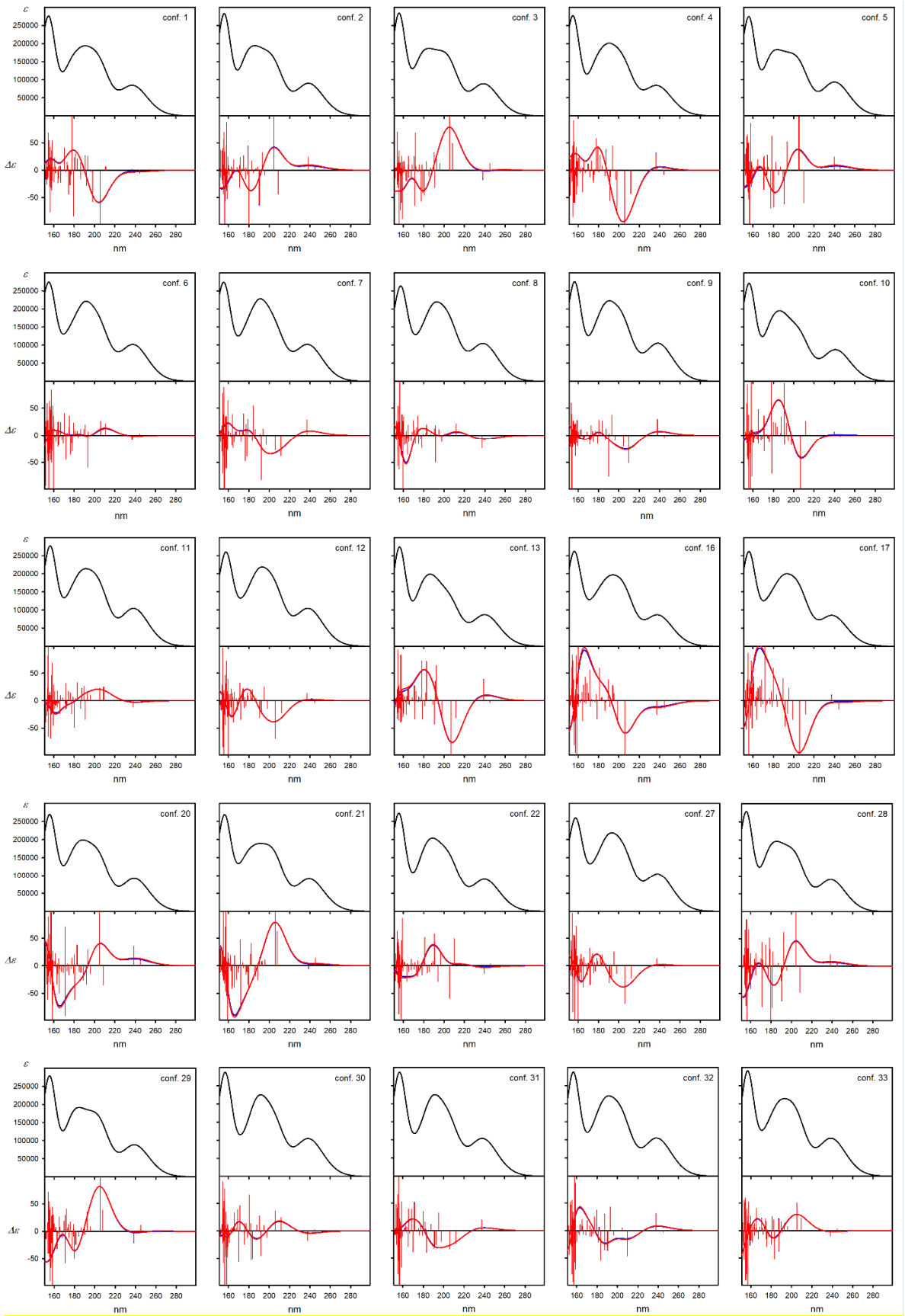


**Figure S64.** UV (upper panels) and ECD (lower panels) spectra calculated at the IEFPCM/TD-CAM-B3LYP/6-311++G(2d,2p) level for individual low-energy conformers of **18**. Wavelengths were not corrected.

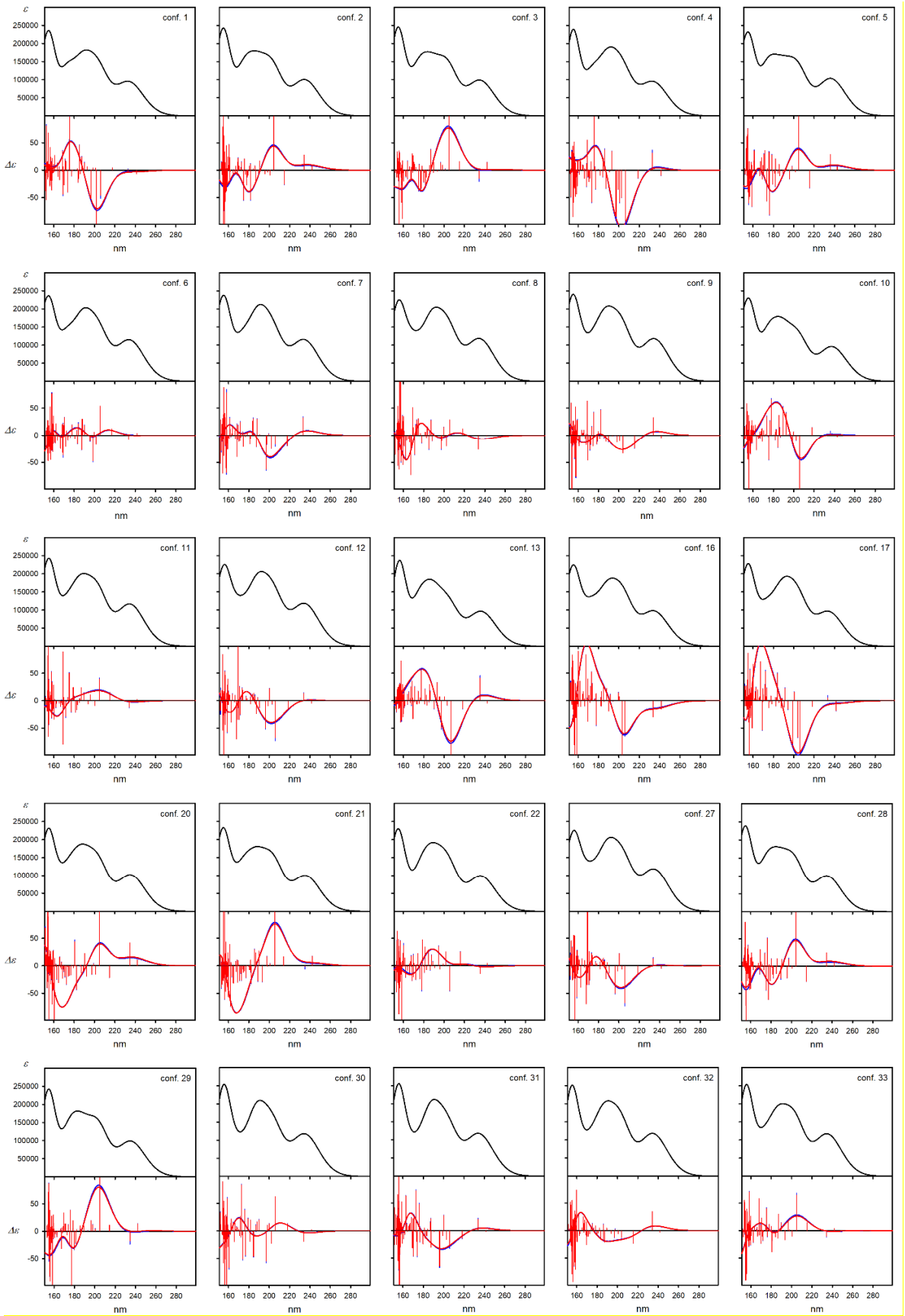


**Figure S65.** UV (upper panels) and ECD (lower panels) spectra calculated at the IEFPCM/TD-M06-2X/6-311++G(2d,2p) level for individual low-energy conformers of **18**. Wavelengths were not corrected.

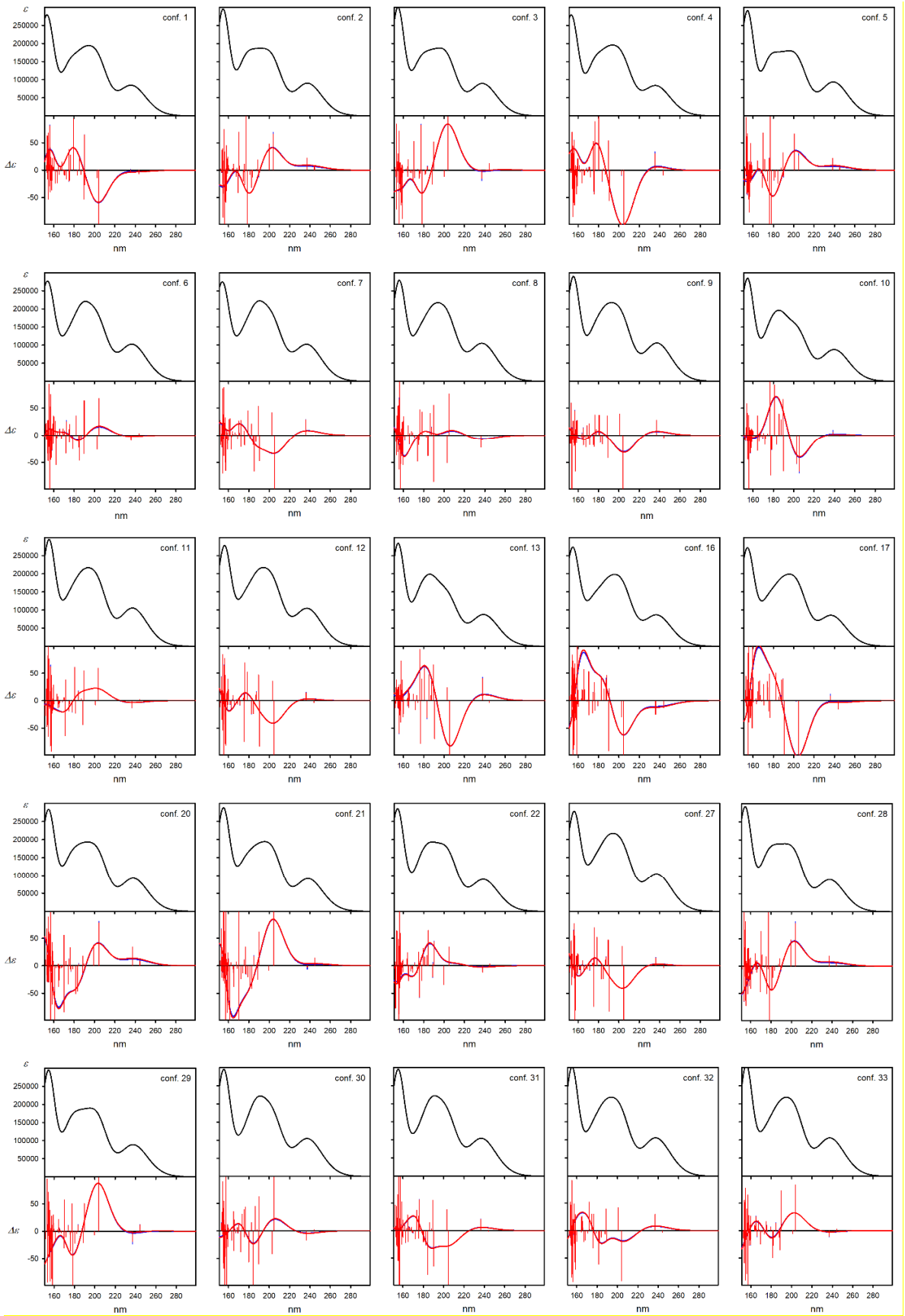


**Figure S66.** UV (upper panels) and ECD (lower panels) spectra calculated at the IEFPCM/TD-$\omega$B97-XD/6-311++G(2d,2p) level for individual low-energy conformers of **18**. Wavelengths were not corrected.

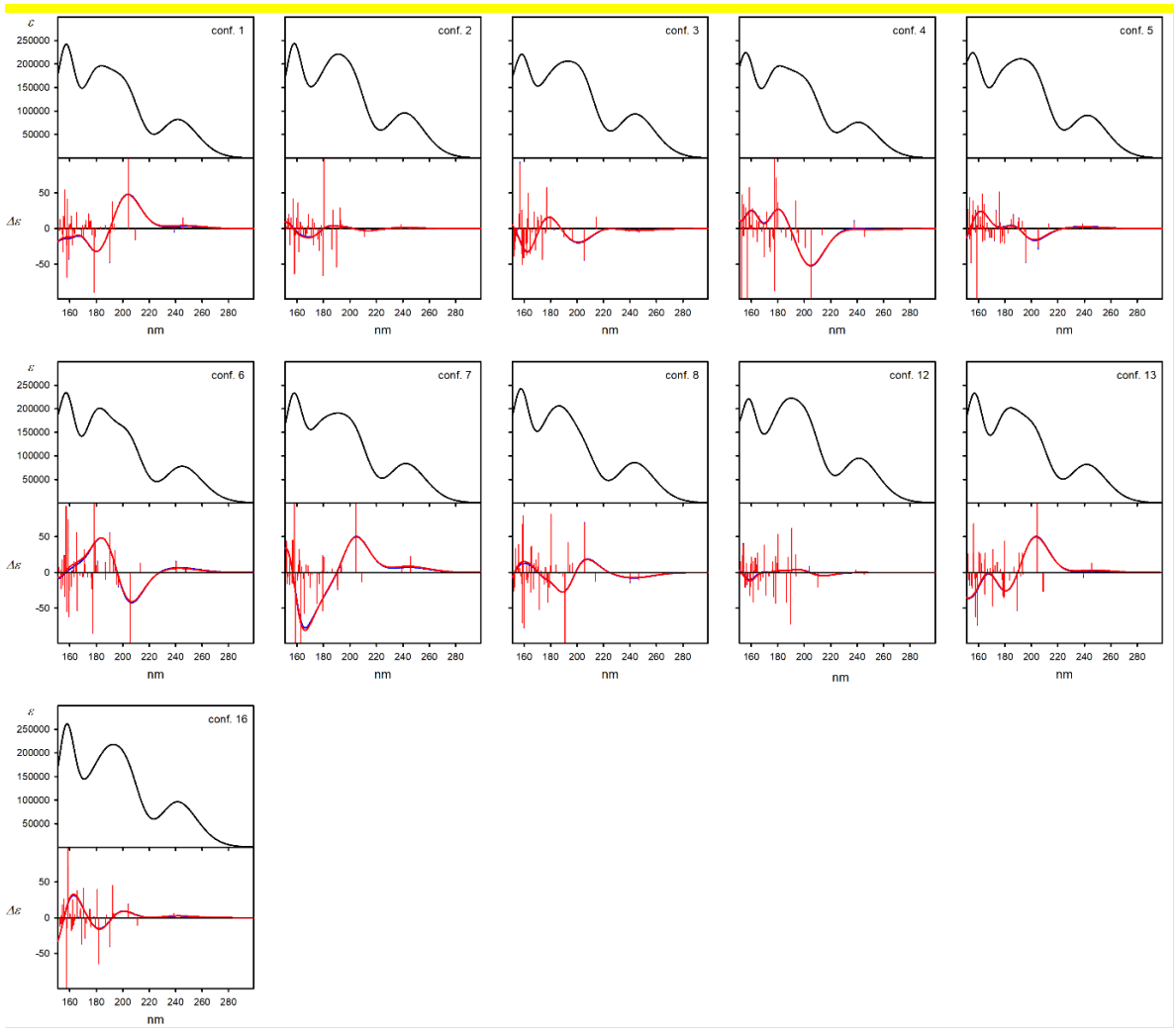


**Figure S67.** UV (upper panels) and ECD (lower panels) spectra calculated at the IEFPCM/TD-CAM-B3LYP/6-311++G(2d,2p) level for individual low-energy conformers of **19**. Wavelengths were not corrected.

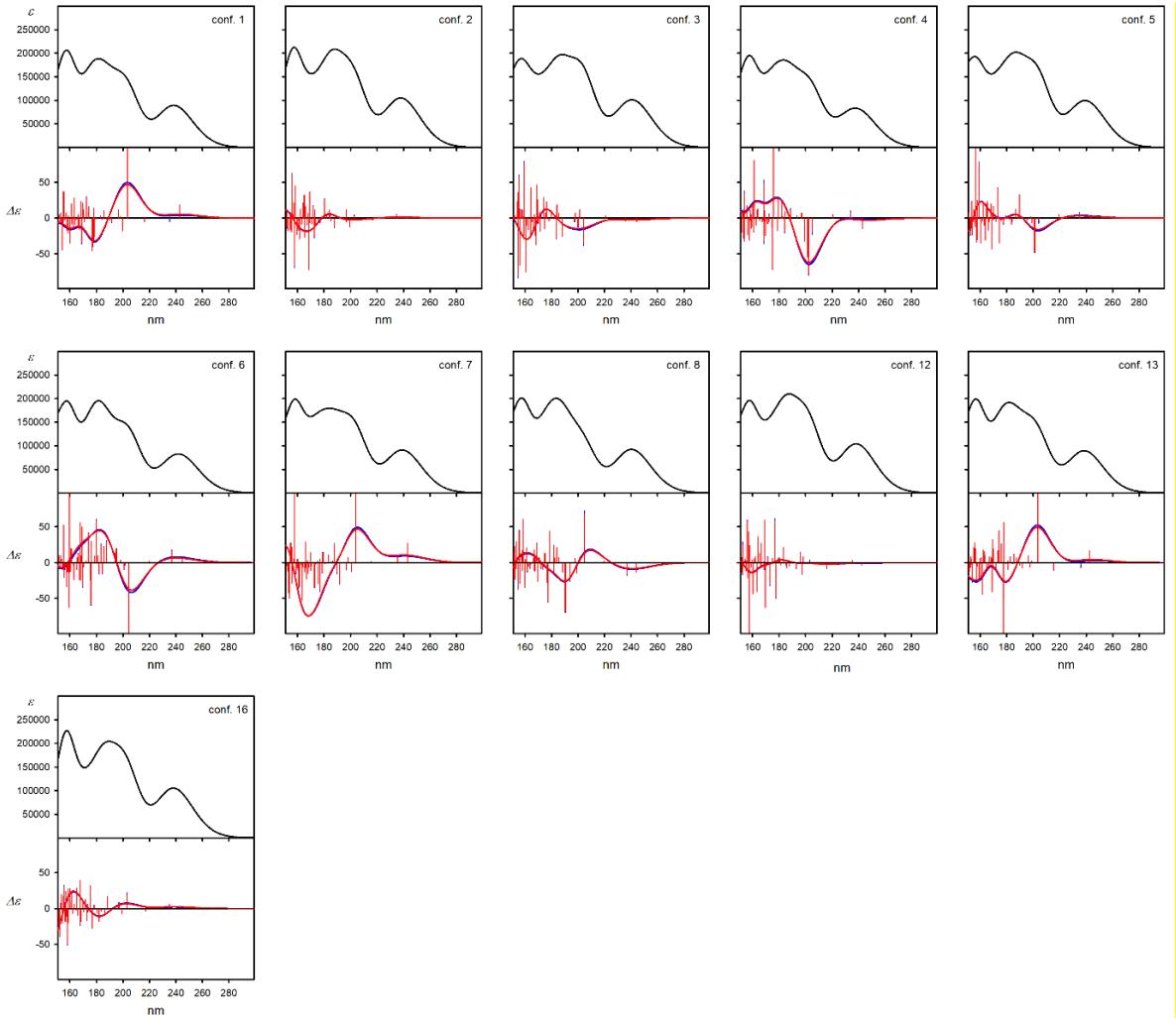


**Figure S68.** UV (upper panels) and ECD (lower panels) spectra calculated at the IEFPCM/TD-M06-2X/6-311++G(2d,2p) level for individual low-energy conformers of **19**. Wavelengths were not corrected.

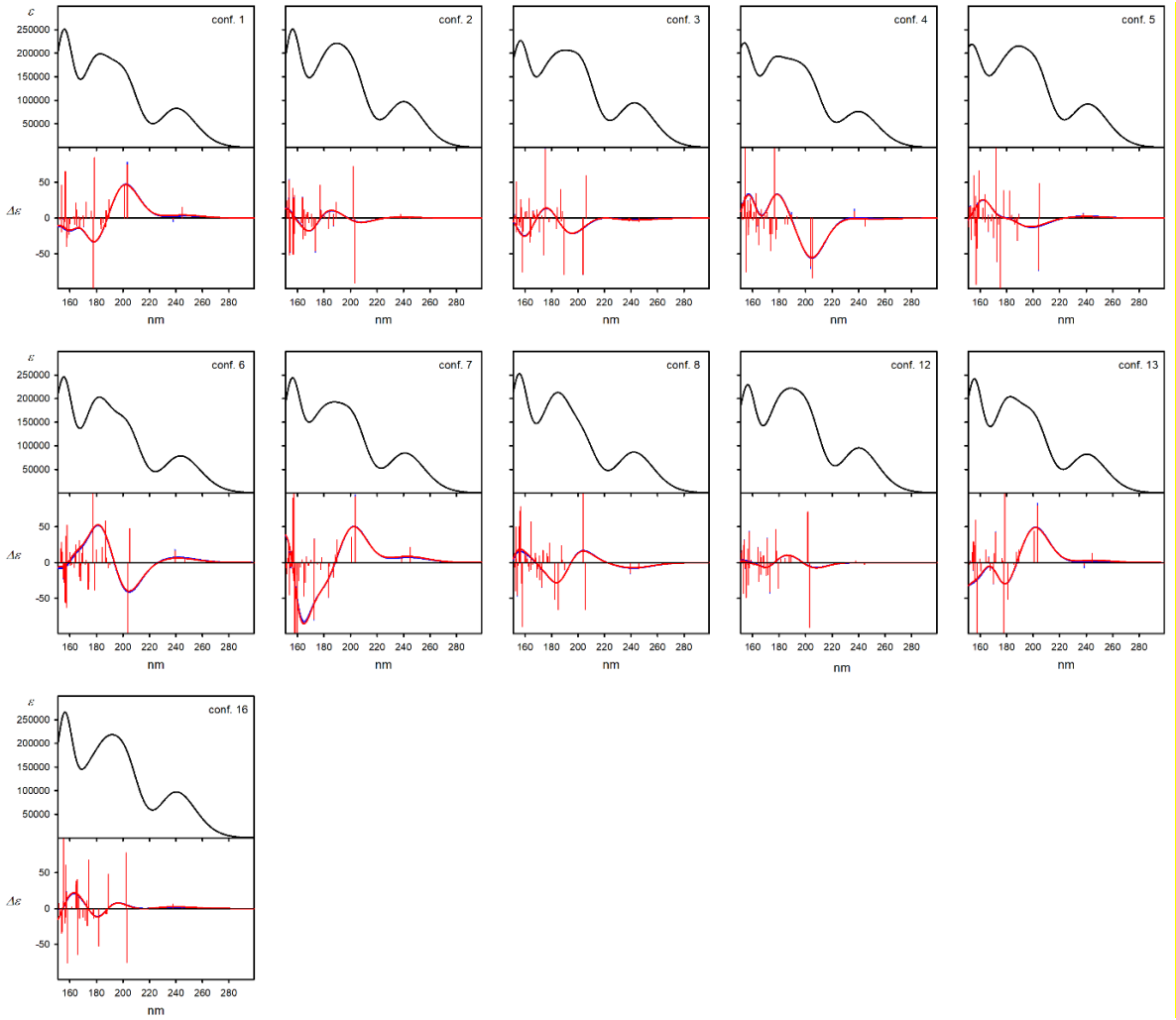


**Figure S69.** UV (upper panels) and ECD (lower panels) spectra calculated at the IEFPCM/TD-$\omega$B97-XD/6-311++G(2d,2p) level for individual low-energy conformers of **19**. Wavelengths were not corrected.

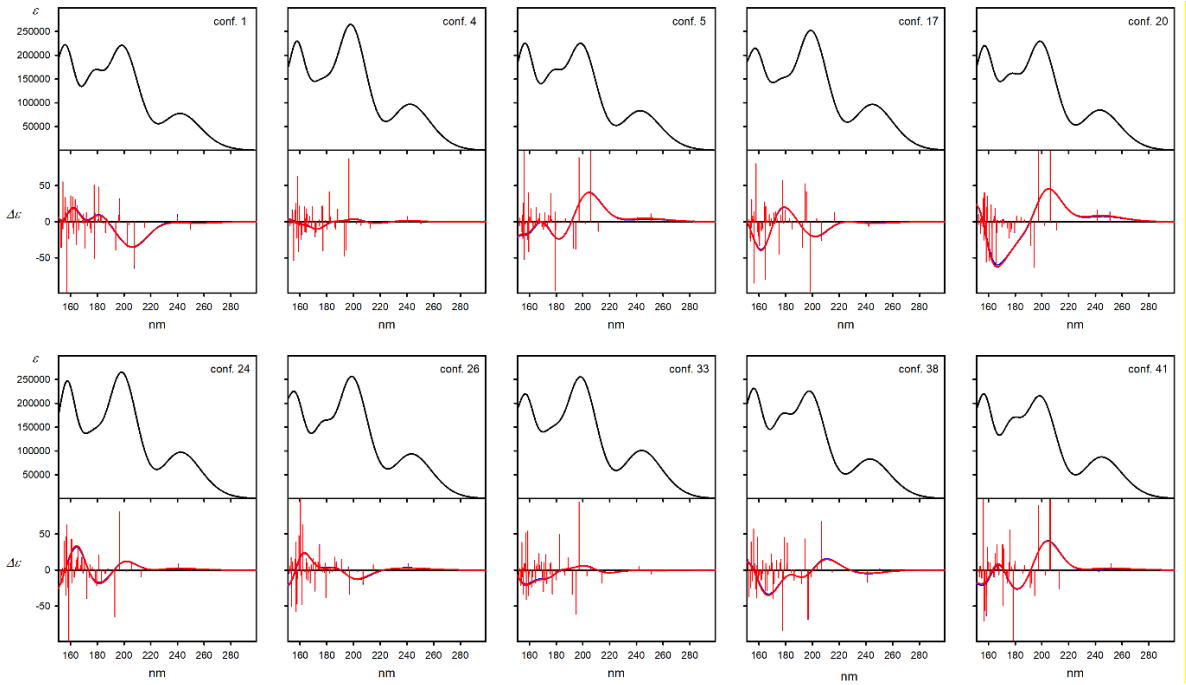

**Figure S70.** UV (upper panels) and ECD (lower panels) spectra calculated at the IEFPCM/TD-CAM-B3LYP/6-311++G(2d,2p) level for individual low-energy conformers of **20**. Wavelengths were not corrected.

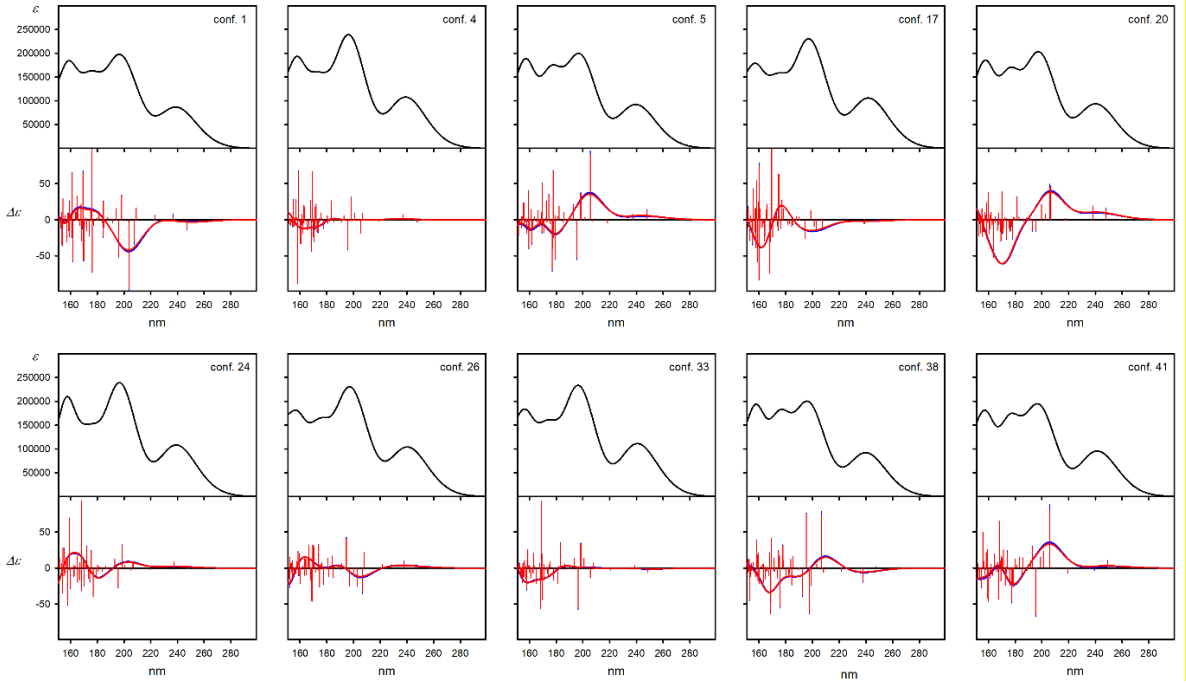


**Figure S71.** UV (upper panels) and ECD (lower panels) spectra calculated at the IEFPCM/TD-M06-2X/6-311++G(2d,2p) level for individual low-energy conformers of **20**. Wavelengths were not corrected.

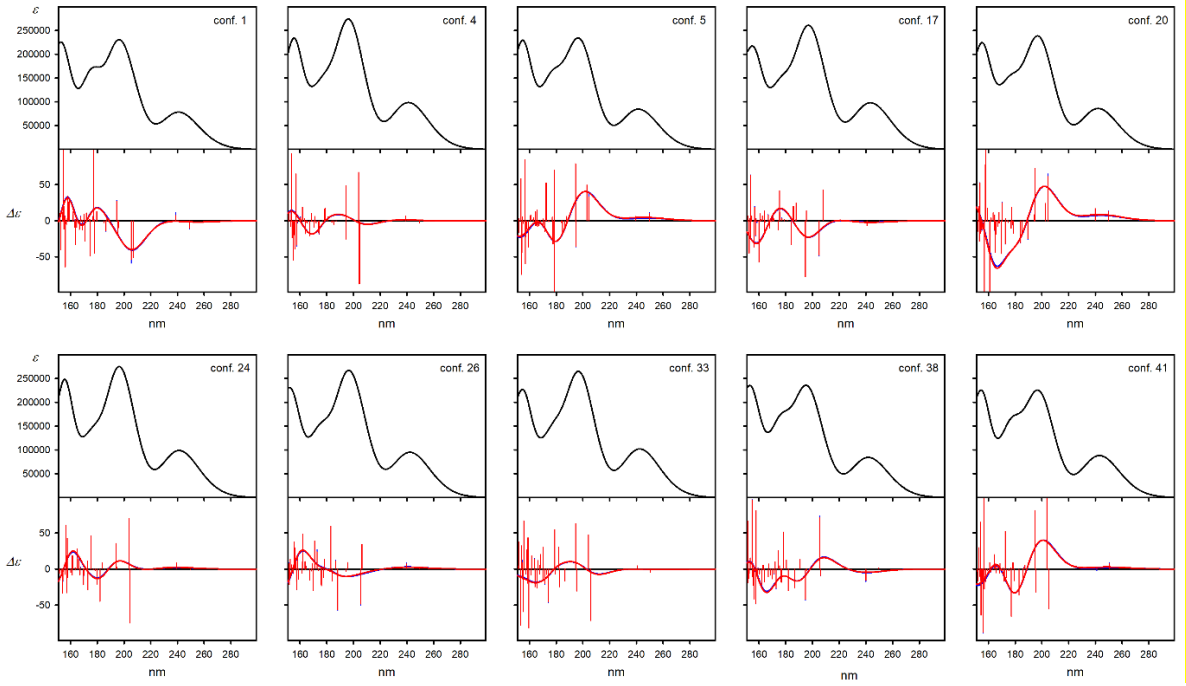


**Figure S72.** UV (upper panels) and ECD (lower panels) spectra calculated at the IEFPCM/TD-$\omega$B97-XD/6-311++G(2d,2p) level for individual low-energy conformers of **20**. Wavelengths were not corrected.

**References**

1. Scigress 2.5, Fujitsu Ltd. FUJITSU Technical Computing Solution SCIGRESS. Available Online: https://www.fujitsu.com/global/solutions/business-technology/tc/sol/scigress/ (accessed on 11 September 2020)
2. Gaussian 09. Available Online: https://gaussian.com/glossary/g09/ (accessed on 9 September 2020)
3. Tomasi, J.; Mennucci, B.; Cammi, R. Quantum mechanical continuum solvation models. *Chem. Rev.* **2005**, *105*, 2999–3093.
4. Kwit, M.; Rozwadowska, M.D.; Gawroński, J.; Grajewska, A. Density Functional Theory Calculations of the Optical Rotation and Electronic Circular Dichroism: The Absolute Configuration of the Highly Flexible *trans*-Isocytoxazone Revised. *J. Org. Chem.* **2009**, *74*, 8051–8063 and references therein.
5. Yanai, T.; Tew, D.; Handy, N. A new hybrid exchange-correlation functional using the Coulomb-attenuating method (CAM-B3LYP). *Chem. Phys. Lett.* **2004**, *393*, 51–57.
6. Zhao, Y.; Truhlar, D.G. The M06 suite of density functionals for main group thermochemistry, thermochemical kinetics, noncovalent interactions, excited states, and transition elements: two new functionals and systematic testing of four M06-class functionals and 12 other functionals. *Theor. Chem. Acc.* **2008**, *120*, 215–241.
7. Harada, N.; Stephens, P.J. ECD Cotton effect approximated by the Gaussian curve and other methods. *Chirality* **2010**, *22*, 229–233.
8. Chai J.-D.; Head-Gordon, M. Long-range corrected hybrid density functionals with damped atom-atom dispersion corrections. *Phys. Chem. Chem. Phys*. **2008**, *10*, 6615–6620.